

First Street Foundation Flood Model

Technical Methodology Document

First Street Foundation Flood Model (FSF-FM) Technical Documentation

Published: 06/17/2020

Acknowledgements

Peer Review Panel: We would like to thank our independent expert reviewers for their agreement to participate on the scientific panel evaluating the First Street Foundation Flood Model through a formal review of this documentation. The reviewers provided us with critical commentary on the methodology contained within the document, insightful adjustments to be integrated into the flood modeling process, and pushed the overall quality to meet the standards of scientific review. This document represents the final version of the methods that successfully passed the independent review process, in which reviewers read the document and provided critical feedback, the First Street Foundation and modeling partners responded to those comments by updating the methodology document and developing a response memorandum, and all parties convened for formal panel review on February, 24th, 2020. Ultimately, the First Street Foundation, and modeling partners, owes a debt of gratitude for the time and effort the review panel put into ensuring a high quality product was developed in the form of the First Street Foundation Flood Model.

Expert Panel Reviewers:

- **Dr. Witold F. Krajewski:** University of Iowa, Director, Iowa Flood Center
- **Dr. C. Adam Schlosser:** Massachusetts Institute of Technology (MIT), Deputy Director for Science Research, Joint Program on the Science and Policy of Global Climate
- **Dr. James Smith,** Princeton University, Professor, Civil and Environmental Engineering
- Past Research and Modeling Partners: We would additionally like to thank all of our modeling partners and acknowledge the tremendous support we received from the availability of public resources from government entities such as NOAA, USGS, FEMA, and many more such groups at the local level. Coupling this publicly available data with the tremendous wealth of expertise among our modeling partners allowed us to bring together the best available data with some of the best available methodologists in this area. Our hydrological modeling partners, Fathom, are led by Professor Paul Bates and bring with them decades of novel and creative approaches to the development of high precision national and global flood risk hazards. Our climate modeling partners, Rhodium Group, allowed for a partnership with some of the leading researchers in the field of environmental change through the Climate Impact Lab. Chief among those contributors is Dr. Kerry Emanuel who's research on climatic influences on the physics of cyclonic activity is at the forefront of our understanding in that area. And finally, our partnership with Dr. Celso Ferreira and the iFlood Lab at George Mason University gave us access to computational capacities allowing for the creation of high precision flood simulations of past and present coastal storm events.

Table of Contents

Executive Summary	4
Methodology	6
Inland Flood Risk...	6
The Fathom Flood Modeling Framework.....	6
Model Builder.....	6
Hydraulic Model.....	8
Advancement 1: Move to NHDPlus Hydrography	8
Advancement 2: Channel Solver.....	11
Advancement 3: Regionalized Flood Frequency Analysis (RFFA) Updates	13
Advancement 4: Downscaler.....	16
Climate Uncertainty.....	17
Uncertainty in Inland Models.....	17
Inland Current (2020) Hazard.....	17
Hydrological Modelling Within Selected Catchments.....	18
Inland: Future (2050) Hazard.....	21
Climate Model Linking and Change Factors for Fluvial Modelling.....	21
Regionalization of Change Factors	22
Future Fluvial Flooding Execution	23
Future Pluvial Flooding Execution	24
Coastal Flood Risk.....	24
Estimating Peak Water Levels for Flood Risk Assessment.....	26
Joint Flood Probability in Coastal Catchments.....	31
Gulf and East 30 Coasts: Current (2020) Hazard.....	31
Defining the Marginal Distributions	31
Defining the Hazard Catalogue	37
Characterizing the Multivariate Tail Dependence	38
Sampling Event Catalogues	40
Uncertainty in Coastal Models.....	41
Gulf and East Coasts: Future (2050) Hazard	41
Application of Methods to the West Coast.....	43
Historical Analysis	43
Coastal	43

Hydrodynamic Modeling of Historical Storm Surges	44
Inland Historic Flood Events.....	45
Localization of National Model.....	46
Adaptation	46
Gray Adaptation.....	47
Levees	47
Dams	48
Other Gray Adaptation.....	49
Green Adaptation	49
Green Infrastructure	49
Soils.....	50
Coastal Adaptation	50
Cost Distance Analysis.....	51
Hazard Layer Processing	52
Creating Cumulative Statistics.....	52
Interpolation.....	52
Interpolation to Create Hazard Layers.....	52
Cumulative Statistics	55
Discussion and Limitations.....	57
Discussion	57
Limitations	57
References	60
Appendix I. Table of Adaptation Structure Types Included in NFM.....	66
Appendix II. Review and Feedback of Preliminary Flood Models	70

Executive Summary

First Street Foundation (FSF), in partnership with Fathom Global, the Rhodium Group, and Researchers at George Mason University, have collaborated to create a high resolution First Street Foundation Flood Model (FSF-FM). The model has been created with a focused purpose of estimating flood risk for the entire continental U.S. (CONUS), with a specific interest in high resolution risk evaluation at the individual property level. The document that follows this summary is organized around the transparent presentation of the methods used in the development of this model in order to give users a clear understanding of 1) how the model was developed, 2) the strengths and weaknesses of the model, and 3) any potential limitations associated with the techniques and decisions made in the creation of the models. Additionally, the document is broken down into a series of discussions around the actual “flood modeling” process, the inclusion of climate uncertainty and environmental factors in the development of future facing portions of the NFM, and post-processing the results of the models for the development of property level derivative statistics. With that being said, the bulk of the document will be devoted to the process of “flood modeling” which serves as the basis for the calculation of the past, present, and future flood risk for all properties in the CONUS as summarized here:

Historical: Past flooding events are recreated through a catalog of data sources related to actual historic observations in spatial and temporal alignment with the peak impacts of the specific events. These include local stream/river gauge information for the simulation of historical fluvial inland flooding events and documented historic storm characteristics along the coast to model extents and depths associated with storm surge from hurricanes, tropical cyclones, and extra-tropical cyclones. In some cases, these events overlap and will include both storm surge and fluvial outputs for coupling related to the unique nature of the flooding event.

Current Risk: The base inland modeling technique is conceptualized around a flood frequency analysis approach, through the development of a regionalized flood frequency analysis (RFFA) methodology. This approach is conceptually consistent with regionalized predictive methods for modeling flow in areas with missing or poor quality of records and, therefore, allow for the modeling of both gauged and ungauged river and stream networks. Ultimately, the RFFA methodology is the basis for our ability to model flood risk nationally, and importantly, in areas where risk information is relatively hard to come by. This method is combined with synthetic coastal cyclones simulations and observed changes in Sea Level Rise, and associated tidal levels, to estimate risk of flooding in joint-form along coastal regions.

Future Risk: The flood model takes into account changing environmental factors including Sea Level Rise, increasing cyclonic intensity, higher probabilities of cyclone landfall locations at higher latitudes, shifting precipitation patterns, and shifts in river discharge. The manner in which each changing factor is incorporated in the model varies, but the results are probability distribution functions created from a blending of observed, synthetic, and forecasted inputs. Ultimately, the future risk models rely heavily on agreed upon Intergovernmental Panel on Climate Change (IPCC) recommendations related to changing environmental conditions and the primary drivers associated with Representative Concentration Pathway (RCP) trajectory 4.5. This information is explicitly integrated along with an ensemble of global climate models in order to estimate expected flood risk, while allowing uncertainty around factors associated with those estimates.

This report further documents our inclusion of climate uncertainty and environmental factors as central to the modeling of both current and future flood risk. As mentioned above, we do so through the utilization of climate inputs originating from the CMIP5 GCMs and the RCP 4.5 scenario so that the resulting flood hazard layers be deemed as the “most plausible” vs. “worst case scenario” (generally referenced as RCP 8.5). The specific CMIP5 GCM outputs are used in the generation of station specific sea level rise projections (Kopp 2014), in the generation of synthetic hurricane tracks used to simulate storm surge and hurricane related precipitation (Feldmann et al. 2019, Emanuel 2017, Emanuel 2016), and in the generation of National Aeronautics and Space Administration (NASA) Earth Exchange Global Daily Downscaled Projections (NEX-GDDP) that perturbed intensity, duration, and frequency (IDF) curves in addition to river discharge distributions.

The observational records utilized in the creation of the NFM primarily come from two sources: the United States Geological Survey (USGS) and the National Oceanic & Atmospheric Administration (NOAA). From the USGS, river gauge specific discharge values and tidal estuary / river water levels are utilized. From NOAA, tide gauge water level and IDF curves are utilized. Both sources are subject to selection criteria that identifies gauges with sufficient record lengths and accurate datum information for coastal gauges. Where such information is missing, unreliable, or sparse; we are able to implement advancements from the Fathom Model Builder approach documented below as the basis from which our NFM is developed.

In order to make national scale models accurate to the property level, additional steps are performed to improve accuracy. First, care is being taken to identify and include adaptation measures that significantly impact flood risk. Information about these features is taken from a variety of sources, both national and local. Second, a series of scripted Geographical Information System (GIS) operations are also implemented in order to compare generated hazard layers against Federal Emergency Management Agency (FEMA) maps, hazard layers against known adaptation features, and to check the influence of DEM resolution & vintage against hazard layer results. Outputs from these processes were reviewed and irregularities flagged for correction through a detailed and rigorous “review and feedback” process. Third, additional validation is performed against the historical FEMA claims dataset in order to ensure model alignment with areas that have previously experienced flooding. Fourth, in addition to historical claims comparisons, remotely sensed and high water mark data is utilized to check recreated historical flooding extents against observed flooding locations to calibrate model performance.

Three hydraulic / hydrodynamic models are deployed in the creation of the NFM: LISFLOOD-FP for hydraulics, GeoCLAW for coastal storm surge, and ADCIRC-SWAN (ADVanced CIRCulation - Simulating WAves Nearshore (SWAN)) for calibrating GeoClaw outputs in addition to historic storm recreation. Due to computational efficiencies, LISFLOOD-FP and GeoClaw were chosen to execute the thousands of simulations needed to create a national probabilistic model. By combining efficient models with observational data and GCM derivatives, a set of hazard layers are being generated that reflect the climate-adjusted flood risk to the United States in 2020, 2035, and 2050. Due to the uncertainty in climate modeling, 3 sets of hazard layers are being generated to reflect the median expectation from the climate models in addition to both lower and higher possibilities, with the high and low thresholds being quantified as the 25th and 75th percentiles. The quantification and communication of future risk, and this uncertainty, is paramount to the focused intention of this project.

Methodology

Inland Flood Risk

The Fathom Flood Modelling Framework

The Fathom flood modelling framework consists of two primary components, namely (1) a model builder, which uses a number of different data sources to automatically construct hydraulic models of a specified geographic region; and (2) a hydraulic model, which executes the models constructed by the model builder by solving a simplified form of the shallow water equations in two dimensions across the model domain. Both of these components have been extensively documented and validated in leading academic peer-reviewed journals (for key references of the hydraulic model see Bates and de Roo, 2000; Bates et al., 2010; Neal et al., 2012; Neal et al., 2018. For key references of the model builder see Sampson et al., 2015; Smith et al., 2015; Wing et al., 2017. All papers have been made open-access and are available to the general public free of charge). The purpose of this section is to provide a high-level overview of the material covered in the aforementioned papers, while providing details of any changes and advancements made since their publication.

Model Builder

Conceptually, the Fathom framework is different from many earlier large-scale flood models because it **does not** employ a rainfall-driven hydrological model to derive boundary conditions for a hydraulic model. The decision to avoid such a model cascade was taken in recognition of the decades-long struggle within the field of hydrology to create behavioral, extreme-flow hydrological models in ungauged catchments (Bloschl et al., 2013). Due to the limited density of river gauges, any national scale model would necessarily consist of a patchwork or river reaches characterized by such models. The alternative to rainfall-driven hydrological-hydraulic model cascades is to use flood frequency analysis of river gauge records to characterize extreme river flows and generate boundary conditions of the hydraulic model. Flood frequency analysis involves the fitting of a curve to the observed tail of a flow distribution (typically gamma or GEV) from a river gauge. Once the curve is fitted, it is possible to estimate the flow associated with any return period. The problem of ungauged catchments remains; however, given the large database of river gauge records available in the U.S. (approximately 9000, 6000 of which have adequate record length and quality for use) it is possible to use regionalization methods to assign curve typologies from gauged catchments into ungauged catchments based on catchment characteristics (see Smith et al., 2015 for original paper; subsequent updates detailed below).

Currently, the ability to estimate flood flow frequency curves in ungauged catchments in the US is a high priority for the USGS and is directly identified in their Guidelines for Determining Flood Flow Frequency Bulletin 17C as a major focus for future research (USGS, 2019). Bulletin 17C does identify two common methods that are used in this process per 1) a regionalized generalized least squares regression approach that allows for a localized estimation of the flow frequency information at ungauged sites (see Tasker and Stedinger, 1989) and 2) rainfall-runoff models (see Pilgrim and Cordery, 1993; McCuen, 2004). It is fairly well documented that these methods

of estimation contain considerable error, however, they are also considered state-of-the-art in an area that has been identified as needing significant methodological attention. To that point, the Fathom model builder incorporates a regionalized information approach through the development of a Regionalized Flood Frequency Analysis (RFFA), which includes the estimation of missing data from ungauged catchments with information from catchments of similar. Ultimately, it is not known how the Fathom model builder compares with the methods documented by the research in Bulletin 17C, but it should be noted that this model does operate within a reasonably similar framework.¹

As a result, the Fathom model builder was developed around the concept of flood frequency analysis rather than a rainfall-driven hydrological model cascade. The model builder performs the following tasks for each geographic area of simulation in an automated manner:

1. Assembles relevant input datasets into harmonized resolution and projection grids (terrain, hydrography, flood defense locations and standards, rainfall and climate characteristics, soil types).
2. Decomposes river network into discrete reaches for simulation using catchment-scale analysis using logic rules based on upstream area change thresholds and reach length limits (i.e., new reaches are triggered when the upstream area has changed significantly or when a maximum reach length condition is met).
3. Calculates fluvial boundary conditions for each river reach (e.g. river discharge at inflow points and water level and downstream boundaries).
4. Calculates pluvial boundary conditions using intensity-duration-frequency (IDF) curves.
5. Estimate river network characteristics (e.g. river channel widths, depths, and defense standards).
6. Constructs high-resolution (~30m) hydraulic model input files for execution to enable simulation of all reaches for both fluvial and pluvial hazards across the desired range of return periods.
7. Constructs “Slurm” server-management files to control batch execution of hydraulic models (as tens of thousands of discrete simulations are undertaken across a domain the size of the U.S.).
8. Assembles the individual reach simulation result files into contiguous hazard layers.
9. Re-project the hydraulic simulations to the final ultra-fine resolution terrain model (~3m).

The stages above are explained in more detail in the aforementioned references, particularly Sampson et al., 2015 and Wing et al., 2017. However, several key advancements have been

¹ We have tried to address sampling error based on the length of the observed records by pooling together suitably homogenous catchments and combining their respective records. However, uncertainties related to the fitting of extreme value distributions will become significant at higher return periods. In the future, it may be possible to attempt to account for this uncertainty by sampling from the GEV parameter spaces.

made in the development of the NFM documented herein, and these are detailed under the “Advancement” headings below.

Hydraulic Model

The Fathom hydraulic model is a raster-based two-dimensional shallow water model capable of simulating the flow of water over a high-precision digital elevation model (DEM). A novel simplified implementation of the shallow water equations (Bates et al., 2010) yielded an algorithm for which the minimum stable time step scales linearly with decreasing grid size, rather than quadratically as had been the case with previous diffusion wave formulations (Hunter et al., 2005). Furthermore, improvements to the software implementations of shallow water algorithms through vectorization and OpenMP parallelization on central processing units (Neal et al., 2009, 2010, 2018) have yielded dramatic reductions in model runtimes totaling several orders of magnitude relative to original serial variants. The model represents channels using a 1D “subgrid” formulation (Neal et al., 2012) that enables river width to be decoupled from model grid scale and therefore allows any river size to be represented within the model. An extended slope-dependent form of the constant-velocity routing method (Sampson et al., 2013) in conjunction with a Froude-limiter ensures that the model solution remains stable in areas where the shallow-water equation assumptions of gradually varying flow are violated (e.g. steep or discontinuous terrain). All hydraulic simulations within this project have been undertaken on a 1 arc-second (~30m) grid.

Advancement 1: Move to NHDPlus hydrography

A new hydrography for the contiguous U.S. was generated by means of the National Elevation Dataset (NED) (Gesch et al., 2009), which is a high precision ground surface elevation data, and the National Hydrography Dataset (NHDPlus) (Simley et al., 2009), a feature-based database that interconnects and uniquely identifies the stream segments or reaches that make up the U.S.’s surface water drainage system. The new hydrography (UShydro) captures main channels and river streams at ~90 m (at the equator) resolution and extends the current coverage of the NHDPlus data set beyond its coverage. The new data set was created using a framework which automatically conditions the DEM and calculates flow direction and flow accumulation maps, taking into account existing inland basins in the U.S. The automatic computational framework allows replication of this methodology with different sources of terrain and river vector data sets. It’s anticipated that the UShydro will expand the current research carried out on river hydrology in the contiguous U.S. The methodology used in the incorporation of UShydro relied on the National Elevation Dataset (NED) (Gesch et al., 2009) at ~30 m (at the equator) as the terrain source. The NED dataset was subsequently upscaled to ~90 m (at the equator) using bilinear interpolation. Additionally, UShydro used the National Hydrography Dataset (NHDPlus) (Simley et al., 2009) to geolocate main rivers and channels. In particular, the entire NHDPlus database was downloaded from the United States Geological Survey (USGS) servers in a stand-alone file in Geodatabase format. In order to facilitate the data processing, the Geodatabase was filtered and only the “NHDFlowline_Network” features were extracted in a stand-alone file in GeoPackage format. From the resulting GeoPackage file, the attribute “DivDASqKm” or Divergence-routed drainage area was extracted as a raster file using the “gdal_rasterize” program from the GDAL geospatial library (www.gdal.org).

Both the upscaled NED terrain data and the rasterized Divergence-routed drainage area were re-projected from NAD83 projection to WGS 84. Also, in order to facilitate the data processing, the

raster files were tiled into 5x5 degree tiles in both datasets, resulting in a 72 tile mosaic for the entire U.S. It is important to mention that it was decided to process the data in this form in lieu of processing the entire datasets at once due to computational expense considerations. The tiling of the data simply allows for a more efficient management and processing of the raster files, but the native resolution of the data is preserved in the tiling process.

The flow direction map was created using an algorithm that indicates the direction of the lowest elevation within a 3x3 cell kernel (O'Callaghan and Mark, 1984). Even though the resolution and accuracy of the NED dataset was enough to let the algorithm identify where the main rivers and channels are, in some cases a second source of data was used (such as in the case of the divergence-routed drainage area). The divergence-routed drainage area corresponds to the drainage area of a particular cell. Thus, the headwaters cells in a basin have a value of 0 km² while the outlet has a value corresponding to its drainage area (e.g., Colorado River 618,000 km²). The divergence-routed drainage area was directly burned into the NED tiles to create new synthetic elevation following the equation here:

$$E = \frac{10}{\frac{\log(N)}{\log(1.5e^{-2})} - 99}$$

Where, E is the new value to be burned in the NED dataset and N is the drainage value obtained from NHDPlus. This procedure of burning main rivers and channels in a DEM is referred to as DEM Conditioning and it has been widely used to produce flow direction and flow accumulations maps (Yamazaki et al., 2019).²

The previous procedure successfully captures main rivers and channels from the NHDPlus database in addition to channels not depicted by the NHD in most of the rivers flowing within the U.S. However, the NHDPlus database does not contain complete information beyond the U.S. in trans-national rivers such as the Columbia, Rio Grande, and Colorado Rivers which share territory with Canada and Mexico. To tackle this issue main channels and rivers from NHDPlus were fused with MERIT Hydro (Yamazaki et al., 2019) to complete the missing information for trans-national

² The equation provides new values for terrain elevation (in meters) along the channels based on the drainage area as input (km²). The divergence-routed drainage area in NHDPlus provides, indeed, upslope areas, however, they can't be used directly to produce a hydrography as it presents channel connectivity issues. To solve the connectivity issues in NHDPlus, the solution is to "burn" NHDPlus into NED to obtain a new hydrography. The process of burning channels into a DEM has been very well studied, basically, it assigns "new" elevation values in the DE. Our methodology used the equation mentioned before to obtain sensible elevation values. For example, in a cell with divergence-routed drainage area (from NHDPlus) with 700,000 km² the equation will produce an elevation of -95.28 m. As the drainage area increases in the downstream direction, the new elevation value will change accordingly. The equation was needed as it helps to handle very high drainage area values. Our methodology used D8 instead of D_trig as most continental-scale hydrographic (HydroSHEDS, MERIT Hydro) uses the D8 scheme. More complex flow direction methods (D16, D-infinity, and D-trig) can be considered perhaps in a post-processing stage.

rivers. Additionally, the same fused vector lines were also used to identify center lines in the Great Lakes area.³

With the NED dataset conditioned using NHDPlus and MERIT Hydro data, a flow direction map for every tile using the D8 method (O'Callaghan and Mark, 1984) was used. To complete this task the RichDEM library (richdem.readthedocs.io) was incorporated into the methodology. Unlike flow directions that can be easily calculated due to the use of 3x3 cell kernels, flow accumulations cannot be calculated so easily. Resulting flow direction tiles require an efficient algorithm which efficiently connects flow direction tiles when calculating the draining area as rivers are mostly contained in different tiles. To tackle this issue, a parallel flow accumulation algorithm with efficient memory management was used (Barnes, 2017).⁴

The results of the move to an NHDPlus hydrography approach are documented in Figure 1. The figure highlights the performance of UShydro at different river outlets in the U.S. and indicates its suitability for accurately capturing river channels under the most common, and sometimes problematic, issues associated with the ways in which these channels are reflected in the original dataset.

- Fig 1a shows the termination of the Mississippi River around Pilottown, Louisiana
- Fig 1b shows the Rio Grande around the Villa Pancho area in Texas
- Fig 1c shows the Sacramento and San Joaquin Rivers around the Rio Vista area in California
- Fig 1d shows the Colorado River termination in the Northeast part of Baja California

Given the results presented in Figure 1 and the methodology outlined here, a new hydrography for the contiguous U.S. was generated by means of the National Elevation Dataset (NED) and the National Hydrography Dataset (NHDPlus). The new data set extends the current coverage of the NHDPlus for trans-national rivers, has a resolution of ~90m (at the equator), and is distributed in GeoTIFF format using 72 tiles of 5x5 degrees which mosaic the entire contiguous U.S. with flow direction and flow accumulation. This standard framework allows for a replicable approach that can be easily used with other data sources of terrain elevation and vector data, and the framework is computationally efficient as the entire computational chain took ~6 hours to obtain flow accumulation map.

³ Endorheic or inland basins are rivers that normally retain water and do not allow outflow to other external bodies of water. It is essential to identify those as an incorrect representation, or the hydrography could result in an improper drainage area for a nearby river. This problem arises as the inland basin could be seen by the flow direction algorithm as a new channel of a main river, which is not the case. To tackle this issue in UShydro inland basin termination from the NHDPlus were extracted, through a feature called "Sinks," and assigned as NODATA value in the Conditioned NED.

⁴ All steps mentioned before were grouped together in an automatic computational framework to facilitate debugging and to allow the use of different source of datasets. The entire framework successfully took ~6 hours to obtain flow accumulation for the entire U.S. on an Intel(R) Xeon(R) CPU E5-2650 v3 @ 2.30GHz, 64GB Ram.

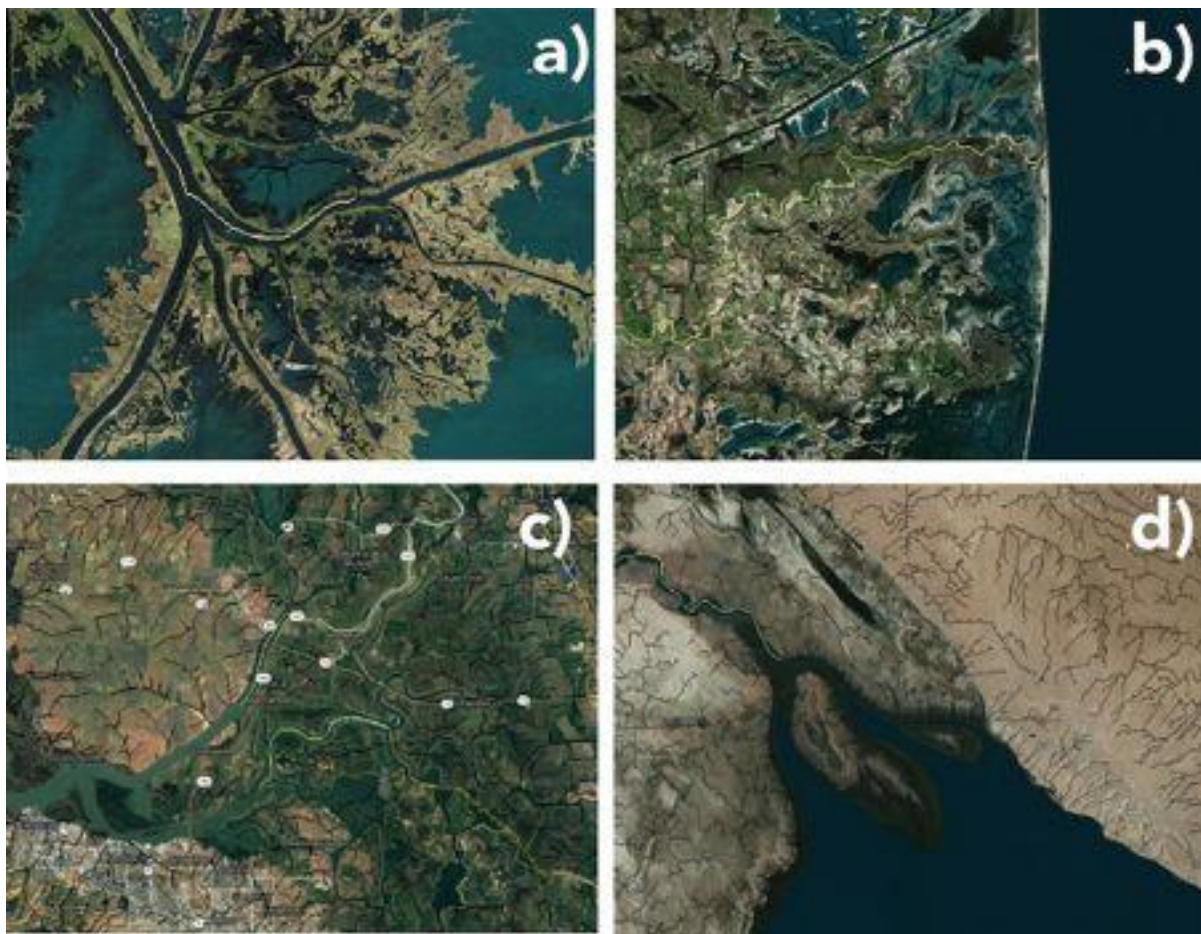


Figure 1: Performance of UShydro at different US river outlets a) Mississippi River b) Rio Grande c) Sacramento River and San Joaquin River d) Colorado River.

Advancement 2: Channel Solver

A critical control on how water moves through a landscape for any riverine model is the definition of the river channel network. In the case of fluvial flooding, the river channel is usually the main conveyor of discharge and will interact with the floodplain in a complex manner as water moves both from and to the channel in a manner dependent on local variability in topography and friction. Even in the case of other types of flooding, such as pluvial and fluvial, the role of channel conveyance can be significant. How channels are represented in a regional scale flood model will therefore influence inundation simulations, particularly at low return periods where small changes in river conveyance can have a disproportionately large impact on the simulated flooding. For traditional hydrodynamic modelling, the quality of river bathymetry data is key to accurate simulation of the relationship between discharge and water level. However, since high-quality versions of such data are not available for national scale modelling contexts, an approximation must be used that best represents the water surface elevation and discharge relationship given the available data. The framework used in approximating this relationship is a 1D gradually varied flow assumption to estimate depth along the channel network.

This is governed by the equations:

$$\frac{\partial h}{\partial x} = \frac{(S_0 - S_f)}{1 - Fr^2}$$

Where h is depth, x is distance downstream, Fr is the Froude number, S_0 is the bed slope and S_f is the friction slope. We assume that the river channel is rectangular, and that friction is represented by Manning's equation such that friction slope is found via:

$$S_f = n^2 \left(\frac{Q}{wh} \right)^2 \left(\frac{wh}{2h + w} \right)^{-4/3}$$

Where n is manning's roughness coefficient w is the channel width and Q is discharge. The Froude number of the channel Fr is then

$$Fr = \frac{Q}{w\sqrt{gh}}$$

Where g is acceleration due to gravity. For any set of bed elevations (z) the gradually varied flow profile is found by solving these equations using the Runge-Kutta method. A first-order approximation of riverbed elevations (z) is made by subtracting depth h_{bf} from the bank height profile, where pixelwise river depths are estimated by using the Manning's equation rearranged for depth

$$h_{bf} = \left(\frac{nQ_{bf}}{S^{1/2}w} \right)^{3/5}$$

Where S is water surface slope approximated by the DEM slope and Q_{bf} is calculated using the RFFA for an assumed bankfull discharge return period (typically 1 in 2 years). Due to backwatering effects these initial bed elevations will result in an overprediction of the water surface elevation at bank full discharge for all river reaches where diffusion of shallow water wave properties are important (most lowland rivers and deltas). Thus, we seek bed elevations that minimises the least squares difference between the desired water surface profile at bank full discharge and that simulated by the gradually varied flow solver. This can be done via least squares nonlinear estimation; however, the computational cost of optimising all bed elevations is too high for continental scale application meaning a simpler bed nudging approach is used in practice. This nudging involved the following steps:

- i) solve for the water surface profile given the initial bed estimate from Manning's equation,
- ii) compute the differences between bank elevations and water surface elevations from step 1,
- iii) apply the differences between the bank elevations and water surface from ii to the bed elevations,

- iv) recompute the water surface profile, and v) repeat ii, iii, iv once more to get a final set of bed elevation estimates and water surface profile errors.
- v) impose the water surface estimates from step iv as the bank heights or calculated defended bank heights for greater return period discharges using the gradually varied flow solver when flood defences are known to exist.

The result of the above process is channel bed and bank estimates that are consistent with both the DEM and the return period discharges at which overbank flow is to commence. Thus, the method creates a set of channel network geometries that behave according to the assumptions of bankfull return period imposed by the model user.

Advancement 3: Regionalized Flood Frequency Analysis (RFFA) updates

The Fathom-US model uses a regionalized flood frequency analysis (RFFA) methodology to provide lateral inflows to the hydraulic model at desired return period magnitudes. Although not without its own uncertainties, the use of direct gauge observations in order to remove the need for atmospheric and hydrological models in such instances has been used in both the academic literature and in industry (e.g. Keef et al. 2009) as an attempt to reduce the introduction and propagation of errors from a variety of sources associated with rainfall and hydrological modelling applications. For instance, Sampson et al. (2015) highlights that precipitation data quality is a significant issue. They state that although a number of global precipitation data sets do exist, based on satellite data (e.g. Huffman et al., 2007; Joyce et al., 2004), model reanalysis (e.g. Dee et al., 2011) or gauge records (e.g. Xie et al., 2007), these products are known to have limitations that are of particular concern to flood modelling including spatially variable biases (Kidd et al., 2012), poor correlation with ground gauges at short (~daily) time scales (Chen et al., 2014; Cohen Liechti et al., 2012), poor representation of spatial variability over smaller catchments (He et al., 2009) and a tendency to underestimate heavy rainfall (Chen et al., 2014; Gao and Liu, 2013). Sampson et al. (2014) evaluated the effect of these differences on flood risk using a cascade model structure that replicates an insurance catastrophe model and found estimates of monetary loss from flooding to vary by more than an order of magnitude depending on whether the cascade was driven with gauge, radar, satellite, or reanalysis data. Similarly, it is well known that extreme flows in ungauged catchments remains a key challenge to the field of hydrology (Bloschl et al., 2013). Therefore, the discharge estimation used by Fathom-US is based upon direct observations of flows, linking extreme flow behavior in gauged catchments to estimate what gauged observations would likely be in ungauged catchments. This process involves taking flow information from gauged catchments and applying those to ungauged catchments that are similar in nature the gauged catchments using a series of indicators related to grouping catchments based on a set of predetermined characteristics.

The main forcing required by Fathom-US is a set of inflow boundary conditions derived from RFFA (Smith et al., 2015). The RFFA utilizes a hybrid-clustering approach in conjunction with a flood-index methodology. The methodology used here is similar to that employed by Smith et al. (2015); however, it has been updated owing to the far denser network of gauges in the U.S. in comparison to global RFFA. The method employed consists of two steps: firstly the estimation of an index flood is undertaken, followed by the scaling of this index-flood using growth curves that describe the relationship between the index flood and extreme flow magnitudes. The index flood

used here is the mean annual flood, with the method used to define the mean annual flood differing from that employed by Smith et al. (2015). To best utilize the far denser USGS gauge network, gauges were partitioned in space to estimate the index flood. Therefore only gauges from the same river or hydrological zone were used in the estimation of the index-flood. However, for the estimation of the growth curves, gauges were pooled together across all catchment zones—this was undertaken to avoid temporal sampling errors.

For the first stage of this procedure, the estimation of the index or scaling flood, gauges are partitioned in space, using both a river identification number and the USGS hydrologic unit data (HUC zones) to place gauges into their respective hydrological groups. The method used here to estimate the mean annual flood uses a hierarchical system to link observed mean annual flood estimates to upstream areas for individual rivers and HUC zones. The method proceeds as follows: firstly, for individual river reaches, the procedure checks whether there are a sufficient number of gauges and a sufficient number of gauge years present. It also checks whether a sufficient sample of the individual river is available; this is defined by checking whether minimum and maximum area thresholds are satisfied. The gauge number, gauge record length, and minimum and maximum area thresholds are pre-defined parameters which when met allow for power laws to be fitted between upstream areas and discharge/index-flood. For gauges on an individual river, when sufficient record lengths and gauges are present and the river is adequately sampled when it is both small and large, individual power laws are stored to estimate discharge across any part of the river.

For other rivers, that do not have either sufficient gauge coverage or sufficient coverage in space, gauges are pooled together with gauges from other rivers according to their respective HUC zones. The procedure then uses a hierarchical system moving from small HUC zones to large HUC zones (Figure 2), checking whether the same threshold parameters described above are satisfied. When the threshold parameters are met for an individual HUC zone, the relationship between upstream area and discharge/index-flood is defined again using a power law. If the parameters are not met, the procedure moves up to the next level HUC zone, pulling in more gauges, with the procedure continuing until the parameters are satisfied.

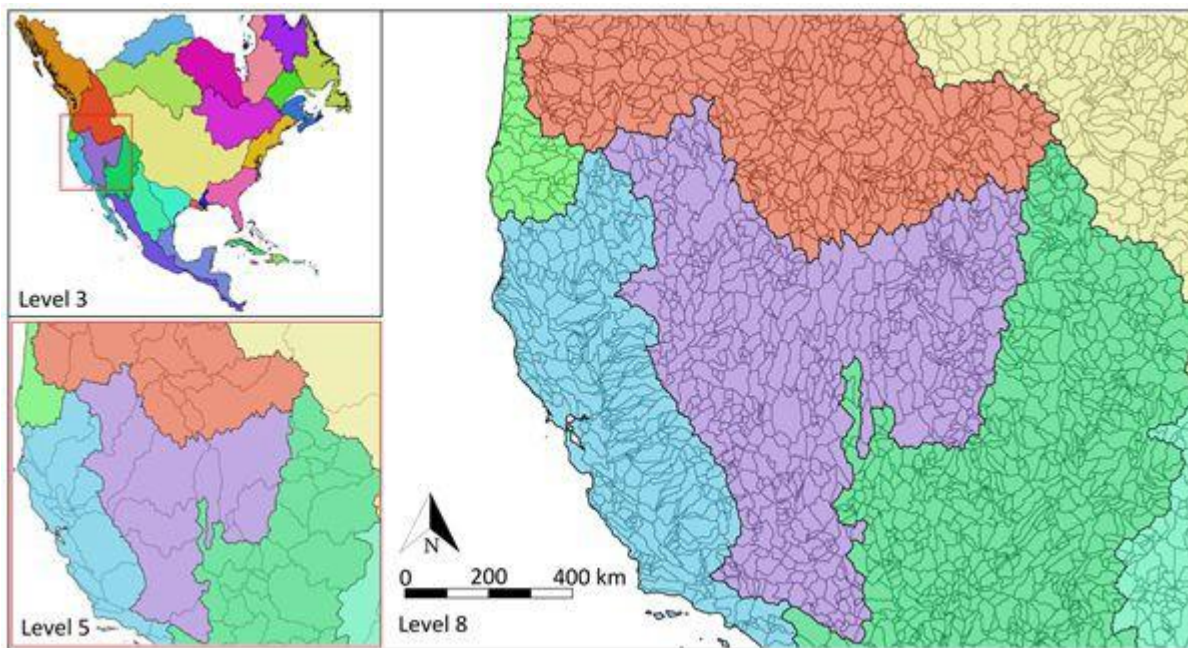


Figure 2: An example of the progressive discretization of catchment data across 3 levels of complexity along the west coast of the U.S.

For the second part of the RFFA procedure, the methodology uses the growth-curve procedure outlined by Smith et al. (2015). As discussed above, the method does not partition gauges in space in an attempt to limit temporal sampling errors. Instead, the method uses catchment descriptors of climate class, upstream annual rainfall, and catchment area and proceeds as follows: data from available river gauging stations are subdivided into the five main categories of the Koppen-Geiger climate classification (Kottek et al., 2006). A clustering method is then used to pool together suitably homogenous catchments; the clustering method used for regionalization is a combination of Ward's algorithm and k-means clustering (Ramachandra Rao and Srinivas, 2006). Extreme value distributions or flood frequency curves are then fitted to each of the pooled groups, providing relationships between the index-flood described above and extreme flows for any recurrence interval, for each of the pooled regions. When combined with the index flood, MAF, the flood frequency curves or growth curves provide a basic means of flood estimation for any region (Meigh et al., 1997; Zaman et al., 2012).

Smith et al. (2015) applied these methods to a global data set of over 3000 gauging stations, sourced from the Global Runoff Data Centre (GRDC) and from the USGS stream gauge network (<http://nwis.waterdata.usgs.gov/nwis>). Although the ability of this approach to provide detailed, localized discharge estimates is limited by the simplicity of the methods, significant uncertainties in the discharge record, and the complexity of anthropogenically modified river systems, these methods have demonstrated skill in providing first-order discharge estimates in data poor regions (Padi et al., 2011; Smith et al., 2015). Estimating extreme discharge via this method is subject to significant uncertainty, as is the case with all generalized global methods; although global mean errors of ~80% were reported by Smith et al. (2015), far larger errors were also reported, in some cases >300%. Even though the errors in estimating flow in the U.S. are anticipated to be far lower,

due to far denser gauging/sampling, significant errors will still exist. Because such errors are currently unavoidable in large scale discharge estimation, discharge estimation bias is explicitly accounted for in the modelling framework by scaling channel conveyance within the hydraulic model according to the estimated bankfull discharge.

Although the RFFA can provide good estimates of return period discharge for rivers and streams, it does not allow for accurate discharge estimation in small channels where flooding is generally driven by intense local precipitation. For small channels (catchment area <50 km²), an alternative method is required, with flow generated by raining directly on to the DEM (“rain-on-grid”). Therefore, in addition to the estimation of discharge, methods were also required for the estimation of extreme rainfall. The relevant design rainfall intensities were taken directly from the NOAA IDF database. The “rain-on-grid” approach or “direct precipitation” is the term used to describe the direct addition of water volume to each pixel of the model at each timestep according to the design rainfall hyetograph (i.e. simulating rainfall). An allowance for infiltration is made based on soil type using a simple Hortonian infiltration model; in urban areas this allowance is based on the assumed/researched design rainfall capacity. These volumes are then moved across the grid using the shallow water equations as normal. In areas that are too steep for the shallow water equations to operate, a slope-dependent variable velocity rainfall-routing scheme is applied to move water downslope until the slope gradient decreases. The basis for this approach is predicated on the work presented in Sampson et al. (2012).

Design discharges for ten different recurrence intervals (5, 10, 20, 50, 75, 100, 200, 250, 500, and 1000-year) were calculated for all river reaches utilizing the methods detailed above. In reference to the relationship between recurrence intervals longer than the span of the historically observed data, the Fathom RFFA method pools together catchments/gauges into homogenous groups. Growth curves are then derived from these groups by normalizing the extreme values for each gauge by their mean annual flow. Therefore, instead of the absolute discharge values, the extreme values for each gauge are a function of Discharge/Mean Annual Flow. Each pooled growth curve typically contains hundreds of years of data.

Advancement 4: Downscaler

To downscale the raw 1/3 arc second Fathom-US model output onto finer resolution terrain data (~3m), a hydraulic downscaler was used. The downscaler uses water surface elevations from Fathom-US which are then projected onto the higher resolution terrain data, it therefore assumes that the relative heights between the lower and higher resolution digital elevation (DEM) data are consistent. The downscaler procedure is as follows: firstly, the water surface elevations at 1/3 arc second are taken from the Fathom-US model. To allow inundation to propagate out from the edge of the coarse resolution data, the model water surface elevations at the edge of the simulated inundation footprint are extended by 1 cell. The coarse resolution, extended water surface elevations are then resampled to the same resolution as the high-resolution DEM, using bilinear resampling. This yields a water surface elevation mask and a high-resolution DEM, both on the same grids; the DEM values are then taken away from the water surface elevation data, where the water surface elevation data are non-zero. Resulting values that are less than zero are set to zero, yielding a new high-resolution inundated depth layer. To avoid discontinuities at the edge of the simulated floodplain related to the extension of the simulated water surface elevation mask, an isolated depth mask is applied. This identifies all cells that are disconnected from the floodplain, using a connected cell threshold of 36, corresponding to 4 cells in the coarse resolution

data; all water bodies in the high resolution depth data that are not connected to water bodies by more than this value are set to zero.

To this point, the document has detailed the base Fathom Model Builder from which the hydraulic models used to create hazards are based. As an additional consideration, climate uncertainty is included in the modeling process as a way of understanding current uncertainty in the modeling process associated with recent environmental change factors, as well as future projections based on agreed upon RCPs. The sections that follow, detail that uncertainty and how it has been included in the development of the current and future hazards from the process presented above.

Climate Uncertainty

The NFM has been developed to explicitly account for climate uncertainty in a way that attempts to reflect current and future changing environmental factors associated with the mechanisms by which flooding occurs naturally. The factors taken into consideration as non-static climate inputs include: sea level rise, changing hurricane intensity and landfall locations, changing hurricane precipitation patterns and impact to river discharge landfall locations, and changing non-hurricane precipitation patterns and impact to river discharge. Additionally, the NFM is created through an approach that allows for the incorporation of uncertainty in both inland (fluvial/pluvial) and coastal models (fluvial/pluvial/tidal/surge) in a way that allows for the consistent communication of risk as it relates to those changing factors.

Uncertainty in Inland Models

In the inland context, the hazards produced following the procedures documented throughout the remainder of the document incorporate climatological changes by incorporating synthetic hurricane tracks and precipitation. The principle here is to update the observed climatology that the current discharge model uses. The process used to accomplish this will be to extract the data for relevant time periods from an ensemble of 21 GCMS, run them through the sample HBV catchments discussed in below, and then produce flow frequency curves for both the observed and the current climatologies. The differences between these flow frequency curves, for each of the model ensemble members and each of the sample HBV catchments, will then be used to perturb original discharge models.

Inland: Current (2020) hazard

To update the model framework detailed above, and in order to account for climatological changes that have occurred over the duration of the USGS and NOAA derived observational boundary conditions, a climate model ensemble will be used, in conjunction with synthetic hurricane tracks and precipitation. The process used here will be to run an “observed” and a “current” climatology through a set of representative rainfall-runoff models across the U.S. This is done in an effort to update the observed climatology that the current Fathom discharge model uses. The “observed” time period will be the 1980-2010 period and the “current” will be the 2010-2030 period. The process used here will be to extract the data for these time periods from an ensemble of 21 GCMS, run them through the sample Hydrologiska Byråns

Vattenbalansavdelning (HBV) catchments discussed in more detail in the subsequent sections, and then produce flow frequency curves for both the observed and the current climatologies. The differences between these flow frequency curves, for each of the model ensemble members and each of the sample HBV catchments, will then be used to perturb the existing Fathom discharge model.⁵ The process is detailed in Figure 3.

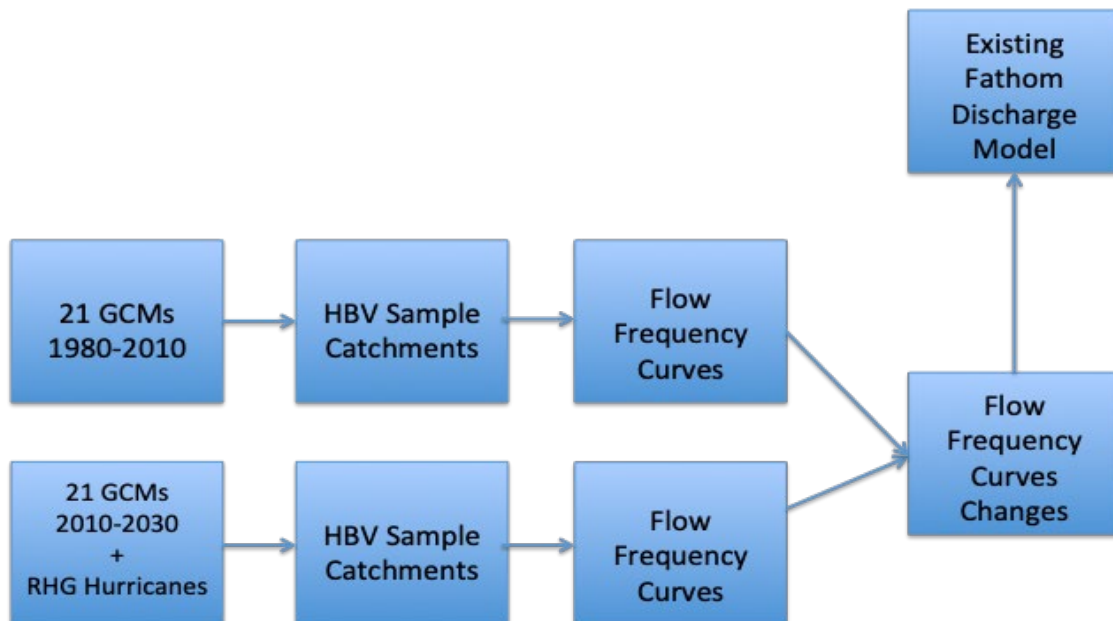


Figure 3. Process for the creation of the climate adjusted inland current model.

Hydrological modelling within selected catchments

Inferring change factors of discharges between current and future scenarios in as many places as possible requires a robust regionalization approach, which in turn needs a representative selection of various catchment characteristics, including historical discharge time-series simulated using a well-calibrated hydrological model.

A total of 147 hydrological basins (Figure 2, above) representing rivers of various sizes and discharge magnitudes were selected across nine different Koeppen-Geiger climate zones (Figure 4), including 23 representative coastal basins. For most basins, a record of observed discharges of at least 30 years was available and used for calibration of a lumped HBV hydrological model.⁶

⁵ HBV was chosen as it has been extensively used in climate impact studies across a wide variety of catchments and scales (Akhtar et al., 2008; Bergström et al., 2001; Cloke et al., 2013; Hinzman and Kane, 1991; Seibert, 1997; Smith et al., 2014; Teutschbein et al., 2011). It is also computationally efficient which is vital when carrying simulations at these scales and with multiple scenarios and models. HEC-HMS is a good suggestion; it would be possible to run models with HEC-HMS also in the future and check that the same conclusions and results are produced."

⁶ The hydrological model is not being used to simulate floods everywhere. A regionalized flood frequency analysis is used to derive the input flows for the hydraulic model framework. The run-off modelling undertaken here is used to derive perturbation factors for the existing discharge model. The absolute discharge values coming out of the calibrated run-off models, which would undoubtedly be subject to significant uncertainty, are not used. We instead only use the relative changes between simulated time-horizons.

The simple conceptual HBV hydrological model (Bergstrom, 1992; Seibert and Vis, 2012) was chosen because of its flexibility, computational efficiency, and proven effectiveness under a wide range of climatic and physiographic conditions. For each selected basin, HBV was set up and parameterized using the global regionalized parameterization provided in Beck et al. (2016). The model uses a total of 14 parameters and requires only daily precipitation and daily minimum and maximum temperature as forcing data to simulate most components of the hydrological cycle (e.g. evaporation, groundwater, soil moisture, snow water equivalent, etc.) needed to obtain output discharge. HBV was set up to simulate historical discharge time-series at river locations of outlet points of all selected basins. HBV forcing data for each basin were taken from the Daymet data product (<https://daymet.ornl.gov/>), which is derived from a collection of algorithms designed to interpolate and extrapolate from daily meteorological observations to produce gridded estimates of daily weather parameters, including minimum and maximum temperature and precipitation, produced on a 1 km² gridded surface.⁷

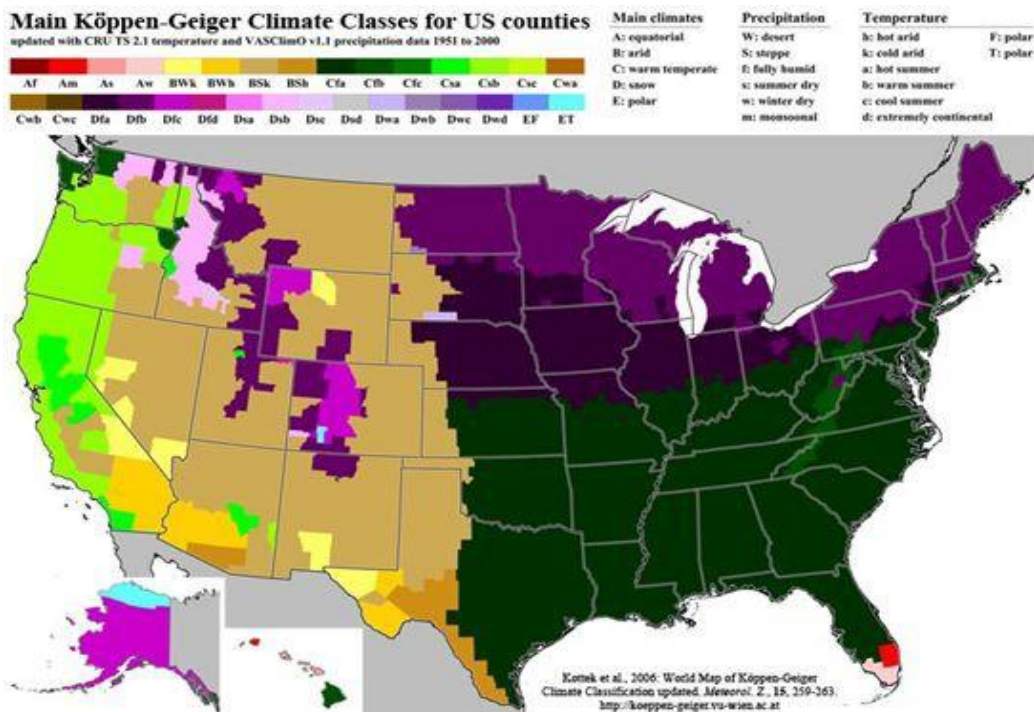


Figure 4: Koeppen-Geiger climate zones across the Continental US
(Source: <http://koeppen-geiger.vu-wien.ac.at/usa.htm>).

⁷ HBV has been tested early on for its performance in Arctic basins and basins affected by significant snowmelt processes. The routine which calculates snowmelt and refreezing is based upon a simple degree day method. A threshold temperature defines the temperature for snowmelt. This threshold temperature also determines if the precipitation will be treated as rain or snow and thus snow accumulation can be simulated. During spring melt, the threshold temperature functioned to control the initiation of simulated snowmelt. Hinzman and Kane (1991) found that the model functioned well but is sensitive to the threshold temperature, TT, and a parameter in the transformation function, MAXBAS. These parameters need to be adjusted to reflect snowpack properties which vary from year to year. The initiation of melt could be controlled by TT and the amount of snow damming is affected by MAXBAS. To account for these parameter sensitivities, and sensitivities of other parameters, we opted to run HBV in an uncertainty framework by computing thousands of simulations for each basin selected, with each simulation using different parameter set values.

Since each basin behaves differently, calibration was performed separately for each. For each basin, a set of model parameter values were generated randomly around the closest validated parameter set provided in Beck et al. (2016) and 2000 realizations of HBV models were performed. This produced a range of discharge time-series for each basin. 63% of the basins included the observed discharge within their simulated range for more than 90% of the time over the total observed record length, with an average of 86% across all selected basins (Figure 5). In almost all cases, HBV simulated the expected discharge within an acceptable range (Beven, 2006) on an average 11600 days out of 13500 days. Unsurprisingly, lower performance was generally observed in flashy basins in semi-arid climate and in snowmelt dominated high-latitude basins. There was no notable difference between coastal and inland basins simulated. Additionally, separating out high flow periods for assessing the model did not significantly change performance.

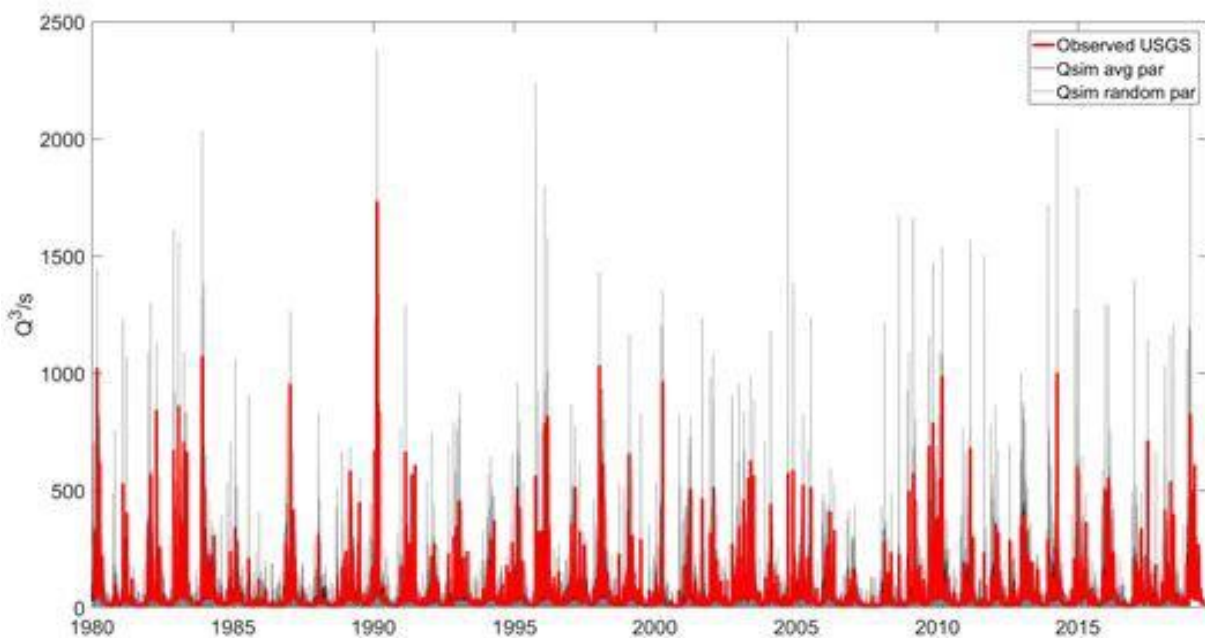


Figure 5: HBV-simulated discharge ranges over a time period of 38 years (1980-2018) for an example basin (USGS 02424000 CAHABA RIVER AT CENTREVILLE AL.).

For simulating current and future change scenarios using the CMIP5 GCMs, the best performing HBV model was selected for each basin using the Nash-Sutcliffe Efficiency (NSE) coefficient, a well-known measure used to assess the predictive power of hydrological models. As an important consideration, uncertainty in the run-off modelling component of the model cascade isn't being undertaken. Instead we select the best performing HBV model based on its performance under the conditions of current climate and with respect to the NSE coefficient. Future iterations of this process will take the time to better account uncertainty in the current climate and potential alignment with future projections. However, to account for the likely situation of an acceptable model parameter set not performing well in future climates, we first looked for behavioral model parameter sets in the two thousand simulations for each basin using gauged discharge records. Given that we're unable to explore uncertainty in the hydrological modelling component, an assumption here is that models performing well under current climate will perform in a satisfactory manner under future climate scenarios. This procedure focused on only retaining those model

parameter sets of the behavioral sets that perform best above the 99% percentile, so it is focused on high flows. Additionally, A Kendall trend test is used to uncover temporal trends in the data. Gauge records with significant trends have not been included within this analysis (after Quinn et al 2019). Further tests search for sudden shifts in the record time series (e.g. due to gauge movement) and again, records are removed if they fail this test.

Inland: Future (2050) hazard

Simulation of future inland flooding, away from coastal regions where compound flooding is not a factor, will follow a more simplified methodology than that used in coastal regions. For the future inland fluvial simulations, output from climate models will be used to generate estimates of current and future discharge, from which discharge “change factors” will be generated. An ensemble of climate models will be driven through a set of representative, calibrated, rainfall-runoff models (Figure 6). The run-off model used will be HBV, a lumped hydrological model that has been widely used in climate impact studies. The assumption used in having representative catchments is the same used in regionalized flood frequency analysis; data for catchments in gauged/sampled areas can be linked to ungauged catchments using a set of catchment descriptors. Following the simulation of current and future time-series through the calibrated run-off models, a set of “change-factors” will be generated between the current and future estimates of discharge. These “change factors” will be linked to the catchment characteristics from which they were generated, allowing them to be mapped onto the existing Fathom-US hydraulic model framework.

Climate Model Linking and Change Factors for Fluvial Modelling

With a set of rainfall-runoff models being calibrated across representative catchments, the next stage is to drive the model set with output from a climate model ensemble.⁸ The model ensemble used will be NASA Earth Exchange Global Daily Downscaled Projections (NEX-GDDP) (<https://cds.nccs.nasa.gov/nex-gddp/>), which are CMIP5 models that have been bias corrected and downscaled across the U.S. Each of the models in the ensemble will be driven through each of the calibrated HBV models for both current and future climates.⁹ This will yield 21 representations of current discharge and 21 representations of future discharge, one for each model in the ensemble. To accurately represent hurricane influence upon precipitation fields, given the relatively short time windows (~30 years), the GCM time series is looped and hurricane tracks, along with their corresponding event precipitation fields, are sampled from the hurricane event sets for the current and future time frames and assimilated into the GCM ensemble

⁸ The total number of catchments being simulated to derive change factors has been dependent on computational resource and time. We are currently expanding this pool; we have now simulated 65 catchments and are hopefully that more will be added. Ultimately, we have to derive future flows for every river in the United States. Unfortunately, gauges do not exist on every single stretch of river. Therefore, we need an alternative methodology to derive future flows. The decision taken here was to use a regionalized method, whereby we use a pool of calibrated models and assume that they are representative of other similar catchments. We are attempting to fill out this sampling pool with more catchments. In the future, with more time, we can build out this sampling pool even further and use the extending sampling to ‘validated’ the pre-existing model pool and the change factors that are generated.

⁹ The aim of this portion of the project is to attempt to capture the range of projections coming out from the CMIP5 models. Although we are not accounting for other uncertainties, such as run-off model uncertainty, the range of uncertainty in the climate models alone will as the reviewer states will already represent a considerable range of uncertainty.

members.¹⁰ Due to the potential representation of some hurricanes within the GCMs themselves, this approach does risk overestimating the frequency of occurrence in some areas, however, without an obvious method by which to extract GCM hurricane events, this is unavoidable.

Current discharge estimates for each ensemble member are generated using the (1980-2017) climate window. This is the same climate window used in the HBV calibration process. Moreover, as the Fathom-US model has been built using the entire USGS gauge record, and the method used to perturb that model is a change-factor approach, it is important that the baseline/current climate chosen is representative of the baseline climate in the existing model framework. Although not an exact overlap, the current climate window of 1980-2010 represents a significant overlap with the USGS gauge record and is deemed to be appropriate for application here. For each climate model ensemble member, simulated evapotranspiration (PET) and precipitation (P) will be driven through the calibrated HBV models, producing 21 time-series' of discharge for the current climate. This process is repeated for the future climatology to produce estimates of future discharge. The future climate window and the future scenario used will be the 2035-2065 time horizons under the RCP 4.5 emissions scenario. Again, PET and P from each climate model ensemble will be driven through the calibrated run-off models to produce 21 time-series' of discharge for the future climate.

With both current and future discharge simulated, the next stage is to convert the discharge time-series into a set of change-factors, representing expected changes to extreme discharge. To enable this, flood-frequency curves will be fitted to the simulated discharge time-series'. This will take the form of generalized extreme value distributions fitted to each discharge time series for each ensemble member. These flood frequency curves will define extreme flow behavior under current and future climates and are used to define change-factors for different exceedance probabilities. In practice, across the range of simulated recurrence intervals, change factors are generated for each climate ensemble member. This will yield 21 change factors for each of the simulated recurrence intervals. Therefore, for each recurrence interval an ensemble spread of potential changes is produced. This range of potential changes for each recurrence interval and for each of the calibrated run-off models will then be sampled from, with resulting values used to perturb the boundary conditions to the existing Fathom-US model framework. The mapping of this catalog of change-factors onto the existing Fathom-US model framework is detailed in the following section.

Regionalization of change factors

The Fathom-US model framework simulates inundation for every single river in the U.S., regardless of size. To allow a commensurate, comprehensive simulation of future flows across all rivers, estimates of future discharge also need to be generated for all rivers. Although extensive, existing gauge networks in the U.S. do not cover all rivers. Therefore, the methodology used here is similar to that used to generate flows for all rivers; potential changes to extreme flows will be linked to catchment characteristics. These characteristics can be generated for every

¹⁰ In summary, we create 100 copies of each of the 21 GCM rainfall ensemble members for each of the 'historic', 'current' and 'future'. Within each of these copies, we use synthetic hurricanes (and their associated annual frequencies) for each of the 3 time windows, drawing from the synthetic hurricanes and replacing the GCM rainfall estimates where the synthetic hurricanes are sampled to. The outcome is 21 long (e.g. 100 * window length) time series of rainfall for each GCM ensemble member, with plausible synthetic hurricane rainfall added, during each of the 3 time windows. Later, the differences in the exceedance probabilities within these time series is used to generate change factors. Further, these time series are put through the hydrological model to provide corresponding discharge outputs which can be used to define change factors in the fluvial boundary conditions.

single river in the U.S. and are the same as those used in the existing Fathom-US discharge model. As a result, the change factors generated for each of the representative catchments can be mapped onto the existing framework using these catchment variables.

The catchment characteristics used are the hydrological unit zone (HUC Zone), upstream area, upstream annual average rainfall, and catchment slope. Each of the catchment characteristics are defined for each of the representative catchments and also for every model boundary condition in the Fathom-US model. This yields a catalog of change factors, linking expected changes in extreme discharge for each of the simulated recurrence intervals to a set of catchment descriptors. The Fathom-US model framework references this catalog, allowing input boundaries to be perturbed for any inland boundary condition point. This referencing is probabilistic in nature, using a clustering approach to calculate the error between the reference catchments and the simulation catchments. In practice, this results in a simulated boundary condition never generating its perturbation factors from one reference catchment alone. Instead, for example, simulation boundary condition point “1” will be perturbed by reference catchments A, B, and C by the respective distance values of 50%, 30%, and 20%.¹¹ This approach prevents any sudden changes between each of the reference catchment change-factors.



Figure 6: Outline of representative catchments used to build calibrated HBV models and derive perturbation factors.

Future Fluvial Flooding Execution

As mentioned in the previous section, Fathom-US defines upstream catchment characteristics for each of the model input boundary conditions. As also mentioned above, these same catchment characteristics will be used to define perturbations of future flooding for each of the simulated recurrence intervals. Therefore, the Fathom-US model framework will be executed in the same way as outlined above, with the addition of a perturbation step referencing the catalog

¹¹ By distance we are referencing the distance between catchment characteristic variables e.g. Upstream Area.

of change factors as described in the preceding section. These change factors provide a range of different change factors for each recurrence interval. To sample across this range, Low, Medium and High scenarios are simulated relating to the 10th, 50th, and 90th quantiles across the ensemble range for each of the representative catchments. Therefore, for each simulated recurrence interval, three separate model realizations are undertaken.

Future Pluvial Flooding Execution

The simulation of future pluvial flooding is more straightforward than the simulation of future fluvial flooding as the future precipitation fields from the assimilated climate model ensemble will be used directly. The current pluvial inundation modelling uses Intensity Duration Frequency (IDF) data from NOAA. These data are used to “rain-on-grid,” providing rainfall inputs to the Fathom-US model framework as opposed to riverine input boundary conditions. To conduct pluvial simulations under future climate scenarios, the assimilated future rainfall fields are used to derive change factors, using changes to maximum 1-day rainfall fields for each model ensemble member.¹² This yields distributed change-factors for each ensemble member nationwide. These distributed rainfall fields are then sampled from in order to provide Low, Medium and High scenarios relating to the 10th, 50th, and 90th quantiles across the ensemble members. These distributed rainfall change factor fields will be referenced in the same way that the NOAA rainfall fields are currently sampled, providing three different explicit simulations of future pluvial inundation.

Coastal Flood Risk

Both fluvial and pluvial components are considered in the development of the portion of the flood risk model in coastal areas, however they must be coupled with the uniquely coastal experiences of storm surge and tidal flooding. Surge is modeled using the GeoCLAW adaptive mesh refinement model (Mandli et al. 2014). As an adaptive mesh refinement model, GeoCLAW is designed to run at a very low resolution by default, both in time and space, and then to increase in resolution in areas near the storm, based on a variety of storm intensity and proximity criteria (see Table 1). The model is run with a spatial resolution of 0.25 degrees on the low end, and is then refined based on a variety of criteria. The refined resolution at each timestep is then set to the maximum refinement specified by each criterion, up to a maximum resolution 64 times the starting resolution, or 14.0625 arc seconds (approximately 430m).

The temporal resolution of the model follows a similar structure, with increases in temporal resolution triggered by a set of stability conditions.¹³ Surge in GeoCLAW is, in part, determined by a specification of the wind field at each time point and relies on an implementation of the Chavas et al. (2015) wind model. Using this model, energy from the wind field is transferred to the water through drag. The drag model used is the linear form specified in Garratt (1976), with a max drag coefficient set to 0.0035. Consistent with Chavas et al. (2015), the radius of max wind

¹² Here the assimilated future rain fields are used to produce change factors as a way of better understanding the impacts of changing environmental factors into the future.

¹³ The model is run with a global digital elevation and bathymetry model, the SRTM15+v2 DEM (Tozer et al. 2019), or higher resolution LIDAR DEMS from NOAA and USGS.

is sampled for each simulated storm from a log-normal distribution fit to historical observational data.¹⁴

Table 1: GeoCLAW model resolution refinement levels and criteria

Refinement level	Base	1	2	3	4
Spatial resolution	0.25 degrees	0.125 degrees	112.5 arc seconds	28.2 arc seconds	14.1 arc seconds
Criteria					
Radial distance from eye	N/A	600km	60km	40km	20km
Wind speed in cell	N/A	20 m/s	40 m/s	60 m/s	N/A
Current speed in cell	N/A	1 m/s	2 m/s	3 m/s	4 m/s
Surge amplitude	N/A	N/A	N/A	N/A	0.5 meters

To test the model calibration, a model specification is used to simulate historical storms and compare the modeled surge with observed NOAA time series tide gauge readings and USGS high water marks. Surge estimates are also compared with eight simulated storms that are run using ADCIRC. Historical storms were characterized using the International Best Tracks Archive for Climate Stewardship (IBTrACS) version 4 dataset (Knapp 2010 and 2018), with preference given to World Meteorological Organization (WMO) best tracks, and utilizing U.S. agency observations where these were unavailable. This data was further supplemented by ATCF track data (Miller 1990) for quality assurance and to infill for historical events or variables missing from the IBTrACS dataset. Tides are not forced in the model, but the time series of predicted tides at each NOAA tide gauge location are added to the storm surge outputs to account for actual tidal variability during the time of the storm. To simulate a hydrodynamic state approximately equivalent to the conditions of the historical event, the model is initialized at the average water levels observed for the week prior to the storm. Predicted tidal variability is then calculated relative to the predicted tides for the week ahead, thus accounting for any bias in the predicted tidal levels relative to observations during the storm. Predictions of water levels at USGS tide gauge sites, where time series predictions and observations are not available, are simulated by adjusting the amplitude of the time series of predictions from the nearest NOAA gauge to match the observed mean MHHW – MLLW range of the USGS gauge. Tidal predictions for other reported points not located at USGS or NOAA gauges are interpolated from the nearest gauge before being added to storm surge.

In simulated storms consistent with the NCEP reanalysis and GCM inputs, a similar approach to the above is followed, but tides are predicted using each NOAA station's harmonic constituents using the maritimeplanning/pytides package (2018). Projections of local sea level rise from Kopp

¹⁴ The Chavas et al model parameterizes the entire wind field, including the maximum storm radius, using these parameters and those available in the storm track datasets provided by WindRiskTech.

et al. (2014) are then added. To correctly simulate future hydrodynamic states, the model is further initialized at the cross-gauge mean of the median sea level predicted in Kopp (2014), which is accounted for when simulating gauge-specific water levels for each simulated storm. These individual events are then resampled into simulated years, using a sampling method that is consistent with historical hurricane activity but allows the frequency of hurricanes to change with changes in environmental conditions predicted by the GCMs, as specified in Emanuel (2017).

Estimating peak water levels for flood risk assessment

While the GeoCLAW package gives us the ability to simulate storm surge on a national scale, it does not inherently include a methodology to account for wave setup, wave run-up, or other contributors to peak surge water levels beyond the basic input it is able to use to produce surge levels across at a large geographic scale. As a result, surge water levels from GeoCLAW are often under representative of actual peak water levels experienced by the storm. Those additional considerations (plus storm surge) can be broken down into six major components (see Figure 7):

1. Local mean sea level: Incorporates local changes in land height and sea level rise. No intra-annual variability, ranges on the order of several meters over the 21st century.
2. Astronomical tide: Varies dramatically (multiple meters), often with 2 maxima per day.
3. Storm surge: Sometimes decomposed into pressure and wind surge, this is the increase in local sea level due to atmospheric conditions (pressure) and the effect of wind speeds on still water levels. This includes large-scale movements of water, and the flow of water based on these movements, but not waves. Storm surge can be significant (3+ meters) for very strong storms, and often varies slowly, on the order of days. Because of this, peak water levels often (though not always) coincide with peak astronomical tide. The combination of sea level, astronomical tide, and storm surge is known as storm tide. The difference between peak astronomical tide and peak storm tide, even if they do not co-occur in time, is known as skew surge.
4. Wave setup: Small-scale effect of wave dynamics on average sea levels, such as persistently higher sea levels immediately adjacent to a sloped beach, as well as average short-run effects of winds and atmospheric conditions generating waves. Note that these are short run (e.g. 6 minute) average effects, meaning the rise in sea levels caused by incoming waves will be represented, but not the high frequency variation in water levels of the waves themselves.
5. Wave run-up: Also known as wave swash, the maximum distance that water is driven by momentum up a shoreline. This marks the instantaneous maximum extent of water. Wave run-up can also be used to mean the total of shoreline wave setup and wave swash (as in the figure below). In low-friction, low-gradient locations, wave run-up can be extensive, and, in some areas, even in the south Atlantic and Gulf coast, these factors make up more than 50% of the FEMA base flood elevation (1-in-100-year flooding level).

6. Freshwater: Finally, interactions with fresh water sources (rain runoff and channel flow) can interact with the above components to increase flooding by adding water or to change water dynamics by affecting currents.

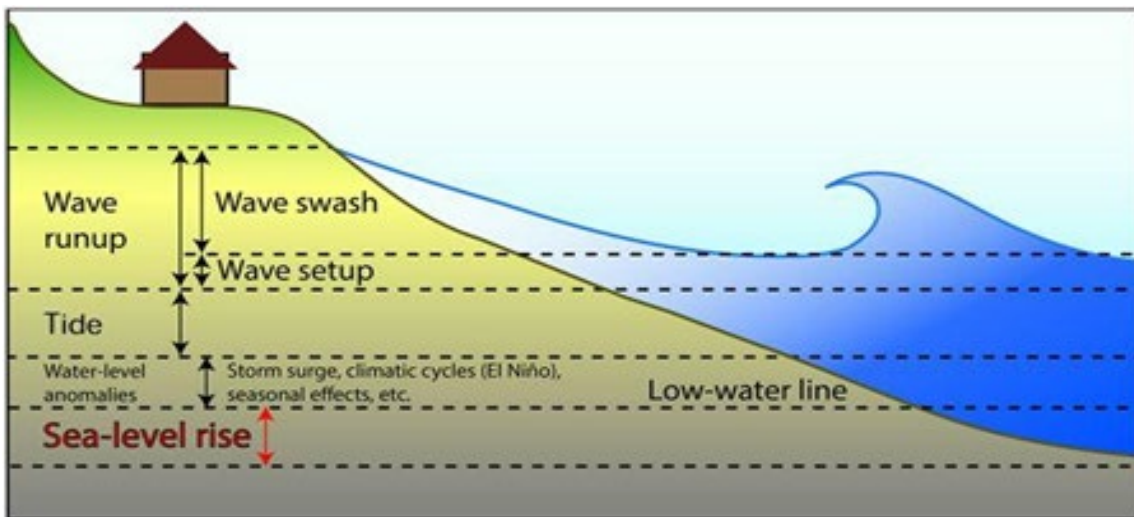


Figure 7. Components of Peak Water Height.

Source: Vitousek et al (2017).

The coastal portion of the integrated NFM being prepared by First Street Foundation, Rhodium Group, and Fathom is being produced in three stages. First, Rhodium Group, using its version of the surge model GeoCLAW in combination with predicted tides at NOAA gauge sites and estimates of sea level rise, is simulating storm tide. This gives us the time series of total static water levels throughout the storm, neglecting the effect of waves. The outputs of Rhodium's modeling are then incorporated by Fathom to their coastal methodology to generate coupled inland and coastal flood estimates, incorporating freshwater flows.

This approach is designed to efficiently simulate the effect of climate change on flood risk. Using observations from NOAA's extensive and long-running tide gauge network, we have validated our predictions of storm tide for over 100 historical storms, and GeoCLAW's results compares favorably with other more computationally-intensive best-in-class models (ADCIRC), lending itself well to this analysis. However, the outputs of GeoCLAW, combined with predicted tides, still miss two components of coastal flooding - wave setup and run-up.

In conventional process modeling approaches such as those used by FEMA to simulate risk, wave setup, and especially wave run-up, are the most difficult to calibrate and computationally intensive parts of the modeling process. Given our goal of providing local flood risk information for a range of time periods, sea level rise scenarios, and simulated future climate states, using such models to simulate wave setup and run-up is not possible. Still, they represent a significant share of the total flood height, even for large storms, meaning that estimates of total flood risk which neglect these components will necessarily be biased low.

Because of this, we developed a simple statistical model to adjust storm tides to approximate total wave run-up levels, based on information available to us in our simulations. For this analysis, we draw on observed high water marks compiled by USGS. The high water mark

dataset is collected after storms by surveying visible markers of flood height and extent, such as mudlines, seedlines, or debris, for the specific purpose of improving flood modeling. Our approach allowed for the estimation of peak water levels against observed high water marks through the application of the statistical model and thus captured the latent indicators associated with the under-estimation of surge heights from the GeoCLAW models. Additionally, the high water mark data includes areas flooded by coastal surge and waves as well as by freshwater sources. Therefore, we also filtered the high water mark data to include only coastal points and combined this with our estimated storm tide and maximum 1-minute sustained windspeed at each point.

The largest predictor of HWM elevation is GeoCLAW predicted surge, with an R² of 0.74 and a regression coefficient of 1.73, meaning we would nearly double our surge estimates to maximize our fit to the HWM data by simply scaling surge. Adding maximum 1-minute sustained windspeed increases the R² to 0.79, and the coefficient on surge drops to 0.98998, meaning that the surge signal is left essentially unmodified and much of the prediction error we see by modeling only storm tide can be explained by windspeed alone. Ultimately, a further refinement in which we removed high water mark data from Hurricane Harvey actually increased the model fit to an R² of about 0.86 (see Figure 8).

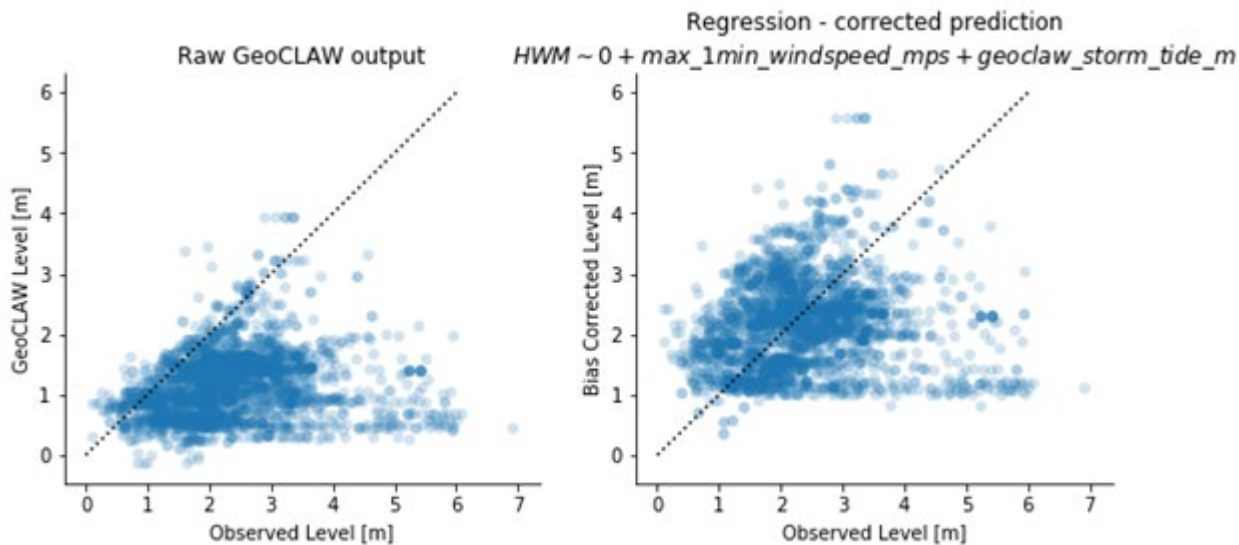


Figure 8. Model Correction of GeoCLAW surge heights to high water mark observed heights.

We next used this model to bias correct simulated water levels from synthetic tracks, produced by Dr. Kerry Emanuel using a climatology from the NCEP reanalysis of 2008-2018, in order to compare our modeled 1-in-100 year flood level to the FEMA Base Flood Elevation (BFE). This should not be considered a comparison of modeled vs. observed 1-in-100 flood risk, as this value is unobservable and the FEMA estimate is only that – another estimate compiled using a variety of different assumptions, modeling approaches, and data sources, and estimated over many years. However, the techniques used in more recent Flood Insurance Rate Map (FIRM) estimates usually represent the best-in-class modeling techniques and information at the local level. Therefore, the FEMA BFE is a useful check for any flood risk assessment.

The corrected model results in a 100-year flood elevation for which the pointwise deviations from the FEMA BFE are centered on 0 (median -0.19m, mean -0.26m nationally). Limiting the results to below the 35th parallel (south Atlantic & Gulf), where unlike in the Northeast we would expect 1-in-100 flood risk to be driven primarily by tropical cyclones, the median discrepancy is reduced to -0.06m (Figure 9).

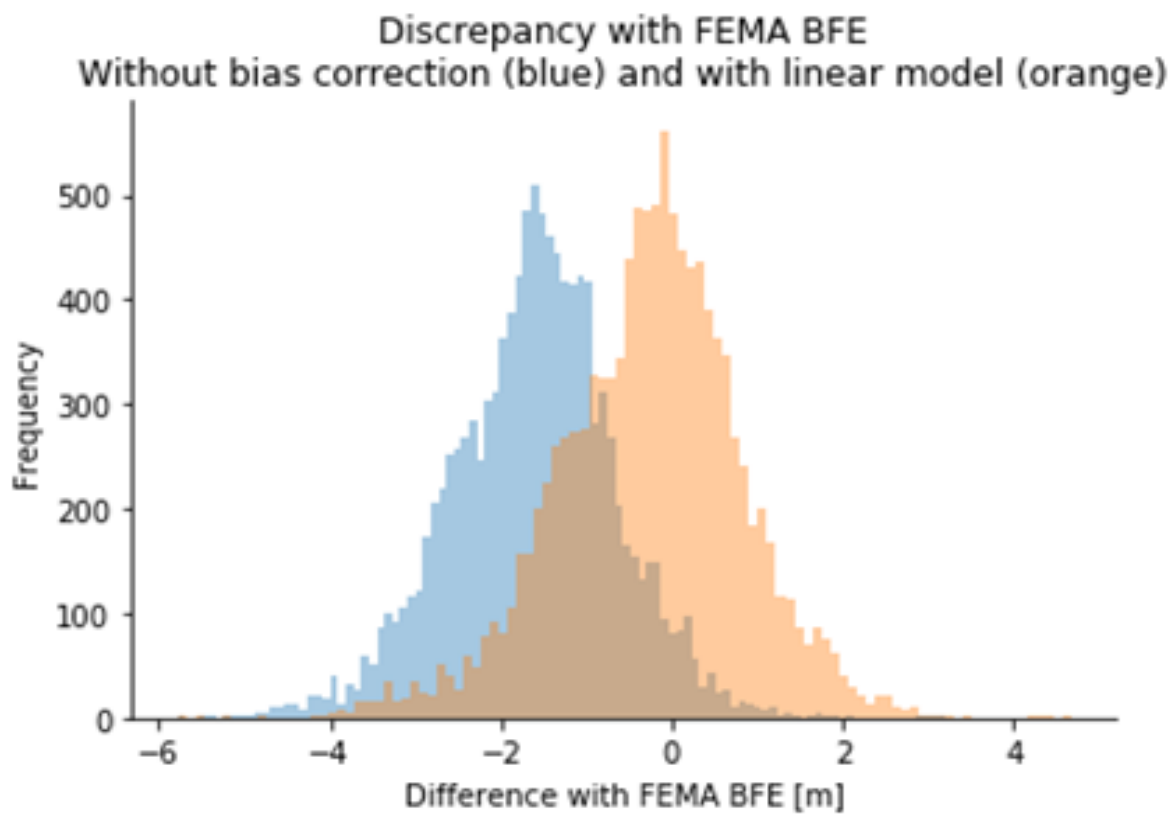


Figure 9. FEMA BFE comparison shift following model correction.

The increased alignment of our results with the FEMA BFE is also apparent when looking at a map of the differences between the FEMA BFE and our modeled 100-year floodplain. The map without bias correction is clearly biased low in all parts of the South Atlantic and Gulf, whereas the bias corrected version is clearly closer to neutral in the south. It is still significantly below the FEMA BFE in the north because of Nor'Easters. However, when looking at the two panels in Figure 10, we can see that the error distributions in our surge heights relative to BFE are much more randomly distributed across the coast outside of the NE and Mid-Atlantic regions. Ultimately, the coastal coupling described in the next section of the document will help to account for some of the non-stationarity introduced by the cyclone-centric nature of the approach being taken in the surge modeling portion of this analysis (more details below).

FEMA difference, no bias correction



FEMA difference, with bias correction

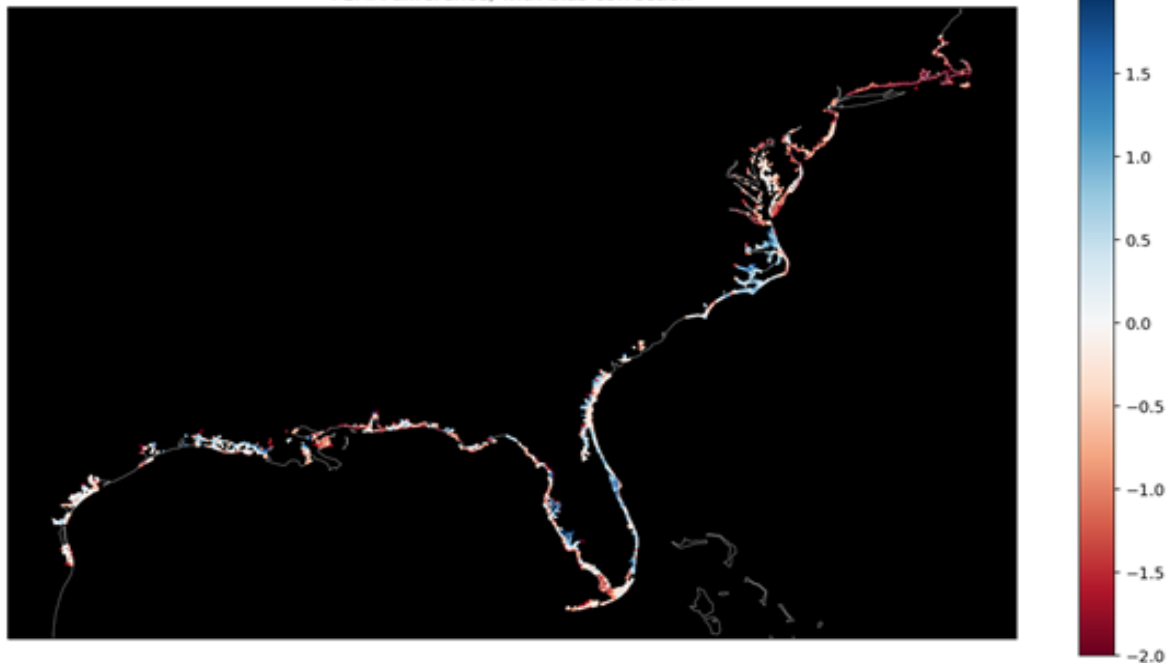


Figure 10. GeoCLAW vs FEMA BFE comparison before (upper panel) and after (lower panel) statistical correction of surge heights.

Joint Flood Probability in Coastal Catchments

Coastal catchments can be influenced by pluvial, fluvial, and coastal (storm, tide, and wave) processes, both independently and in compound flooding situations. In such regions, to accurately define the risk of inundation both the boundary conditions of all processes to the hydraulic model and the frequency at which event processes occur jointly (compound events) must be characterized. Further, historical records are prohibitively short for defining all plausible event scenarios, therefore, relatively long synthetic event sets (e.g. hundreds or even thousands of “today”) are required. Finally, a flood inundation model can then be used to derive depth-event (hazard) layers associated with the synthetic events, from which depth-return period distributions (agnostic of driving process) can be calculated.

Within this project, the aim is to define the “agnostic” (in terms of driving process) risk to coastal regions from three processes (fluvial, pluvial, and coastal) along all CONUS coastlines for a “current” time period and a future scenario. The methodology (described below) separates the process into 3 broad work packages, splitting the area spatially into the West Coast and the Gulf and East Coasts, and temporally into current (2020) and future (2050) risk. The spatial separation is used in recognition of the significant role of rare, intense hurricanes play in the gulf and east coastal regions. The inclusion of these events, particularly when correctly representing event frequencies, requires additional modelling processes that are not needed along the West Coast.

Gulf and East Coasts: Current (2020) hazard

Along the Gulf and East Coasts, pluvial, fluvial, and all coastal drivers can lead to flooding. The presence of hurricanes is highly influential upon coastal populations within these catchments, as hurricanes bring both strong rainfall, which leads to pluvial and fluvial flooding, and strong winds and low atmospheric pressures, which generate large storm surges and waves, all of which can lead to coastal flooding. Within this area, 4 key steps are used to define the flood risk:

1. Definition of the marginal distributions of the flood driving processes which will act as boundary conditions to the hydraulic model
2. Generation of the hazard layer catalogue
3. Characterization of dependence between the tails of the flood driving processes
4. Sampling from event catalogues to produce agnostic depth-return period distributions across all catchments

Defining the marginal distributions

The hydraulic model is driven by boundary conditions, representing inflows that can then be propagated through the computational domain. The model framework requires boundary conditions that are representative of distinct return period magnitudes, applied at specified spatial resolutions. For instance, pluvial hazards require an intensity duration value representing event rain-on-grid across a catchment, while at the coast, a time series of water levels representing

storm surge and astronomical tidal elevations are used. Currently, the additive influence of waves is not represented in the modelling framework. For the fluvial model, each river reach will require a series of hydrographs representing inflow discharge that will be routed through the hydraulic model to provide a resulting hazard map for that region (where the number of hydrographs represents the number of return period scenarios desired). For further information on the boundary specification and the hydraulic model framework see Sampson et al. (2015).

Pluvial boundary conditions for the current period are built using the IDF curves provided by NOAA and updating them to more explicitly account for hurricane activity (see Figure 7).¹⁵ Updating the existing IDF functions is done through the creation of ‘change factors’ across a set of 13,000 locations (corresponding to the GCM grid loci). Within each time window a 55,000 year timeseries consisting of sampled precipitation events from the synthetic hurricane track sets years were generated, within each of the 7 models. This resulted in 7 realizations of a 55,000 year time series of hurricane events. To assimilate the GCM and hurricane precipitation outputs, at each location, for each GCM ensemble member, an equivalent 55,000 year set of GCM annual maximum rainfall (AMAX) events was produced. This was done by extracting AMAX events within the GCM point timeseries, fitting a GEV distribution to the data, and then sampling from these distributions. For each synthetic year, at each location, within each model and time window, the largest of the AMAX values was retained. The output was 147 (21 GCM members combined with 7 hurricane ensemble members) AMAX timeseries at each location, for each time window. This data was then used to produce 147 estimates of the 10-year event magnitude at each location, where hurricane activity was influential upon the precipitation tails while the 98th quantile was used in the non-hurricane regions, within each time window. Hurricane track information is combined with a conservative (500km) buffer, replacing existing precipitation with the synthetic hurricane estimates. The above steps result in a significantly extended semi-synthetic precipitation record across the CONUS, from which daily intensity-frequency (IF) curves can be produced which adequately address the sampling issue encountered when attempting to characterize extreme, rare event influence (hurricanes) upon marginal distributions. Finally, the underlying NOAA IDF curves are updated using “change factors” based on the daily data provided using the steps above. These uplift factors characterize a proportional alteration in the intensity of rainfall for a given return period at the daily duration, represented as the difference between the “best guess” and the NOAA estimates. Currently, as the synthetic data is modelled at a daily resolution, the change factors are assumed to hold across the IDF duration ranges of interest.

The approach used to obtain “best estimate” current pluvial IDF curves (boundary conditions) requires two key assumptions. First, the synthetic hurricane event set is based on a time window (~10 years) that differs from the non-hurricane observed network data (~37 years). The reason for this is that hurricane characteristics are highly variable temporally and, therefore, conditions beyond windows of ~10 years are not considered to be stationary. However, for the fitting of marginal distributions, the use of relatively short time windows is problematic, as many rare

¹⁵ To do this, observed precipitation data is obtained from the NALDAS, which is a gridded precipitation record from 1980-2017, constructed through the interpolation of the daily gauge network across the U.S. In developing these boundary conditions, historical hurricane precipitation measurements are removed from this record using the International Best Tracks Archive (IBTrACS) historical hurricane information, assuming conservative spatial buffers. Non-hurricane rainfall fields, for the period of 1980-2017, are looped in order to provide N realizations for the period.

events may be missed.¹⁶ The assumption made here is that the non-hurricane processes are largely stationary over the longer time window, so a 37-year record can be used as a compromise allowing a long enough time series to adequately represent rare non-hurricane events, while still maintaining a high enough degree of stationarity to be representative of present-day conditions (for which synthetic hurricane precipitation already exists).¹⁷ The second assumption is that our best estimate of pluvial rainfall is defined by using change factors between the ‘historic’ and ‘current’ time window GCM’s plus synthetic hurricane rain fields. As a result, any model bias is incorporated into the resulting marginal distributions. It is important to note that without a method to characterize this bias, and remove it, this is unavoidable.

Fluvial boundary conditions utilize a similar approach to the pluvial and coastal water levels. However, an additional modelling step is required due to the complexity in relating rainfall to the estimation of river discharge. Figure 11 provides an overview of the process. In this instance, the looped rainfall product (containing non-hurricane observations with synthetic hurricane rainfall assimilated into it) is used to drive a series of hydrological models established in 23 key “representative” coastal river catchments in order to define hurricane related discharges.

¹⁶ The rapidity in which hurricane conditions can vary between decades is the reason why ‘historic’, ‘current’ and ‘future’ hurricane sets are given for 10 year windows. For example, we specify some time window from which to obtain synthetic hurricanes that represent expected 2050 conditions, but do not go beyond 2045 - 2055 to do so.

¹⁷ In reality, this is an assumption that emerges from the method rather than an assumption on which a method is then developed. The choice we are faced with is whether we restrict the non-hurricane record to a shorter window (for instance 10 years matching the hurricanes) and risk serious sampling errors when defining marginal distributions (as we have only one realization of the past) or extending the historic period to gain more observations but risk non-stationarity creeping into our predicted distributions.

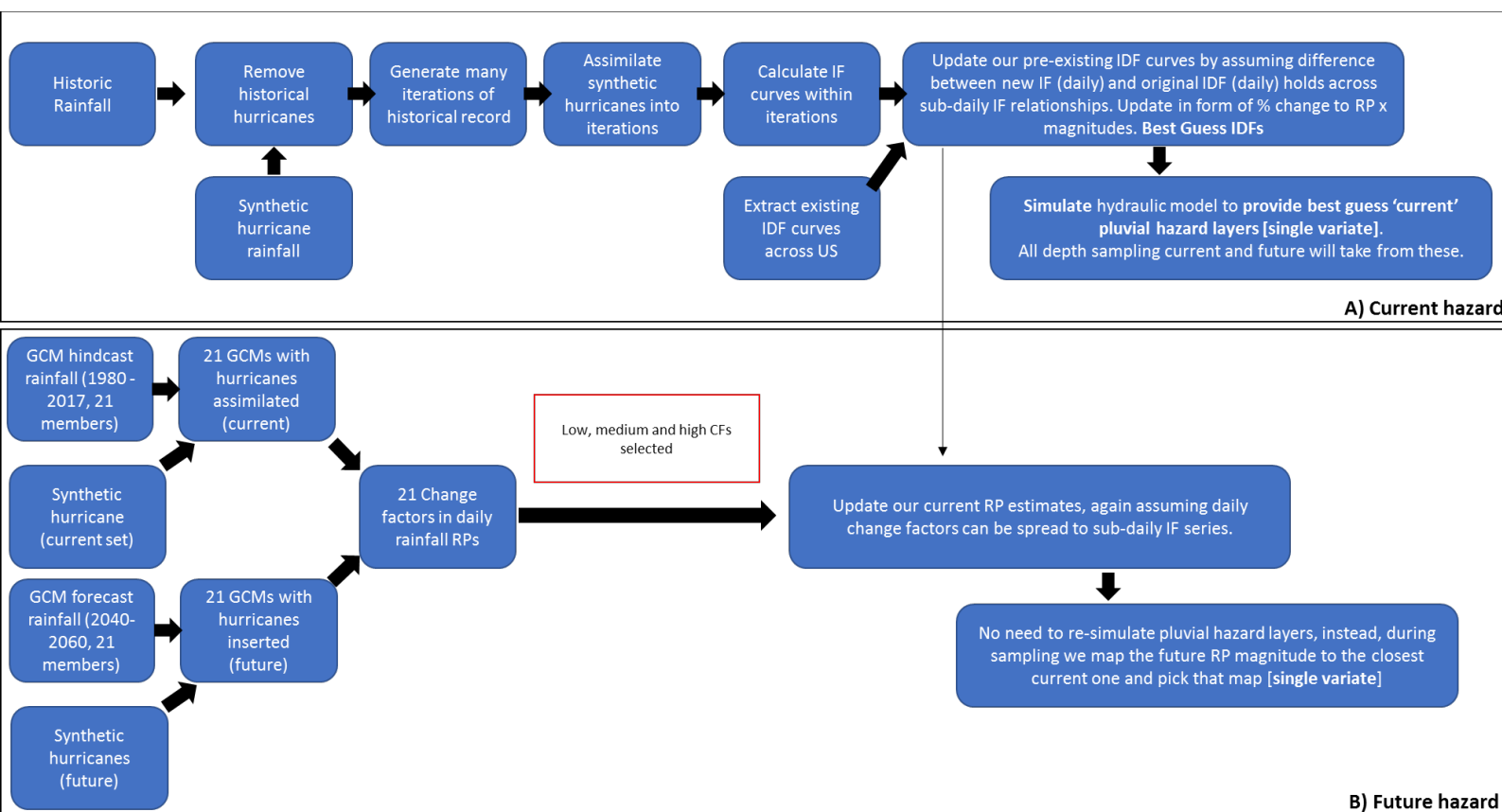


Figure 11. The specification of current and future pluvial boundary conditions to the hydraulic model.

The selection of “representative” river reaches is a requirement due to computational constraints on the construction of a U.S.-wide hydrological modelling framework. The sites selected represent significant ($>1000 \text{ km}^2$ upstream accumulation) rivers of varying size within 10 broad coastal regions along the Gulf and East Coast of the U.S., with relatively close proximity to NOAA tide gauges, which were used to define the multivariate tail dependence in fluvial, pluvial, and skew processes (detailed further below). Given the semi-synthetic, extended discharge record at each of the modelled river catchments, change factors between the new marginal distributions and existing marginal distributions (defined using regionalized flood frequency analysis, defined in more detail in Sampson et al., 2015; Smith et al., 2015; and Quinn et al., 2019) can be calculated. As the majority of river reaches are not modelled, change factors from the modelled river reaches are applied to surrounding reaches based on distance and upstream accumulation criteria. The methodology for the estimate of fluvial boundary conditions contains the same assumptions as that of the pluvial and sea level data sets. However, further assumptions surrounding the bias introduced by the hydrological model and, most importantly, the assumption that change factors at only 23 river reaches can adequately represent the expected changes in event discharges across very large regions (Figure 12a and 12b).¹⁸

¹⁸ At the time of this document, we settled on change factors at 23 river reaches, but future work could look to create more representative regions or sample more rivers local to each NOAA gauge when calculating dependencies. In many of the regions there will not be alternative, suitable, rivers, but certainly where there are, this could potentially

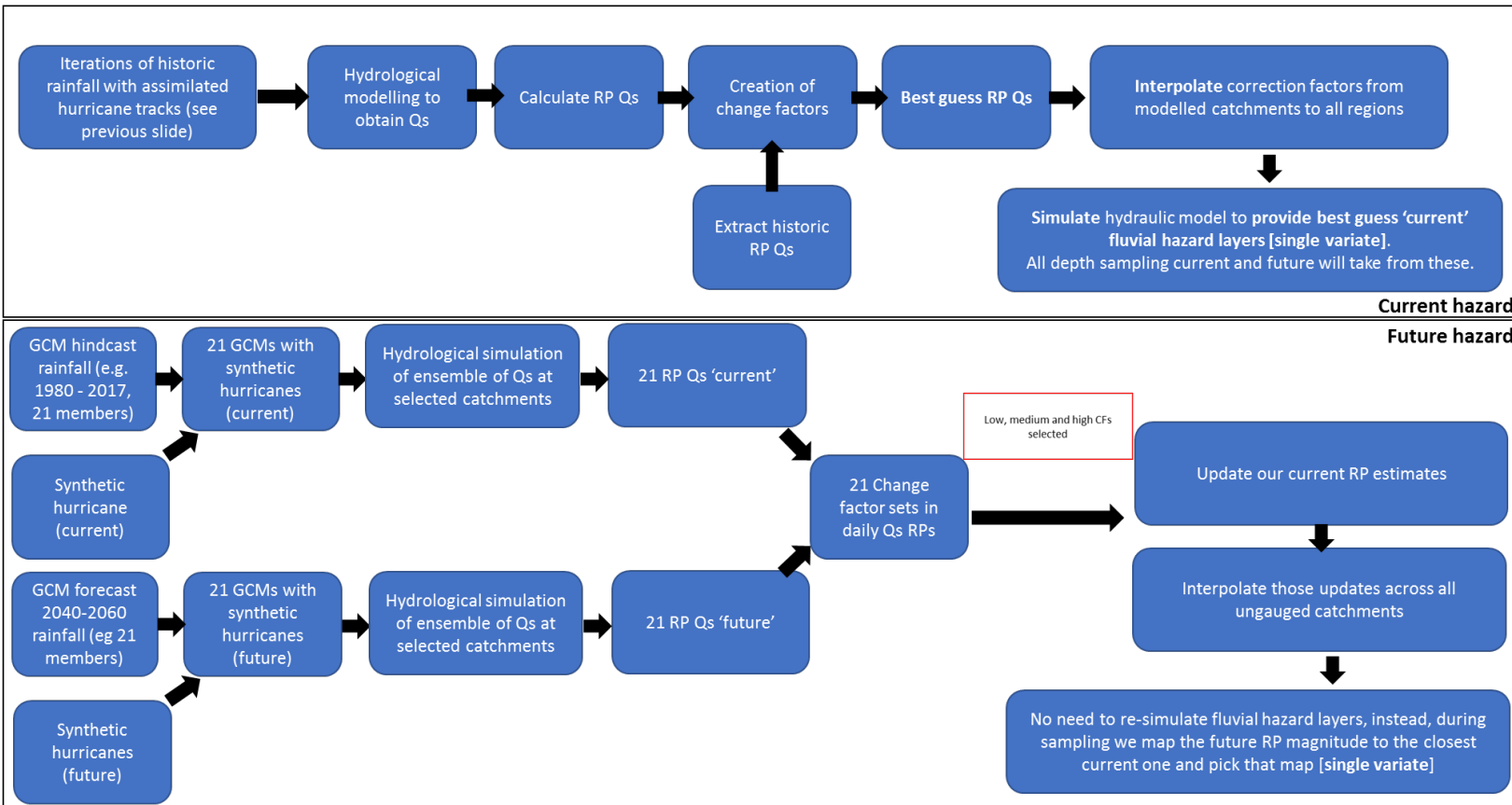


Figure 12a. The specification of inflow discharge boundary conditions to the hydraulic model.

provide improved results.



Figure 12b. Coastal regional units

Coastal water level boundary conditions are characterized using a similar strategy the one applied to the pluvial data, where available observations within the 1980-2017 period are processed to have historical hurricane conditions removed, then synthetic hurricane events are augmented into extensive looped observed records (see Figure 13). Observed water level and predicted tides are extracted from the NOAA tide gauge network (<https://tidesandcurrents.noaa.gov/>) along the U.S. coast for the 1980-2017 period. Gauges with less than 25 years of data are excluded from the analysis. 68 gauge stations (20 along the west coast and 48 in the Gulf and east) were retained for analysis. Coastal water levels are the supposition of three main factors: (1) mean sea level, (2) astronomical tides, and 3) non-tidal residual. To account for this, the underlying tidal elevations are taken directly from the NOAA gauge network, while the non-tidal signal is characterized by a “skew surge” (see <https://www.ntslf.org/storm-surges/skew-surges>). As a “skew surge” is defined as the difference between the highest recorded water level and the predicted tide, while the tide provided by NOAA assumes a given epoch, it is important to account for changes in mean sea level (MSL) in the recorded water levels over time. To do this, a 19-year, moving temporal window is applied to each gauge water level, within which the MSL is calculated. A polynomial is then fitted to the trend to define annual MSL changes throughout the record, and the water levels are adjusted to become normalized to the current NOAA epoch (typically 1983 – 2001) level, on which the tidal predictions are based.¹⁹ Skews are defined based on a comparison between the recorded water levels and the predicted tide.

Using the semi-synthetic, extended records, water level and skew marginal distributions are created at each of the NOAA gauges. To account for changing mean sea levels, the polynomials defined above are then applied to the data, normalizing to current (2020) MSL conditions. All levels are given relative to NAVD88, which corresponds to the datum used in the hydraulic model DEM (see https://nationalmap.gov/PERS_Jan2002_NED_highlight_article.pdf). As the hydraulic

¹⁹ The skew records are intersected with historical hurricane information (see pluvial description above) and looped over N iterations of the 37-year period. Hurricane event skew information provided at a series of coastal points is assimilated into the looped observations. The combined water levels at the NOAA sites, during these synthetic events, is given by adding NOAA tidal predictions on the event days with the corresponding synthetic skew estimates.

model requires inflow boundary conditions along the coastal boundary, the marginal distributions at the NOAA gauges are interpolated along the coastline with the aid of shorter records provided by the USGS, as well as the full set of “skew surge” and synthetic storm outputs, to more accurately characterize the changes to marginal distributions along complex coastlines. The interpolations are performed with an inverse distance weighting function that allows for the use of barriers, such as islands or other elevation related features that separate surface continuity. This helps better characterize the individual behavior or disconnected tidal water bodies that are in proximity. The methodology requires the same assumptions as those discussed in the pluvial section above.

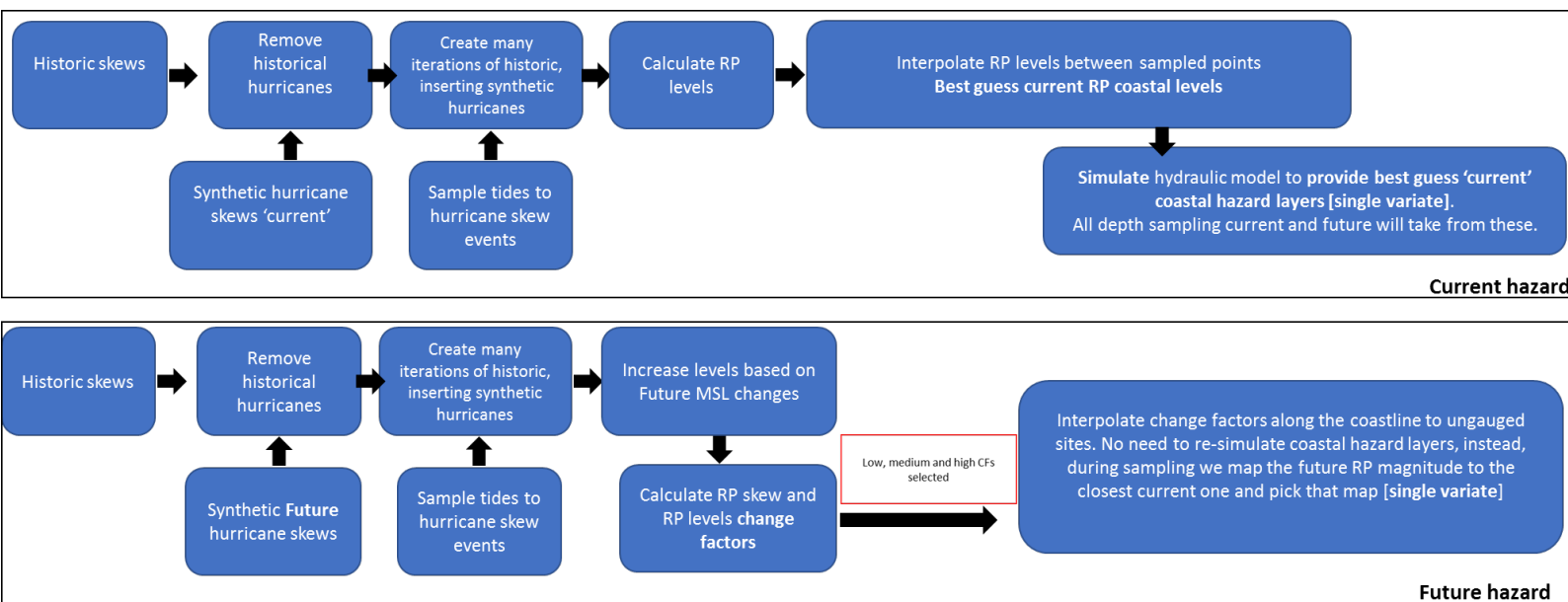


Figure 13. Method for selecting best ‘current’ and ‘future’ SKEWS / LEVELS RP boundary conditions and resulting hazard layers

Defining the hazard catalogue

The marginal distributions defined above are used to force the hydraulic model to produce resulting flood hazard layers. Due to the inclusion of pluvial, fluvial, and coastal flood processes, as well as the potential for joint occurrence (compound flooding), many more layers are computed than the 19 outlined in Sampson et al. (2015) and Quinn et al. (2019). This component of the workflow attempts to represent this large multivariate parameter space.²⁰ Once simulated, the

²⁰ A clear trade-off exists between attempting to represent as much of the parameter space as possible, while accounting for computational and research timeline constraints. In this project, this is achieved by selecting approximately 10 bins within each of the 3 marginal distributions and modelling each combination of those process bins to account for potential compound flooding. This is done over all coastal tiles within the hydraulic model, where coastal tiles are defined as those containing catchments that may, plausibly, be impacted by coastal water levels, either directly or through event interactions. This threshold is currently defined using an elevation of 50m. Although flood driving processes may peak at the same time, completely separately, or at any point between the two extremes, computationally it is infeasible to model this range of interactions. Therefore, in this research, where flood processes are modelled to interact, their peaks are assumed to occur at the same time.

resulting tiled hazard layers are dissected into catchment-specific catalogues that can be sampled from, following the methods and catchment units outlined in Quinn et al., (2019) (see Figure 14). Compound flooding was not considered for all 3 processes – only fluvial and storm surge were assessed as delays meant that we could not simulate a large number of pluvial layers required to include it in the compound flooding analysis. Synthetic events that saw a pluvial event occurring within a day of another process took the max of the compound Q/surge layer and the independent pluvial layer. In total, 81 hazard layers are simulated for each coastal catchment, representing all potential binary interactions between the storm surge and fluvial processes within 8 return period bins. In this instance, each process is modelled to either peak at the same time as another, or completely independently of them. The catchments defined as ‘coastal’ were given as those thought to be plausibly impacted by storm surge water levels, either directly or through interactions with fluvial or pluvial processes. This was estimated by simulating an extreme coastal water level (given as the 5000-year current return period + 2 meters) and finding any catchments in which inundation occurred. A 20km buffer was then applied to this layer to create a mask, any catchments within which would be included in the coastal impact zone.

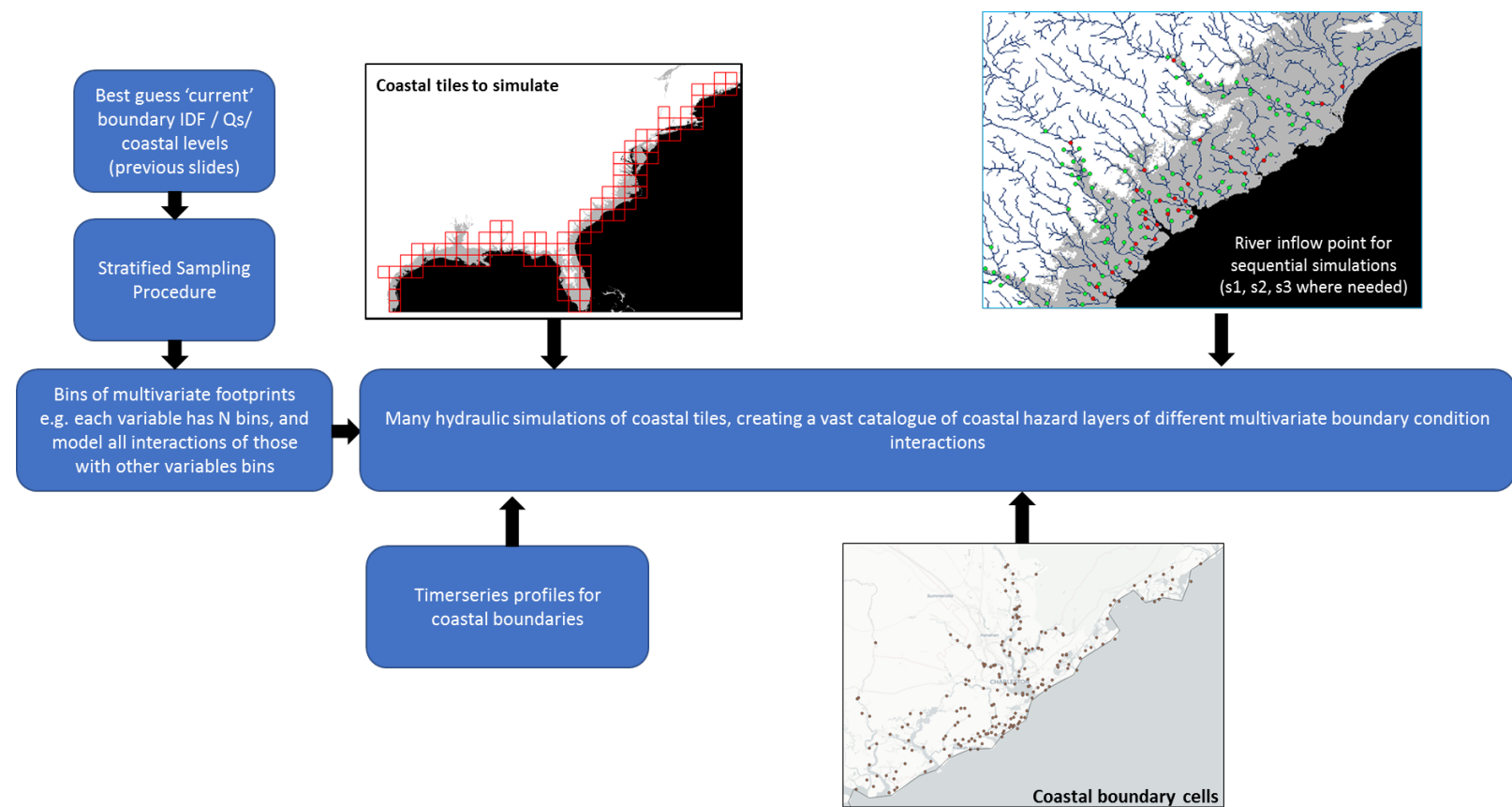


Figure 14. Creating Multivariate Hazard Layers

Characterizing the multivariate tail dependence

The above steps provide a method by which one can create a best estimate of flood driving marginal distributions and use them to produce a large catalogue of flood hazard layers that accounts for a wide range of plausible compound flooding events. However, in order to accurately

define risk to a given location, the expected frequency of flood causing events must be characterized. To do this, the methodology aims to produce a large semi-synthetic time series of events, sample depths from the corresponding hazard layer, and then use that information to derive a process agnostic depth-frequency curve (Figure 15).

The approach used in this research follows that of previous research that has considered compound flooding frequencies across continental scales (e.g. Wahl et al., 2015; Ward et al., 2018). In summary, “representative” regions in which it’s possible to find NOAA tide gauges, river reaches with significant upstream areas ($>1000 \text{ km}^2$), and rainfall records within close spatial proximity (and that contain a sufficiently large data record) are selected and used to characterize tail dependence between the flood driving processes. All gauges lie within 100km of the corresponding NOAA tide gauge with outflows points within 50km. Few exceptions to this rule were made for extremely large rivers such as the Mississippi in which river gauges further upstream had to be used. In total, 127 unique coastal, fluvial and pluvial sets were used to characterize the marginal tail dependencies, 64 within the West coast and 63 within the Gulf and East coast. Due to limitations in the number of potential sites, priority is also given based on proximity to large urban centers. As indicated above, 10

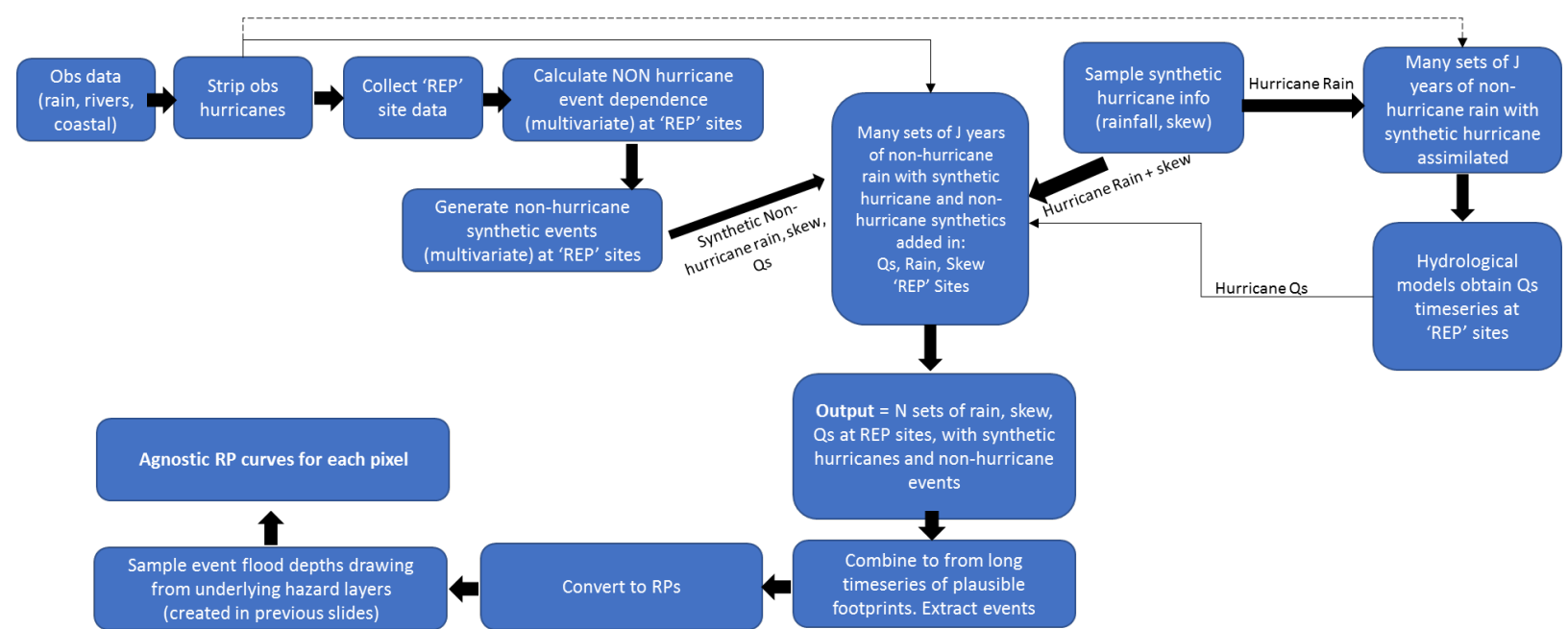


Figure 15. The characterization of compound flooding frequency and hazard layer sampling.^{21,22}

²¹ The RPs calculated here have no bearing on what inflows go into the hydraulic model, they are only there to convert time series to RPs to then say which of the underlying hazard RP layers to pick.

²² For future scenarios, the same method is used, but we apply to many new hurricane event sets from Rhodium. In doing so we assume the dependence between the variables is stationary for non-hurricane events.

regions, and 23 specific river reaches were used due to computational restrictions. Future research may wish to build upon this data set, adding more sites for modelling. The 10 large regions were selected based on availability in NOAA tide gauges and manual assessment of historical storm tracks and coastline typology, with the aim of deriving regions in which the dependence between processes will be largely represented by the sampled sites.

The approach used in this research begins with extracting the observed datasets for the 1980-2017 period and removing the historical hurricanes, as described in previous sections. These time series at the “representative” data points are used to define the multivariate tail dependence in non-hurricane events using the approaches defined in Quinn et al. (2019). This process produces a series of models in which, given an “event” occurring at a given site, can be used to predict conditions in the other processes in the same region. These models are used to define a large catalogue of non-hurricane events within which the conditioning site exceeds a specified event threshold (given here as the 99th quantile of the corresponding marginal distribution). Within the coastal regions, five days is used to define an event window.²³ Looping the observed, non-hurricane records at these “representative” sites, N times, historical non-hurricane events are found and, in each case, the conditional site is defined, the corresponding model is selected, and a Monte Carlo sampling scheme is used to insert a synthetic non-hurricane event into the record. Sampling of hurricane-induced pluvial, fluvial, and coastal water levels into the semi-synthetic time series provides a relatively long time series of plausible, compound events.

Sampling event catalogues

The time series created at the “representative” sites described above can be used to derive a series of independent events (where at least one variable exceeds a specified event threshold). Within each event, variable estimates can be represented as return period magnitudes, the combination of which are used to define which underlying hazard layer to sample from within the containing catchments. Interpolation is required to ungauged catchments. As spatial dependence is not required to do this, it is assumed that the dependence (and event conditions) at the “representative” sites are also found in all other catchments within the large containing region (see Figure 2, presented previously). The process by which this is undertaken requires that we sample the dependence and generate synthetic events only at a small set of ‘representative’ points within much larger regions. The synthetic event characteristics (e.g. the magnitudes of pluvial / fluvial / coastal boundary conditions) at these points during an event are then applied to all river / rainfall / coastal inflow points within the wider region – in doing so we ensure that all catchments within the wider region experience the same frequency of compound event combinations as those generated at the ‘representative’ sites.

Through the implementation of this process, an estimate of return period magnitudes associated with each process, within every coastal catchment, can be defined. Given each set of event magnitudes, coastal hazard layers from the large catalogue established in Section 2 can be sampled to provide many years of plausible event depths associated with “current” conditions, in every coastal cell. The time series of event depths, in any given location, can then be collated and used to provide a marginal distribution (describing the depth – frequency relationship) that is

²³ A specified time period is used by the stochastic model to define the number of lags over which to assess tail dependence between the fluvial, pluvial and skew parameters. The use of a 5 day value follows that used by Ward et al (2018) in their work defining the dependence between extreme sea levels and river discharges across global deltas and estuaries.

agnostic of flood driving processes, for the “current” (2020) time period.

Uncertainty in Coastal Models

In the context of coastal flooding, the NFM is more complex in that it includes the same risk as the inland models (pluvial and fluvial events) but also uniquely coastal flooding risk from tidal and storm surge sources. In regards to the uncertainty around storm activity and associated surge, the historical record does not provide a sufficient number of observations to fully characterize the flooding risk posed by hurricanes at all locations for current risk or into the future. To address this, flood risk is modeled by simulating storms consistent with a specific climate state and sea level and integrating simulated hurricane tracks and rain field estimates provided by WindRiskTech (see, e.g. Feldmann et al., 2019; Emanuel, 2017; Emanuel, 2016). The model used to generate these storms incorporates environmental variables simulated by a climate model.

Current risk is characterized using storms consistent with the climates of a reanalysis produced by the National Centers for Climate Prediction (NCEP) (see Kalnay et al., 1996). Future changes are modeled using the climates simulated by seven global climate models, consistent with Representative Concentration Pathway 4.5 (Meinshausen, 2011). Rain fields, hurricane skew surge, and storm tides for 400 synthetic tracks are simulated for each year in the years 2007-2017, consistent with the NCEP reanalysis, as well as 200 synthetic tracks for each year for each GCM for the periods 2007-2017, 2015-2025, 2030-2040, and 2045-2055, for a total of 66,000 individual events.²⁴

Gulf and East Coasts: Future (2050) hazard

In order to move from current to future risk, the ensemble of models contained within the CMIP5 data set (<https://www.wcrp-climate.org/wgcm-cmip/wgcm-cmip5>) are utilized. This research focuses on the 2050, RCP4.5 scenario when defining future risk. The methodologies used to derive changes in the various boundary conditions are outlined in Figures 4, 5, and 7b, and briefly summarized below. The future pluvial boundary conditions are obtained by extracting the GCM ensemble members’ data for the current time period (1980-2017), looping the series N times, and assimilating the synthetic hurricane precipitation fields, as described previously. The same process is applied to future GCM data (defined using a 30 year window centered on the 2050 year of interest) and assimilating hurricane precipitation fields forced under future climatic conditions. The difference between the 21 resulting marginal distributions provides an ensemble of change factors that can be used to perturb the original (“current”) boundary condition return period magnitudes.²⁵

²⁴ The global climate models (GCMs) used to examine changes in the environmental conditions which affect hurricane activity in this study are CM3 from the NOAA Geophysical Fluid Dynamics Laboratory, HadGEM2-ES from the UK Met Office Hadley Center, CM5A-LR from the Institut Pierre-Simon Laplace, MIROC-5 from the Atmosphere and Ocean Research Institute (The University of Tokyo), National Institute for Environmental Studies, and Japan Agency for Marine-Earth Science and Technology, MPI-ESM-MR from the Max Planck Institute for Meteorology, MRI-CGCM3 from the Meteorological Research Institute, and CCSM4 from the National Center for Atmospheric Research. These models were downscaled and then used to simulate hurricane activity by Kerry Emanuel (see Emanuel 2017 and Emanuel 2016).

²⁵ “ N ” (the number of realizations of each GCM member, for each time window) is defined as 100 currently as that approaches the number of synthetic hurricane tracks provided for a given time window period (~4000). Effectively that gives us 4000 years of synthetic hurricanes within the ‘historical’ period under each of the 21 GCM ensemble members. However, it could be possible to do some convergence testing around this. The same method is used in

The future fluvial boundary conditions are obtained by simulating the numerous GCM-hurricane augmented time series through the coastal hydrological models. This provides 21 marginal distributions at the modelled river reaches which can then be used to derive change factors, all of which are then interpolated throughout the ungauged coastal catchments using the interpolation approaches detailed above. The future coastal water level boundary conditions are obtained in a similar manner, in which future synthetic hurricane events are assimilated into looped observations for each of the 21 ensemble members. In addition to the changes in hurricane skew, predictions of changes to MSL are also applied to the resulting ensemble of future time series. Change factors are then applied as with the pluvial and fluvial boundary conditions. No changes to non-hurricane skews are considered in the current research.

Given the continental scale of this project, and the lack of agreement on surge changes into the future, we rely heavily on historical data and existing literature to understand how surge may change into the future. A review of the literature seems to indicate that, broadly, there is little consensus on the significance of changes to surge characteristics upon extreme sea levels in the future, with the most important factor being relative sea level rise. For instance, Menéndez and Woodworth (2010), and Mawdsley and Haigh (2016), report that consistently changes in extreme still water levels follow trends in relative sea level. For this reason many studies such as Wahl et al (2017), and Vitousek et al., (2017) employ a static approach, only considering changes in MSL on extreme water levels in the future. We do acknowledge that there will be some sites where extreme levels are expected to change beyond MSL fluctuations (either increasing or decreasing) but we hope that more often than not, the assessment of MSL changes will account for the vast majority of future change in risk.²⁶

In each case, change factors are used to describe the change in magnitude associated with a given return period boundary condition magnitude. However, new hazard layers are not produced as this would be computationally infeasible. Instead, during sampling of the hazard layers, a lookup table approach is used in which the closest hazard layer from the original catalogue is selected, based on the boundary condition magnitude plus the change factor. For instance, in the current time window an event with a 5-year fluvial boundary condition would sample the corresponding 5 year fluvial hazard map for the river reach in question. However, in the future scenario, it may be that the 5-year boundary condition is closer to the original (“current”) 20-year magnitude, in which case, during a future event which has a 5 year fluvial boundary condition, the 20-year hazard layer will be selected.

The production of many change factors, based on the ensemble of models within the GCM data set, enables the estimation of uncertainty bounds on the future flood risk predictions. 21 sets of time series can all be used to sample from the underlying hazard layers, each producing an estimate of the depth – frequency distribution at a given location. The spread within these distributions can be used to inform uncertainty within the model predictions for the future scenario.

subsequent time windows of interest.

²⁶ The exception in our method is within the Gulf and East Coast hurricanes where we were able to use synthetic hurricane outputs, which we felt, although it introduced inconsistencies between the east and the west coastal region methodologies, was a valuable addition to the workflow. Future research might wish to expand the model/ develop new models to also provide synthetic non-hurricane future events around the US coastlines, but it was beyond the scope of this project.

Application of methods to the West Coast

Along the West Coast of the U.S., a simplified version of the method described here is applied due to the lack of hurricane activity influencing the region. The observed record alone (1980-2017) is used to define the current boundary conditions to the model, using the same regionalized approach as outlined above (see Figure 5 for the regional units specified). In order to provide a longer duration record from which to sample plausible events, the dependence model on this coast utilizes all available data within the 1980-2017 window. Synthetic realizations of plausible event conditions on this period are then used to produce a synthetic record of many thousands of years following the methods outlined in previous sections.

When creating change factors for future scenarios, the approaches described above are used, however, only the GCM components are considered (as hurricanes are not required). Furthermore, as no coastal storm surge model is developed for this region, no change to skew characteristics are defined and changes to coastal boundary layers are controlled entirely by changing MSL conditions.

Historical Analysis

The historical portion of the analysis concerns the recreation of past flooding events in two different contexts, inland and coastal. The inland methodology begins with observed precipitation and stream gauge discharge which are used to recreate flooding extents with combined pluvial and fluvial simulations. The coastal methodology centers on recreating historical extreme surge events with a combination of hydrodynamic modeling, remote sensing, interpolations, and statistical modeling.

Coastal

The recreation of historical flooding from coastal storm events takes place in multiple steps. First, synthetic aperture radar (SAR) data was obtained in spatial and temporal alignment with a series of significant coastal flooding events. The SAR data was processed using distributions of backscattering values and Ashman coefficients that permitted the distinguishing between water and dry surfaces in the image. Once water was identified, high precision DEMs were incorporated in order to estimate depth at any given sensed water pixel, based on a series of steps beginning with an estimation of water elevation and followed by a calculation of inundation depth. Subsequently, the remote sensing depth estimation was coupled with depths from the USGS high-water mark data / depth grids and hydrologically simulated water levels coming from ADCIRC simulations. The ADCIRC water levels were obtained from specific storm recreations at points representing mesh nodes where the water level was determined to be higher than the elevation (thus identifying flooding from storm surge).

To train the model, tidal water levels, elevation, and cost surfaces are used to calibrate the prediction of water levels. The tidal water levels were extracted from NOAA and USGS gauges in the impacted areas and are interpolated across the spatial extent of the storm. Elevation is represented by the highest precision available DEM in that area, and cost surfaces are created

using an ArcGIS Cost Distance function that allows for the creation of a cumulative cost surface that identifies areas subject to some constraint, either based on land cover types or due to elevation ridges that restrict flow of water to very minimal depths at any place within the inundation extent (depth penalization).

Hydrodynamic modeling of historical storm surges

The historical storm recreation on the coast relies heavily on the ADCIRC model runs that have been created to simulate water levels associated with each of the modeled storms. The numerical simulations of storm surges are based on the coupled version (Dietrich et al., 2011a) of the ADCIRC hydrodynamic model (Luettich, Westerink, & Scheffner, 1992) and the wave model SWAN (Booij, Ris, & Holthuijsen, 1999) to simulate waves and hydrodynamics from tides, hurricanes, and Nor'easters. ADCIRC is a finite element, shallow water model that solves for water levels and currents at a range of scales and is widely used for storm surge modeling (Bunya et al., 2010; Forbes et al., 2010; Garzon & Ferreira, 2016). SWAN is a third-generation spectral wave model that computes random, short crested wind-generated waves and waves transformation in near shore and inland waters for the purpose of including mean wave effects on surge elevations (Garzon & Ferreira, 2016). Simulations were performed in the context of a supercomputing environment provided by the Extreme Science and Engineering Discovery Environment (XSEDE), supported by the National Science Foundation (NSF).

The performance of ADCIRC+SWAN to simulate hurricane storm surge was validated through the U.S. IOOS modeling test bed (Kerr et al., 2013) and the performance and scalability of the coupled ADCIRC+SWAN model was tested successfully with up to 9,216 cores (Dietrich et al., 2011b) in a High Performance Computing (HPC) environment. Tidal forcing from seven tidal constituents were incorporated based on the Western North Atlantic, Caribbean and Gulf of Mexico Tidal Databases. The land cover and land use information are represented in the model through parameterizing the shear stress on the sea bottom as well as on the free sea surface. Manning's roughness coefficient is applied to address different sea bed surfaces and respective frictional resistance by different land cover in the study areas. Additionally, using Garratt's drag law (Garratt, 1977) the model accounts for reduction in wind shear stress on the sea surface due to canopies and other land uses present in the model domain. Friction parameters in the model are computed using the land cover information collected from several national land cover databases such as the National Land Cover Dataset (NLCD).²⁷ The simulations are based primarily on existing numerical meshes for the region of interest based on each individual landfall location.

For this study, variations of the best available meshes for each study area were applied according to the hurricane tracks and the impacted areas. Historical storms were simulated based on an asymmetric wind model forced by the National Hurricane Center (NHC) best track databases, the North American Mesoscale Forecast System (NAM) developed by the National Centers for Environmental Prediction (NCEP), and any additional publicly available weather dataset to ensure the best representation of the wind and pressure fields for each of the historical storms. The results demonstrated that while the NAM presented the best results hindcasting selected

²⁷ For example, the Mason Flood Hazards Research Lab has developed several numerical meshes specially designed for the Mid-Atlantic Region and the Chesapeake Bay (resolution of approximately 30 meters in the Chesapeake Bay region). NOAA has recently developed the HSOFS covering the entire U.S. East Coast and Gulf of Mexico (GOM) with ~1.8 million nodes and approximate resolution of 160+ meters.

historical storm surges in the Chesapeake Bay, other systems might better represent the atmospheric fields for different storms and locations (Garzon et al. 2018). Historical hindcasting and validation of the modeling framework were performed based on high water marks, USGS and NOAA tide gages, and any other available data. A model validation report will be produced to document the model performance for each storm and location. Coastal flooding inundation maps will be produced based on a GIS framework based on *ArcStormSurge* (Ferreira, Olivera, & Irish, 2014) that will be used to convert the model outputs, creating spatial and temporal tropical storms inundation maps, wave heights, and maximum inundation extent. The downscaling of the coupled ADCIRC+SWAN produced results will be performed using the GRASS based *Kalpana* script. This script uses extrapolation module “grow” to extend the water levels to the same elevation on the high resolution DEM. These maps will incorporate the resulting water levels from storm surge, tides, and waves, streamlining the flood map delineation. Each historical storm simulation is documented in Jupyter notebooks demonstrating the model validation and specific methods utilized for the study.

Inland: Historic flood events

Historical inland flood event footprints will be simulated using the Fathom-US hydrodynamic modeling framework. This will be undertaken by linking the modeling framework to the USGS gauge network, to explicitly simulate observed events. These hindcast simulations will be limited to simulations of large magnitude events on relatively large fluvial floodplains. An upstream area threshold of 10,000km² was applied with a minimum annual exceedance probability of 0.98. A minimum observational gauge record length of 50 years was also applied. An examination of the USGS observational record yielded ~150 observed events suitable for hindcast simulation. Each event simulation was undertaken using the observed event hydrograph from the gauge record, implementing the hydrograph as a boundary condition in the Fathom-US modeling framework. Given the known uncertainties in measuring discharge during extreme events, each observed event will be simulated within an uncertainty framework, exploring uncertainty around observed peak flows. A Monte Carlo sampling approach will be used to sample from an assumed normal distribution of errors around the observed peak hydrograph, with errors ranging from +20% to minus 20%. Each sample of this error space will yield a separate simulation, providing numerous realizations of the event footprint. The final layer will rank the likelihood of inundation from 0 to 1, as shown in Figure 16.

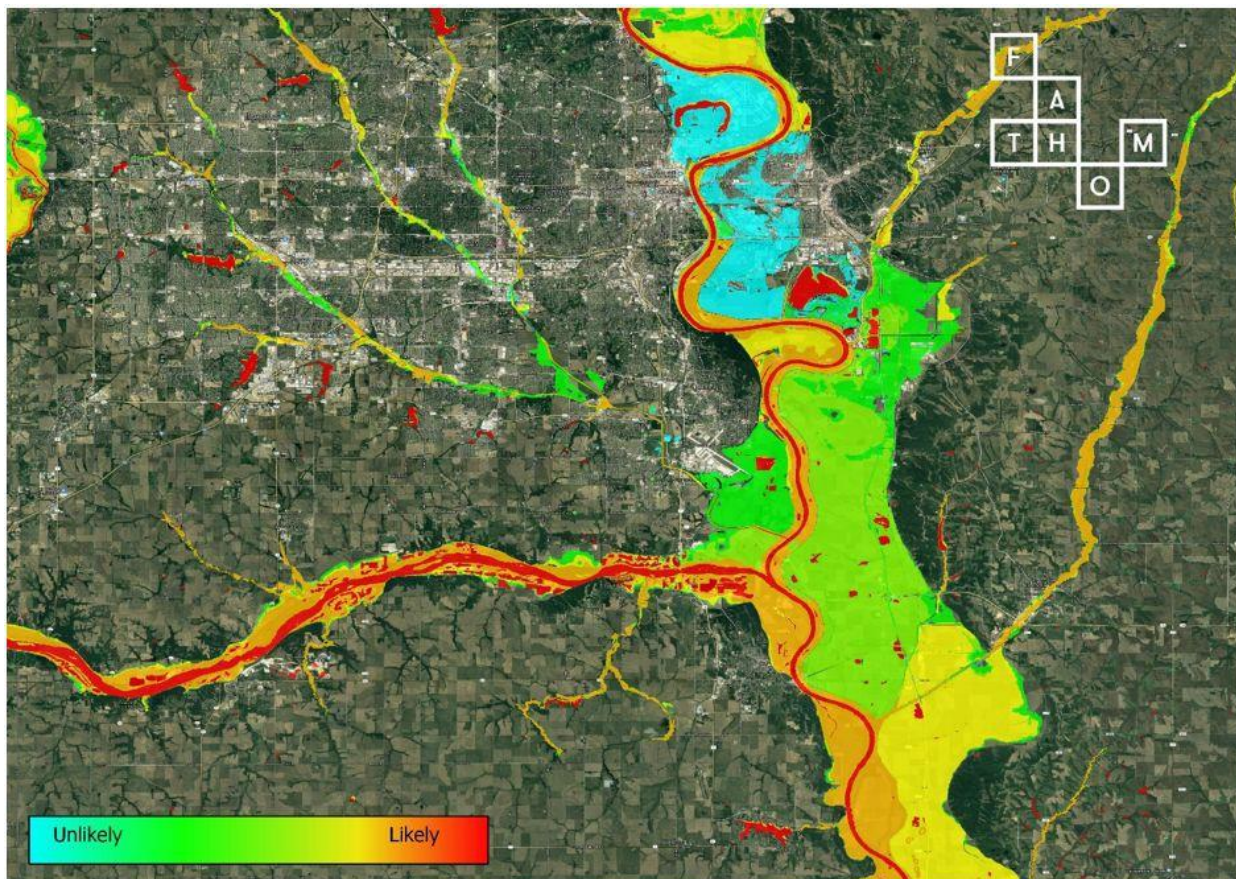


Figure 16: Probabilistic event footprint of 2019 flooding around Omaha, Nebraska.

Localization of National Model

Adaptation

To supplement the model data on hydraulic characteristics, it is also important to capture information on hydro-modifications made through human intervention. In many places, urbanization and development has caused changes to natural flows, and infrastructure protects communities in ways that may not always be captured in the inputs to the flood models. Flood adaptation infrastructure are built works projects constructed in flood prone areas to mitigate the risk of flooding. The purpose of adding flood adaptation structures to our modeling process is to increase the accuracy of our flood inundation layers. Flood adaptation projects can generally be categorized as (1) traditional hard engineering or “grey” infrastructure, such as levees, dams, hardened ditches, etc., or (2) nature-based soft or “green” infrastructure projects designed to

mimic nature, capturing and slowing the advance of floodwaters (e.g. wetland creation, living shorelines, mangrove planting, etc.). Policy-driven, non-structural flood adaptation also exists, however, the following discussion pertains to physical grey and green infrastructure adaptation. Only adaptation measures that are currently built and operational were included in the data. The goal of the exercise is to show how today environment is interacting with flooding, and projecting future projects was deemed too uncertain to include.

There are five modeling mechanisms through which the flood reduction potential of adaptation infrastructure projects are incorporated into the modeled flood inundation layers:

1. Return period — Modeled flooding is excluded within the adaptation structure's service area for all modeled flood events up to the return period year for which the structure is rated (e.g. 10-year, 50-year, 100-year, etc.).
2. Reduction percentage — Modeled flooding is reduced by an assumed percentage within the estimated service area behind an adaptation structure designed to mitigate flooding.
3. Increased infiltration rate — Soil infiltration rates associated with the soils data underpinning FSF internal hydraulic models are modified within the footprints of adaptation projects to increase infiltration within these areas. This mimics the flood reduction impact of these structures.
4. Friction parameter — Modeled flooding in coastal areas is reduced by an assumed percentage within the estimated service area behind adaptation structures such as coral reefs and oyster beds. The momentum of advancing floodwaters is dissipated by friction related to the roughness of the substrate over which the water is moving and the resulting "choppiness" of turbulent surface water. This friction is increased by structures like coral reefs and oyster beds.
5. Elevation model edit — When the elevation of a structure such as a levee or seawall is known, but its return period is not, the structure's average elevation is added to the entire service area to better reflect the protection that structure provides.

Adaptation data collection efforts were divided into two separate work streams: coastal adaptation and inland adaptation. This was related to the dominant influence of tidal flooding and storm surge in coastal regions, whereas these variables don't impact flooding in inland regions. Because of differing flood drivers in coastal and inland regions, adaptation infrastructure projects tend to vary regionally as well. Focusing research efforts through the lens of coastal versus inland flooding allowed the adaptation team to be more focused and efficient throughout our data collection efforts.

Grey Adaptation

Levees

Levees are the most ubiquitous and widely applied adaptation structure incorporated into the FSF modeled flood inundation layers. Levees are an example of "grey" infrastructure and are defined by the US Army Corps of Engineers (USACE) as man-made barriers along a water course,

constructed for the primary purpose of providing flood, storm, and hurricane protection. Levees are used to mitigate flooding in both coastal and inland areas. Levees were incorporated into FSF modeled flood inundation layers using the “return period” mechanism described above.²⁸

Multiple data sources were used to identify levees to be incorporated into the model. The USACE National Levee Database (NLD) is the most comprehensive inventory of levees within the U.S., containing data on roughly 30% of the country’s existing levees (Wing 2017). Nearly all levee data incorporated into the flood models came from NLD. This includes spatial data representing the service areas protected by levees, and the level of protection offered by these levees (e.g. return period maximum for which the levee protects). Additional levee projects were visually identified with the support of a DEM-driven elevation ridge modeling approach. Additional data on levees was derived from news articles, USACE technical manuals, visual inspection of internally modeled flood data, and assumptions based on level of protection offered by levees for which documentation was limited.

Dams

Dams are another nationally ubiquitous type of grey adaptation. They are structures that are designed to impound and utilize the flow of water for multiple purposes, including flood control. Dams are used to mitigate flooding in both coastal and inland areas. Dams were incorporated into FSF modeled flood inundation layers using the “return period” mechanism described above. The National Inventory of Dams (NID) provided the spatial and hazard classification data for dams. Dams in the NID database were assigned return periods associated with the spillway design capacity. When unavailable, the 2012 FEMA Summary of Existing Guidelines for Hydrologic Safety of Dams was utilized to assign return periods. The flood protection service areas of dams were based on availability of inundation maps according to the dam’s Emergency Action Plan. Service areas were captured by downloading available shapefiles or by digitizing them manually. When the spatial extents of a dam’s service area of flood protection couldn’t be found in documentation, service areas were digitized manually. This was done at the location of the adaptation structure by overlaying the internally modeled flooding extents of the return period year that matches the return period for which the structure was designed. This procedure was used to estimate where flooding should logically be removed.

Flooding caused by high tides and storm surge along tidal rivers can also be prevented by dams. Major dams in coastal regions block the influx of tidal floodwaters upstream of the dam’s location on the river. NID was used to identify dams in coastal areas, and service areas upstream of the dam were manually digitized to represent the area where tidal waters cannot feasibly reach, based on elevation of the dam. The area was assumed to reduce flooding by 100% and a maximum return period of protection was assigned, if known.

²⁸ The adaptation return period mechanism is applied during a part of the modeling process where it does have an impact on areas downstream of the adaptation area. Water is not removed from these adaptation zones as a post processing step but rather through its incorporation as a modeling input. The water is “forced” to travel somewhere else since it cannot enter the adaptation zones as defined by the return periods assigned to the applicable adaptation features.

Other Grey Adaptation

Although there were no national adaptation datasets outside the NLD and NID, additional research was conducted to ensure that a comprehensive inventory of adaptation projects beyond levees and dams was incorporated into the modeled flood layers. FEMA Flood Insurance Studies (FIS) provide a detailed narrative of “principal flood problems” and “flood protection measures” that have been documented at the county level throughout the U.S. These FIS reports were used to investigate the presence of any additional flood protection present beyond the levees and dams accounted for in the NLD and NID within a county. The reports also revealed the existence of levees and dams not accounted for within the NLD and NID.

Grey infrastructure projects outside of levees and dams (see Appendix) were often identified using FIS reports and incorporated into the modeled flood layers by generally applying the “return period” method. FIS reports would often provide a return period for which the structure was designed to protect. When a return period wasn’t provided in the FIS, further research was conducted in order to assign a return period. FIS generally did not provide the spatial data representing the service areas for which a project protects. Service areas were therefore digitized manually at the location of the adaptation structure by overlaying the internally modeled flooding extents of the return period year that matches the return period for which the structure was designed. This procedure was used to estimate where flooding should logically be removed. Following inspection of FIS reports, a general web search of the county was completed to find any additional information on adaptation.

Green Adaptation

Green Infrastructure

Green infrastructure adaptation projects are designed to mimic natural systems to reduce flooding. These green adaptation projects rely on natural materials like plants and soils to capture, slow, and infiltrate the advance of floodwaters. This differs from most grey infrastructure projects that reduce flooding by physically excluding water from a service area (e.g. levees, dams, seawalls, etc.), or by rapidly moving flood water out of the structure’s service area (e.g. hardened ditches, emergency spillways, etc.). The flood reduction impacts of green infrastructure were therefore generally incorporated into the modeled flood inundation layers through use of the “reduction percentage” and “increased infiltration rate” methodologies described above. While these features are not part of our main target for this version of the adaptation dataset, when we do find features like storm water basins, catch basins, retention ponds, rain gardens, etc. we include them in our increased infiltration rate methodology. A newer methodology that we have incorporated into our adaptation work stream is called “conveyance” and it will be described in greater detail in the second release of the technical document. In short, the conveyance method incorporates channels into our model that we know have been enhanced, fortified or deepened such that we can apply a return period for inclusion in the water source aspect of our flood modeling process. In the future we would like to figure out ways in which we can find, digitize and include in future iterations.

Soils

The use of soils data was critical to both the overall hydrologic model and the modeling mechanism used to incorporate green infrastructure into FSF modeled flood layers. Internal fluvial and pluvial hydraulic flood models relied on the national USDA Gridded Soil Survey Geographic Database (gSSURGO) to provide the soil infiltration rates required to model overland flows and resultant flooding during flood events. The gSSURGO dataset was used for its superior spatial resolution compared to other national soil database alternatives (e.g. UN Harmonized World Soil Database). Soil infiltration rates were based on hydrologic soil groups assigned to the mapped soil types within gSSURGO. Hydrologic soil groups ranged from Group A (highest infiltration rate; well drained to excessively drained sands or gravelly sands) to Group D (lowest infiltration rate; consists chiefly of clays). Soils were integral in incorporating green infrastructure projects into the modeled flood inundation layers using the “increased infiltration rate” mechanism described above.

Coastal Adaptation

Accounting for the diversified approach to coastal flood risk prevention, from structural flood protection measures to natural solutions, better reflects real world scenarios. Incorporating these adaptation measures into the research stream greatly increases the accuracy of the flood hazard layers. Researching and locating green and grey infrastructure allows areas to be marked as either protected or semi-protected from flooding. Close attention is paid to whether a structure is designed to protect against tidal flooding, storm surge, or both. Additionally in the case of seawalls, the relative heights (elevation above nearby ground surface) is collected in order to model overtopping scenarios. Digital elevation models are altered to reflect these relative heights.

For tracking dams, seawalls, shoreline characteristics, and natural areas, researchers relied on resources such as the State-level GIS databases, Coastal Zone Management Authorities, the Georgetown Climate Adaptation Clearinghouse, and groups such as the American Society of Adaptation Professionals (ASAP). This research is redone at the local level once initial (lower resolution) inundation layers have been produced and analyzed for areas with more than 50 homes inundated. Levees, hurricane barriers, and dams are incorporated from the NLD or the NID, both provided by USACE.

The first round of inundation modeling is exported at a low-resolution raster file. This file is used to determine “hot spots” of flooding by visualizing greatly impacted places. These locations identified through this visualization process are the focus of the next round of research on tidal flooding reports.

News reports, public meeting minutes, foundation funded studies, university papers, environmental, and planning nonprofit reports all provide insights on local histories of flooding and the construction of flood-protection infrastructure. Within these reports it is possible to find information on when certain types of infrastructure was built, how much it cost, who paid for it, the community or area it serves (protects), and what type of scenario it was created for. Within this research stream, a great deal is learned about what type of flooding is most intrusive to a place and what has been done to address it. From there, local or state officials are contacted to see if the adaptation structure has been digitized and if not, then it is included for later digitizing into the final adaptation service area file.

Once as much data as possible is gathered on adaptation structures and the areas they protect from flooding events, these data are digitized into polygon service areas. Some adaptation infrastructure completely protect an area (e.g. levees), while other methods reduce water depth (e.g. pumps). Areas that get completely removed from the flood layers are mostly leveed areas or those behind hurricane protection systems. Attention is paid to what scenario the systems were built to withstand. For example, if a barrier can only sustain floods related to the worst case scenario for a category 2 storm, then flooding will not be removed from hurricane category 3+ scenarios.²⁹

The structure of the adaptation service area files include the name of the structure, the type of structure (see Appendix I), the event the structure protects the area from (tidal, hurricane, pluvial or fluvial), the return period, the soil change category, the reduction percentage, state, the source of the data, the year built, and any additional notes on information relevant to the structure.

Cost Distance Analysis

A cost distance test was used to ensure the accuracy of hazard layers, particularly inundation extents. The hazards are corrected for “unrealistic inundation” by creating a cost surface related to the depth of the water in order to achieve two goals;

1. We refer to that cost internally as a “depth penalty” whereby low depths of water have high costs associated with the ability of water to flow to the next cell. The process has been used to ensure that we if water gets to the point of only being a few cm, that it shouldn’t naturally flow to the next cell, or it should be decreased so that eventually the flow is halted by the depth penalty.
2. We use this approach to account for any water that is hydrologically disconnected from a water source. In both cases, these are applied to fluvial, tidal, and surge events. The nature of pluvial events does not make them eligible for this post-processing step due to the lack of water source.

In application, water levels were calculated using the flood depth layer and low resolution (3m) elevation data. A local water depth maximum was then calculated by assigning the maximum water level value of pixels within a set radius to all pixels within that distance. This process ensures that a water level was calculated for the local water source (e.g. rivers), and for areas adjacent to that source. A new water depth layer was then generated by subtracting high resolution (3 meter) data from the local water level maximum layer. That layer, along with the water source layer, was used as a friction layer to identify areas that were either hydrologically disconnected, or that were protected from a local elevation barrier. Areas identified by this process were flagged for further review by the research team.

²⁹ Since we cannot know how the structure will prevent any given amount of flooding in the event of a failure we assume a total failure at the point past the structure’s design in the modeling process. Having adaptation areas represented in the DEM allows for the model to capture the “x amount of flooding at the point of failure” value automatically when we move to a return period beyond the one indicated for the adaptation feature. For features not represented in the DEM, either because they are very narrow, small or built underground, a total failure is assumed.

Hazard Layer Processing

All explicitly modeled hazard layers were reviewed by the research team for accuracy. Various automated checks were established to observe specific conditions. These checks included a comparison against FEMA floodplains in order to identify areas where the model could benefit from the additional information contained in FEMA flood modeling documents and Flood Insurance Studies. Other sources of validation information included databases of aggregated news reports of flooding created through web scraping and Natural Language Processing. Hazard layers were also reviewed to ensure consistency within the model across return periods, to validate output against claims of historic flooding made available by the National Flood Insurance Program, and to verify flood hazards in areas of high population and large concentrations of impacted structures. This review process also included much manual review from the project team to follow up on the automated checks. This provided for visual review over a significant portion of the data (See Appendix II for information on the Review and Feedback Process).

Creating Cumulative Statistics

Interpolation

The fluvial and pluvial hazard layers in inland areas were created separately, and explicitly modeled at the selected return periods. In order to present a single hazard layer at each return period, the project team needed to determine the joint probability of occurrence for the pluvial and fluvial hazards. Because this naturally varies by location, the team identified the interdependence of the different hazards at locations that had both stream and rainfall gauge data. A historical analysis yielded this interdependence, and values were identified per basin so the layers could be combined into a hazard layer that represents the depth of flooding at the probabilities associated with each return period.

Interpolation to Create Hazard Layers

Due to computational constraints, only a limited number of hazard layers for different years and recurrence intervals were explicitly modeled. However, it was necessary to create hazard layers for all unseen recurrence intervals by the use of statistical methods. The objective here is to use statistical methods to create hazards for several recurrence intervals not explicitly modeled and for all recurrence intervals at 5-year increments from 2020 to 2050, based on the limited number of “seen” raster hazard layers. Based on some initial analysis using explicitly modeled hazard layers at 10 recurrence intervals in 2020, it was shown that for every individual pixel, a non-linear logarithmic relationship can be trained based on every pixel’s ($P_{i,j}$) associated flood depth at a set of specific return periods ($D_{i,j,RP}$) and then predict D at other return periods, where $a_{i,j}$, $b_{i,j}$, and $c_{i,j}$ are parameters that are calibrated for each individual $P_{i,j}$.

The initial model setup to train a larger model for recreating “unseen” hazards required that we had the 10 explicitly modeled hazards listed below (5,10,...,1000) with an approach that held out the green RPs in an attempt to recreate them and use the real values for validation. Ultimately, interpolation was necessary given the scale and scope of the hazard layers we were modeling (9 RPs, across 7 time periods, by 3 climate uncertainties = nearly 200 scenarios for the entire country). Instead, we settled on core scenarios and worked to develop the methods below to fill in the gaps. The first step in this process was to interpolate “within-year/across-RP” using the method below (Figure 16).

Non-Linear Regression:

$$D_{i,j} = a_{i,j} + b_{i,j} \times [\log_{10}(RP)]^{c_{i,j}}$$

Return Periods:

[5, 10, 20, 50, 75, 100, 200, 250, 500, 1000]

Green: “unseen” rasters
 Black: “seen” rasters

Calibration → train a, b, c for each pixel based on the seen Rasters

Validation → test modeled depths against the unseen rasters

Figure 16. Methodology for training model to interpolate hazard layers.

The results of the interpolation was ultimately trained to the equation above so that every pixel’s explicitly modeled hazards (seen raster’s) could be used to interpolate hazards that were not modeled (unseen raster’s). The model selection was based on our ability to minimize the error in the newly interpolated unseen raster’s per the results shown below in Figure 17.

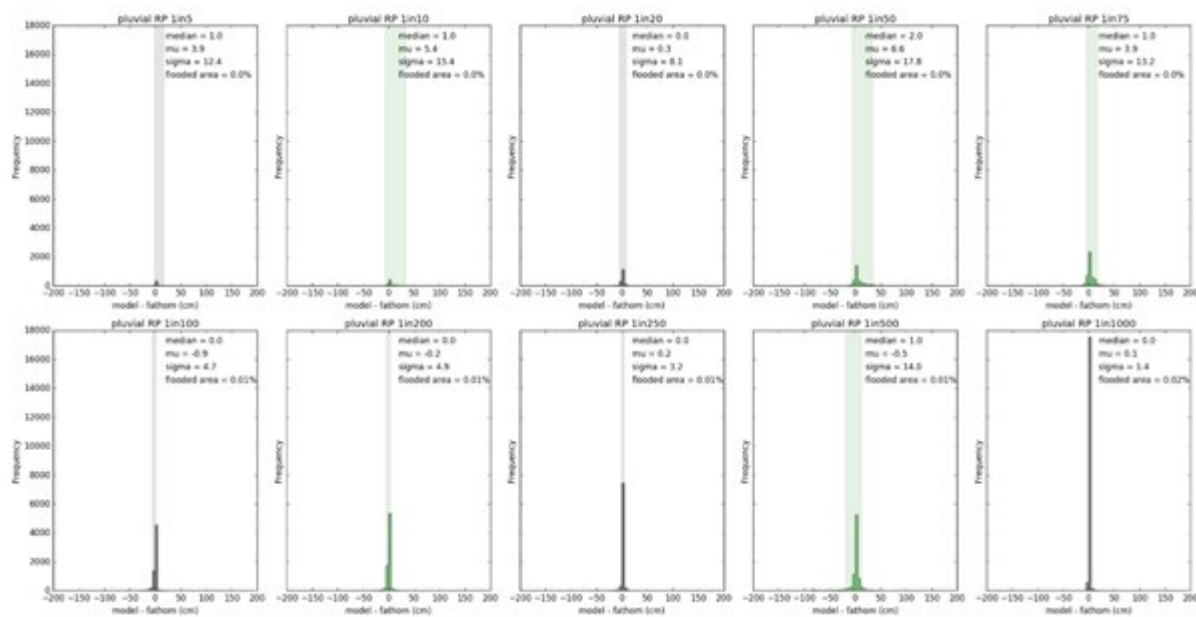


Figure 17. Validation of method for reproducing “unseen” hazard layers (error in cm).

The within year interpolation (above) was applied to both the 2020 and the 2050 modeled hazards and then a weighing function was developed to allow for the interpolation of unseen hazards between years (left panel in Figure 18) and then a method was required to interpolate across years to fill in the grid (right panel in Figure 19).

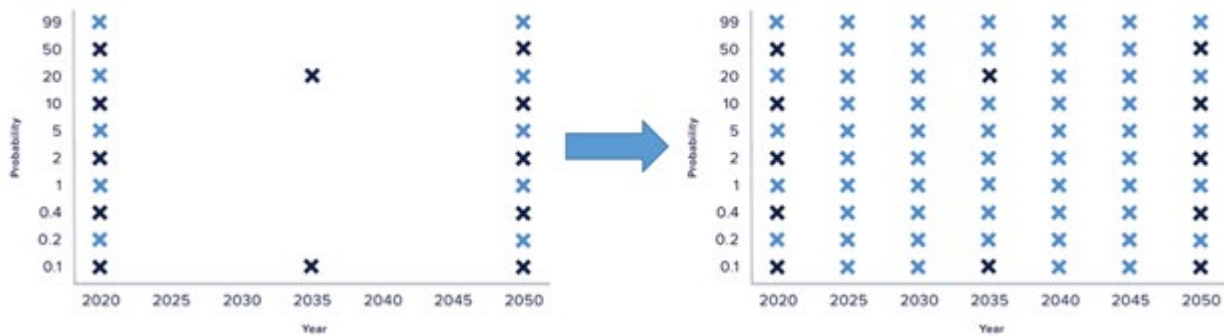


Figure 18. Interpolation process (dark blue were explicitly modeled, light blue were interpolated).

The method used to perform the across year interpolation is a 2D interpolation whereby two weights are produced at given RPs in 2035 and a surface is fit to those weights in order to interpolate any hazard across any year within the scope of our data production. The process is a series of piecewise linear interpolations at the largest and smallest RPs with a surface fit in between (see Figure 19).

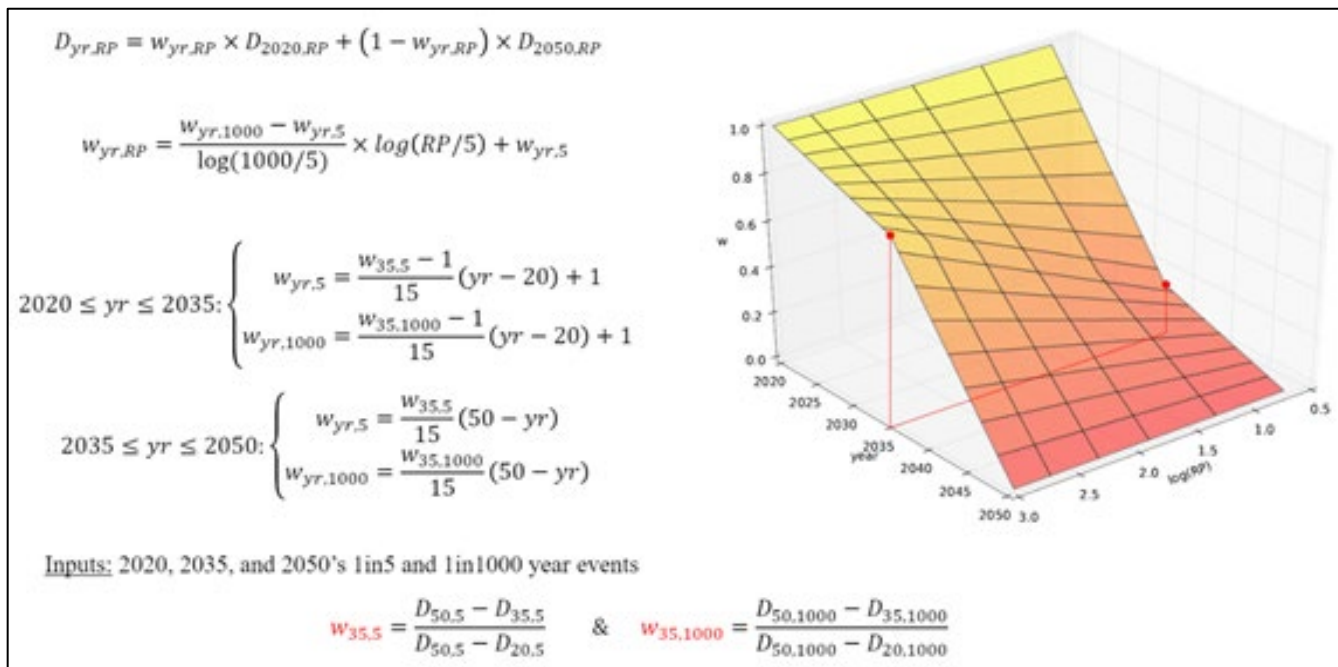


Figure 19. 2D Interpolation of missing hazards across years.

Cumulative Statistics

Upon completion of the interpolation processes across recurrence interval and time, every pixel-based location throughout the U.S. has a modeled water depth at specific recurrence intervals for every five years. This enabled the creation of a single set of cumulative statistics to communicate aggregated flood risk at any given location. Through user testing and research, the project team then chose several significant depths of flooding (e.g. 1", 6", 1', 5', etc.) that could cause different levels of damage to structures and determined the overall risk of that depth being realized at a location in a given year. Additionally, the project team was able to use the relationship of likelihood of reaching those same depth thresholds over time to create a cumulative likelihood over a chosen duration of time. This was achieved by first calculating that likelihood of depth reaching, or exceeding, each depth threshold in any given year. Probability distribution functions were fit to match the hazard layer depth values at each property (e.g. 0.1% layer 5 ft., 0.2% layer 2 ft., 10% layer 0.2 ft., 20% layer 0 ft., etc.). Figure 20 represents the process by which for each property specific PDF the exceedance probability of each depth threshold was obtained. Additional curves were fit to the exceedance probabilities at each 5-year interval in order to generate exceedance probabilities for the intervening years. The curve value for each year was utilized to generate the cumulative likelihood (Figure 21).

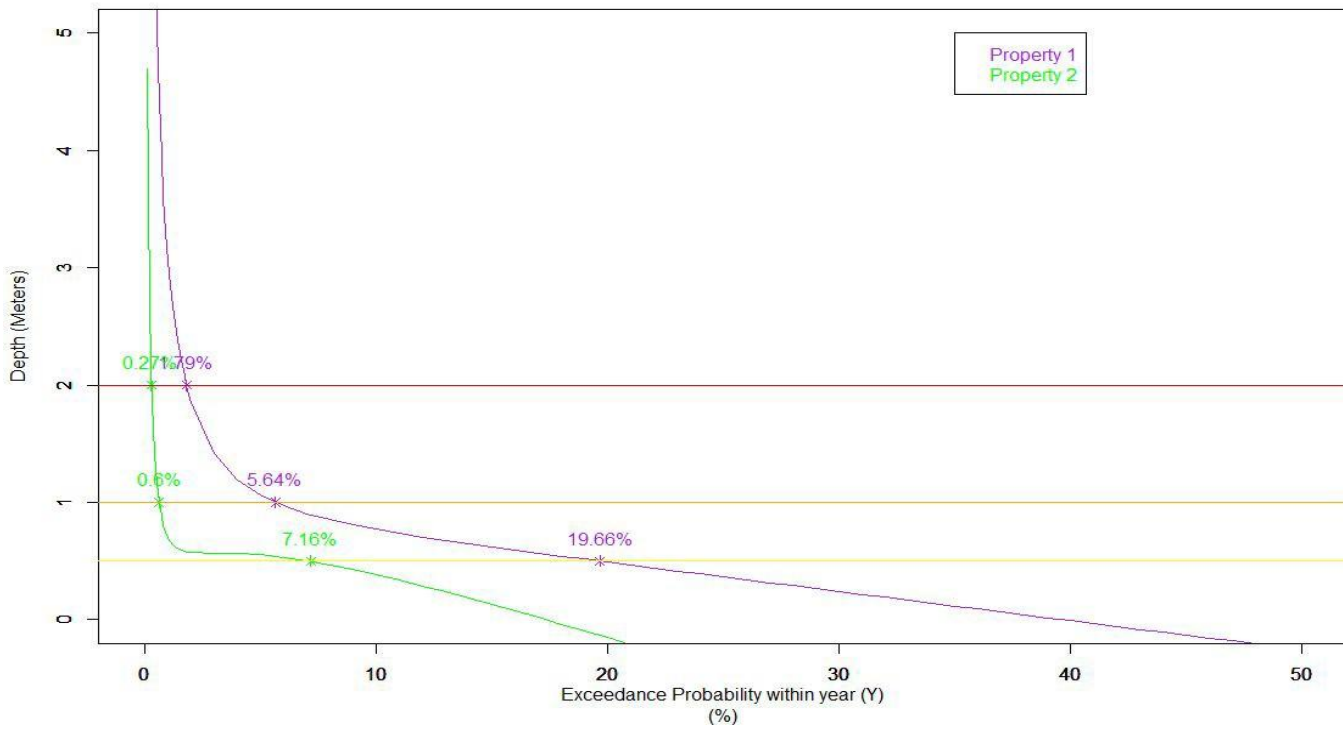


Figure 20. Extracting depth exceedance probabilities within year.

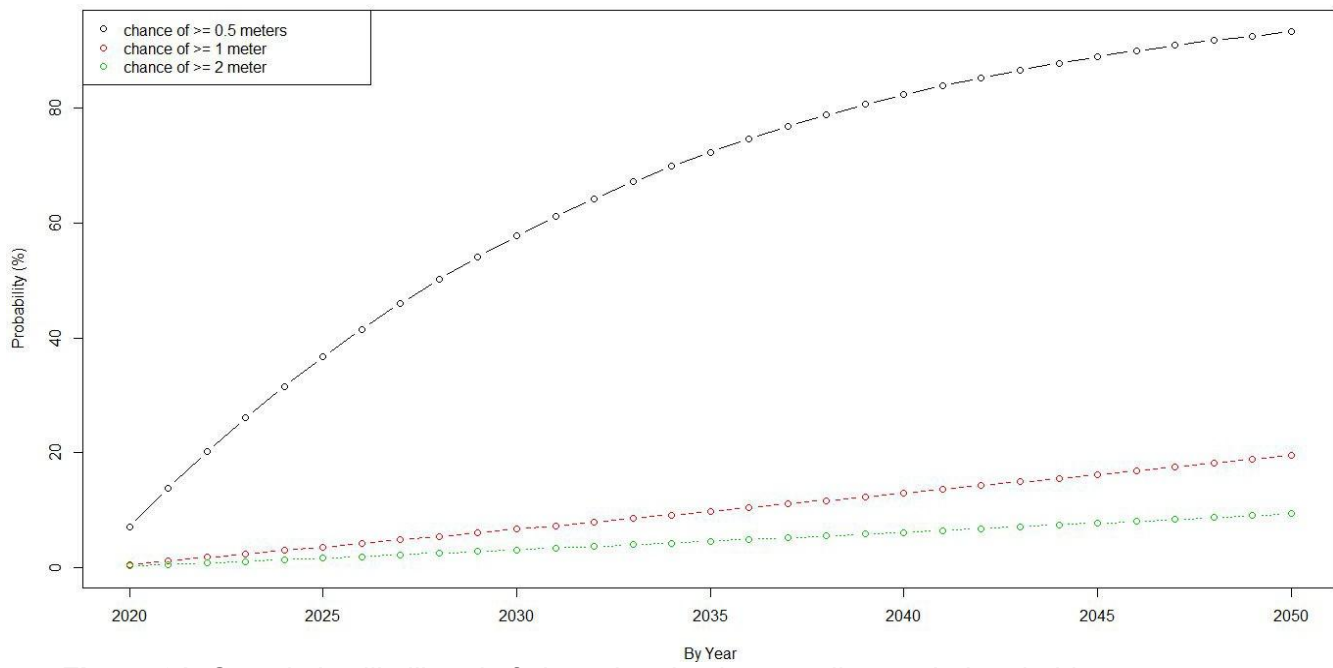


Figure 21. Cumulative likelihood of observing depth exceeding each threshold.

Discussion and Limitations

Discussion

The sections above outline the development of a NFM that encompasses inland and coastal flooding risk into a single comprehensive model. Both the inland and coastal models are created to account for climate uncertainty current (2020) and into the future (2050) in the unique ways that climate will impact risk as a non-stationary process. The inland models are developed using LISFLOOD and Fathom's state-of-the-art national scale fluvial/pluvial risk models with the added refinements of being downscaled to a higher resolution in order to facilitate the development of risk profiles for every property in the non-coastal U.S. Likewise, coastal risk models are developed using GEOCLAW, with significant alignment and calibration checks in comparison to ADCIRC, and downscaled to the same high resolution as the inland models in order to produce the same flooding risk profile at the property level. The coastal models are further coupled with localized tidal water levels and the same fluvial/pluvial models developed for the inland risk models to allow for a full range of risk to be accounted for in the more complex coastal regions of the country.

The high resolution hazard layers in both the inland and coastal contexts are reviewed and refined across multiple iterations to account for issues associated with discontinuity, overly aggressive flooding extents, the absence of flooding in areas with flooding reports/FEMA claims, and missing adaptation infrastructure. The resulting hazard layers are then trained in order to understand their relationship across return-periods within the current year state (2020) in order to interpolate missing periods and then trained across future years using a strategic set of explicitly modeled hazards through 2050. The resulting set of high-resolution interpolated hazards allows for the production of cumulative statistics at a property level for selected flooding depths, across selected return periods, for every property in the U.S.

Limitations

There are a number of known limitations that must be understood in the interpretation and use of the NFM. Those limitations relate primarily to the original resolution of the hydraulic and hydrodynamic flood models as well as the introduction of climate uncertainty into the larger risk modeling scheme. The limitations are not unknown to risk modelers and the methods outlined in the document above actually reduce the impact of these limitations significantly when accounting for the scope of the model. That being said, these limitations should be understood in order to evaluate the utility of the model for any single purpose.

- Even though there are thousands of usable river gauges in the U.S., there are still ungauged catchments that require estimation methods for flow. In these areas, it is more likely hazard layers will under or over represent flood risk. This limitation is similar to the sparsity of gauges along the coasts that measure water levels, which is particularly more important for estuary like tidal water bodies that are behind barrier islands. The tidal

harmonics in these locations are less likely to be accurately represented, and it is harder in these areas to validate and calibrate storm surge model behavior.

- Since the hydraulic modeling is executed at 30 meter horizontal resolution using a 30 meter DEM, it is possible that smaller elevation features affecting the flow of water may be missed. A series of GIS steps using higher resolution elevation datasets (1-3 meters) attempts to identify any elevation feature that can impede flow, which leads to either DEM updates or identification of areas protected by adaptation, however some areas are likely to be missed.
- The adaptation mesh utilized in GeoClaw is computationally efficient, however if the mesh resolution is too low in key areas water behavior is likely to be mischaracterized. This is particularly true in narrower water bodies such as canals. Therefore, water level estimates in these locations can deviate from what would be obtained if a higher resolution mesh were used to propagate water through narrow passageways.
- The exact climate response to already emitted greenhouses gases is unknown, and therefore possible sea level, hurricane intensity, hurricane precipitation, non-hurricane precipitation, and stream discharge projected changes will deviate from reality. In addition, the choice of RCP 4.5 assumes a concentration pathway with no guarantee of occurring. By creating hazard layers reflective of both the high and low ends of the climate models some uncertainty is being communicated, but it is possible some climate responses will end up outside the modeled extremes.
- A key component of flooding modeling is accurate elevation inputs, and due to the nature of elevation projects some areas have older, less accurate DEMs. In these areas, the hazard layers are more likely to miss the impact of recent development or key elevation features than can impact hydraulic modeling.
- Surge effects were not included on the Great Lakes or other large, non-ocean water bodies. This is a model feature in development that will be added in a future version.
- The existence and operation of flood control structures and adaptation measures can significantly impact flooding and therefore model results. The NFM attempts to account for these measures as much as possible. However, several limitations should be acknowledged for the adaptation data used in modeled flood layers.
 - Service areas were sometimes digitized manually when the spatial extents of an adaptation structure's service area couldn't be found in the available documentation. This was done at the location of the adaptation structure by overlaying the internally modeled flooding extents of the return period year that matches the return period for which the structure was designed. This procedure was used to estimate where flooding should logically be removed, but is in no way an exact science.
 - Flood risk related to an adaptation project's structural integrity was not accounted for. Structures were universally assumed to protect for all flood events up to the

documented return period level of protection they were designed for, regardless of structure age, risk of degradation, lack of maintenance, etc. This notably includes dams and levees, where the NFM does not quantify the risk of failure.

- The “increased infiltration rate” mechanism used to incorporate green infrastructure into the flood models is a simplified approximation for how these types of structures reduce flooding. The flood reduction capabilities of green infrastructure projects are far more nuanced than this simple mechanism, but this method does offer a simple and consistent solution to account for the increased infiltration rates offered by the pervious surfaces associated with these types of structure.
- Very few comprehensive adaptation databases exist at the municipal/county level, and no known comprehensive datasets exist at the state or national level. The development of a comprehensive national adaptation dataset for use within our flood models required a level of effort greater than what could be produced by the five team members tasked with this objective. In the interest of time and efficiency, geographic research areas for adaptation data collection were prioritized. A research approach was therefore developed, limiting areas of investigation to the 10 most populous counties in each state.

References

- Akhtar, M., Ahmad, N., Booij, M.J., 2008. The impact of climate change on the water resources of Hindukush–Karakorum–Himalaya region under different glacier coverage scenarios. *J. Hydrol.* 355, 148–163.
- Archuleta, C.M., Constance, E.W., Arundel, S.T., Lowe, A.J., Mantey, K.S., and Phillips, L.A., 2017, The National Map seamless digital elevation model specifications: U.S. Geological Survey Techniques and Methods, book 11, chap. B9, 39 p., <https://doi.org/10.3133/tm11B9>.
- Barnes, R. (2017). Parallel non-divergent flow accumulation for trillion cell digital elevation models on desktops or clusters. *Environmental modelling & software*, 92, 202-212.
- Beck, H. E., A. I. J. M. van Dijk, A. de Roo, D. G. Miralles, T. R. McVicar, J. Schellekens, and L. A. Bruijnzeel (2016), Global-scale regionalization of hydrologic model parameters, *Water Resour. Res.*, 52, 3599–3622.
- Bergstrom, S. (1992), The HBV model—its structure and applications, SMHI Rep. RH 4, Swed. Meteorol. and Hydrol. Inst., Norrkoping, Sweden.
- Bergström, S., Carlsson, B., Gardelin, M., Lindström, G., Pettersson, A., Rummukainen, M., 2001. Climate change impacts on runoff in Sweden assessments by global climate models, dynamical downscaling and hydrological modelling. *Clim. Res.* 16, 101–112.
- Beven, K. (2006) A manifesto for the equifinality thesis. *Journal of Hydrology*, 320, 1-2, 18-36.
- Bloschl, P. G., Sivapalan, P. M., Wagener, P. T., Viglione, D. A., and Savenije, P. H. (2013). Runoff Prediction in Ungauged Basins: Synthesis across Processes, Places and Scales, Cambridge Univ. Press, Cambridge, U. K.
- Booij, N., Ris, R. C., & Holthuijsen, L. H. (1999). A third-generation wave model for coastal regions 1. Model description and validation. *Journal of Geophysical Research: Oceans*. <https://doi.org/10.1029/98JC02622>
- Bunya, S., Dietrich, J. C., Westerink, J. J., Ebersole, B. A., Smith, J. M., Atkinson, J. H., ... Roberts, H. J. (2010). A High-Resolution Coupled Riverine Flow, Tide, Wind, Wind Wave, and Storm Surge Model for Southern Louisiana and Mississippi. Part I: Model Development and Validation. *Monthly Weather Review*, 138(2), 345–377. <https://doi.org/10.1175/2009MWR2906.1>
- Chavas, D.R., N. Lin, and K. Emanuel, 2015: A Model for the Complete Radial Structure of the Tropical Cyclone Wind Field. Part I: Comparison with Observed Structure. *J. Atmos. Sci.*, 72, 3647–3662, <https://doi.org/10.1175/JAS-D-15-0014.1>.
- Cloke, H.L., Wetterhall, F., He, Y., Freer, J.E., Pappenberger, F., 2013. Modelling climate impact on floods with ensemble climate projections. *Q. J. R. Meteorol. Soc.* 139, 282–297.

Cohen Liechti, T., Matos, J. P., Boillat, J. L., and Schleiss, A. J. (2012). Comparison and evaluation of satellite derived precipitation products for hydrological modeling of the Zambezi River Basin. *Hydrol. Earth Syst. Sci.*, 16, 489–500.

Dee, D. P., et al. (2011). The ERA-Interim reanalysis: Configuration and performance of the data assimilation system. *Q. J. R. Meteorol. Soc.*, 137, 553–597. doi:10.1002/qj.828.

Dietrich, J. C., Zijlema, M., Westerink, J. J., Holthuijsen, L. H., Dawson, C., Luettich, R. A. Stone, G. W. (2011a). Modeling hurricane waves and storm surge using integrally-coupled, scalable computations. *Coastal Engineering*. <https://doi.org/10.1016/j.coastaleng.2010.08.001>

Dietrich, J. C., Zijlema, M., Westerink, J. J., Holthuijsen, L. H., Dawson, C., Luettich, R. A., ... Stone, G. W. (2011b). Modeling hurricane waves and storm surge using integrally-coupled, scalable computations. *Coastal Engineering*, 58(1), 45–65. <https://doi.org/10.1016/j.coastaleng.2010.08.001>

Emanuel, Kerry A. "A fast intensity simulator for tropical cyclone risk analysis." *Nat Hazards* (2017) 88: 779. <https://doi.org/10.1007/s11069-017-2890-7>.

Emanuel, Kerry A. "Tropical cyclones in CMIP5 simulations." *Proceedings of the National Academy of Sciences* Jul 2013, 110 (30) 12219-12224; DOI: 10.1073/pnas.1301293110.

Feldmann, Monika, Kerry Emanuel, Laiyin Zhu, and Ulrike Lohmann. "Estimation of Atlantic Tropical Cyclone Rainfall Frequency in the United States." *Journal of Applied Meteorology and Climatology* 58.11 (2019). DOI: <https://doi.org/10.1175/JAMC-D-19-0011.1>.

Ferreira, C. M., Olivera, F., & Irish, J. L. (2014). Arc StormSurge: Integrating Hurricane Storm Surge Modeling and GIS. *JAWRA Journal of the American Water Resources Association*, 50(1), 219–233.

Forbes, C., Luettich, R. A., Mattocks, C. A., Westerink, J. J., Forbes, C., Jr., R. A. L., ... Westerink, J. J. (2010). A Retrospective Evaluation of the Storm Surge Produced by Hurricane Gustav (2008): Forecast and Hindcast Results. *Weather and Forecasting*, 25(6), 1577–1602. <https://doi.org/10.1175/2010WAF2222416.1>

Gao, Y. C., and Liu, M. F. (2013). Evaluation of high-resolution satellite precipitation products using rain gauge observations over the Tibetan Plateau. *Hydrol. Earth Syst. Sci.*, 17, 837–849.

Gesch, D., Evans, G., Mauck, J., Hutchinson, J., & Carswell Jr, W. J. (2009). The national map—Elevation. US geological survey fact sheet, 3053(4).

Garratt, J. R. (1977). Review of Drag Coefficients over Oceans and Continents. *Monthly Weather Review*, 105(7), 915–929.

Garzon, J., & Ferreira, C. (2016). Storm Surge Modeling in Large Estuaries: Sensitivity Analyses to Parameters and Physical Processes in the Chesapeake Bay. *Journal of Marine Science and Engineering*. <https://doi.org/10.3390/jmse4030045>

Garzon, J., Ferreira, C., Garzon, J. L., & Ferreira, C. M. (2016). Storm Surge Modeling in Large Estuaries: Sensitivity Analyses to Parameters and Physical Processes in the Chesapeake Bay. *Journal of Marine Science and Engineering*, 4(3), 45. <https://doi.org/10.3390/jmse4030045>

He, Y., Wetterhall, F., Cloke, H. L., Pappenberger, F., Wilson, M., Freer, J., and McGregor, G. (2009). Tracking the uncertainty in flood alerts driven by grand ensemble weather predictions. *Meteorol. Appl.*, 16, 91–101. doi:10.1002/met.132.

Hinzman, L.D., Kane, D.L., 1991. Snow hydrology of a headwater arctic basin: 2. Conceptual analysis and computer modeling. *Water Resour. Res.* 27, 1111–1121.

Huffman, G. J., Bolvin, D. T., Nelkin, E. J., Wolff, D. B., Adler, R. F., Gu, G., Hong, Y., Bowman, K. P., and Stocker, E. F. (2007). The TRMM Multisatellite Precipitation Analysis (TMPA): Quasi-global, multiyear, combined-sensor precipitation estimates at \square ne scales. *J. Hydrometeorol.*, 8, 38–55. doi:10.1175/JHM560.1.

Joyce, R. J., Janowiak, J. E., Arkin, P. A., and Xie, P. (2004), CMORPH: A method that produces global precipitation estimates from passive microwave and infrared data at high spatial and temporal resolution. *J. Hydrometeorol.*, 5, 487–503.

Kalnay E, Kanamitsu M, Kistler R, Collins W, Deaven D, Gandin L, Iredell M, Saha S, White G, Woolen J, Zhu Y, Leetmaa A, Reynolds R, Chelliah M, Ebisuzaki W, Higgins W, Janowiak J, Mo KC, Ropelewski C, Wang J, Jenne R, Joseph D (1996) The NCEP/NCAR 40-year reanalysis project. *Bull Am Meteorol Soc* 77(3):437–471.

Knapp, K. R., M. C. Kruk, D. H. Levinson, H. J. Diamond, and C. J. Neumann, 2010: The International Best Track Archive for Climate Stewardship (IBTrACS): Unifying tropical cyclone best track data. *Bulletin of the American Meteorological Society*, 91, 363–376.

Knapp, K. R., H. J. Diamond, J. P. Kossin, M. C. Kruk, C. J. Schreck, 2018: International Best Track Archive for Climate Stewardship (IBTrACS) Project, Version 4. Version 4 revision 00. NOAA National Centers for Environmental Information. non-government domain
<https://doi.org/10.25921/82ty-9e16>. Retrieved October 20, 2019.

Kopp, Robert E., Radley M. Horton, Christopher M. Little, Jerry X. Mitrovica, Michael Oppenheimer, D. J. Rasmussen, Benjamin H. Strauss, Claudia Tebaldi. Probabilistic 21st and 22nd century sea-level projections at a global network of tide-gauge sites. *Earth's Future* 2.8 (2014): 383-406. DOI: 10.1002/2014EF000239

Keef, C., Svensson, C., & Tawn, J. A. (2009). Spatial dependence in extreme river flows and precipitation for Great Britain. *Journal of Hydrology*, 378(3-4), 240–252. <https://doi.org/10.1016/j.jhydrol.2009.09.026>.

Kerr, P. C., Martyr, R. C., Donahue, A. S., Hope, M. E., Westerink, J. J., Luettich, R. A., ... Westerink, H. J. (2013). U.S. IOOS coastal and ocean modeling testbed: Evaluation of tide, wave, and hurricane surge response sensitivities to mesh resolution and friction in the Gulf of Mexico: IOOS TESTBED-RESOLUTION AND FRICTION. *Journal of Geophysical Research: Oceans*, 118(9), 4633–4661. <https://doi.org/10.1002/jgrc.20305>

Kidd, C., Bauer, P., Turk, J., Huffman, G. J., Joyce, R., Hsu, K. L., and Braithwaite, D. (2012). Intercomparison of high-resolution precipitation products over Northwest Europe. *J. Hydrometeorol.*, 13, 67–83. doi:10.1175/JHM-D-11-042.1.

Lehner, B., and Grill, G. (2013). Global river hydrography and network routing: Baseline data and new approaches to study the world's large river systems. *Hydrological Processes*, 27(15), 2171–2186. <https://doi.org/10.1002/hyp.9740>.

Luettich, R. A., Westerink, J. J., & Scheffner, N. (1992). ADCIRC: an advanced three-dimensional circulation model for shelves coasts and estuaries, report 1: theory and methodology of ADCIRC-2DDI and ADCIRC-3DL. *Dredging Research Program Technical Report DRP-92-6*, U.S. Army Engineers Waterways Experiment Station, Vicksburg, MS.

Mandli, Kyle T., and Clint N. Dawson. "Adaptive Mesh Refinement for Storm Surge." *Ocean Modelling* 75 (2014): 36–50. DOI: 10.1016/j.ocemod.2014.01.002.

Marsooli, R., Lin, N., Emanuel, K. et al. "Climate change exacerbates hurricane flood hazards along US Atlantic and Gulf Coasts in spatially varying patterns." *Nat Commun* 10, 3785 (2019) doi:10.1038/s41467-019-11755-z.

Meinshausen, M.; et al. (November 2011), "The RCP greenhouse gas concentrations and their extensions from 1765 to 2300", *Climatic Change*, 109 (1–2): 213–241, doi:10.1007/s10584-011-0156-z.

Miller, R.J., A.J. Schrader, C.R. Sampson, and T.L. Tsui, 1990: The Automated Tropical Cyclone Forecasting System (ATCF). *Wea. Forecasting*, 5, 653–660, [https://doi.org/10.1175/1520-0434\(1990\)005<0653:TATCFS>2.0.CO;2](https://doi.org/10.1175/1520-0434(1990)005<0653:TATCFS>2.0.CO;2).

Neal, J.C., Fewtrell, T.J., and Trigg, M. (2009), Parallelisation of storage cell flood models using OpenMP, *Environ. Modell. Software*, 24, 872–877, doi:10.1016/j.envsoft.2008.12.004.

Neal, J.C., Fewtrell, T.J., Bates, P.D., and Wright, N.G., (2010), A comparison of three parallelisation methods for 2D flood inundation models, *Environ. Modell. Software*, 25, 398–411, doi:10.1016/j.envsoft.2009.11.007.

Neal, J.C., Schumann, G., and Bates, P.D., (2012), A subgrid channel model for simulating river hydraulics and floodplain inundation over large and data sparse areas, *Water Resour. Res.*, 48, W11506, doi:10.1029/2012WR012514.

Neal, J.C., Dunne, T., Sampson. C.C., Smith, A., & Bates, P., (2018). Optimisation of the two-dimensional hydraulic model LISFOOD-FP for CPU architecture, *Environmental Modelling and Software*, 107, 148-157, doi: 10.1016/j.envsoft.2018.05.011

O'Callaghan, J. F., & Mark, D. M. (1984). The extraction of drainage networks from digital elevation data. *Computer vision, graphics, and image processing*, 28(3), 323-344.

Pytides, version 0.0.6. Maritime Planning Associates, 2018. GitHub,

[https://github.com/maritimeplanning/pytides.](https://github.com/maritimeplanning/pytides)

Quinn, N., Bates, P.D., Neal, J., Smith, A., Wing, O., Sampson, C., Smith, J., and Heffernan, J. (2019). The spatial dependence of flood hazard and risk in the United States. *Water Resources Research*, 55, 1890-1911. <http://doi.org/10.1029/2018WR024205>.

Sampson, C. C., Bates, P.D., Neal, J.C., & Horritt, M.S. (2013), An automated routing methodology to enable direct rainfall in high resolution shallow water models, *Hydrol. Processes*, 27, 467–476, doi:10.1002/hyp.9515.

Sampson, C. C., Smith, A. M., Bates, P. D., Neal, J. C., Alleri, L., and Freer, J. E. (2015). A high-resolution global flood hazard model. *Water Resources Research*, 51, 7358–7381. <https://doi.org/10.1002/2015WR016954>.

Sampson, C. C., Fewtrell, T. J., O'Loughlin, F., Pappenberger, F., Bates, P. B., Freer, J. E., and Cloke, H. L. (2014), The impact of uncertain precipitation data on insurance loss estimates using a Flood Catastrophe Model. *Hydrol. Earth Syst. Sci. Discuss.*, 11, 31–81. doi:10.5194/hessd-11-31-2014.

Seibert, J., and M. J. P. Vis (2012), Teaching hydrological modeling with a user-friendly catchment-runoff-model software package, *Hydrol. Earth Syst. Sci.*, 16(9), 3315–3325.

Seibert, J., 1997. Estimation of Parameter Uncertainty in the HBV ModelPaper presented at the Nordic Hydrological Conference (Akureyri, Iceland-August 1996). *Hydrol. Res.* 28, 247–262.

Simley, J. D., & Carswell Jr, W. J. (2009). The national map—hydrography. US Geological Survey Fact Sheet, 3054(4).

Smith, A., Sampson, C., and Bates, P. (2015), Regional flood frequency analysis at the global scale. *Water Resour. Res.*, 51, 539–553. doi: 10.1002/2014WR015814.

Smith, A., Freer, J., Bates, P., Sampson, C., 2014. Comparing ensemble projections of flooding against flood estimation by continuous simulation. *J. Hydrol.* 511, 205–219.

Teutschbein, C., Wetterhall, F., Seibert, J., 2011. Evaluation of different downscaling techniques for hydrological climate-change impact studies at the catchment scale. *Clim. Dyn.* 37, 2087–2105.

Tozer, B., Sandwell, D. T., Smith, W. H. F., Olson, C., Beale, J. R., & Wessel, P. (2019). Global bathymetry and topography at 15 arc sec: SRTM15+. *Earth and Space Science*. 6. <https://doi.org/10.1029/2019EA000658>

USGS. (2019). *Guidelines for Determining Flood Flow Frequency: Bulletin 17*. Chapter 5 of Section B, Surface Water: Book 4, Hydrologic Analysis and Interpretation.

Vitousek, S, Barndard, PL & P Limber. (2017). Can Beaches Survive Climate Change? *Earth and Space Science*. Apr. 2017.

Wahl, T., Jain, S., Bender, J., Meyers, S.D., Luther, M.E. (2015). Increasing risk of compound

flooding from storm surge and rainfall for major US cities. *Nature Climate Change*, 5, 1093-1097, doi:10.1038/nclimate2736

Ward, J. P., Couasnon, A., Eilander, D., Haigh, I.D., Hendry, A., Muis, S., Veldkamp, T.I.E.,

Winsemius, H.C., Wahl, T. (2018). Dependence between high sea-level and high river discharge increases flood hazard in global deltas and estuaries. *Environmental Research Letters*, 13, 084012, doi: <https://doi.org/10.1088/1748-9326/aad400>.

Xie, P., Chen, M., Yang, S., Yatagai, A., Hayasaka, T., Fukushima, Y., and Liu, C. (2007), A gauge-based analysis of daily precipitation over East Asia. *J. Hydrometeorology*, 8, 607–626. doi:10.1175/JHM583.1.

Appendix I. Table of adaptation structure types included in NFM

Project Type	Green/ Grey/ Both	Coastal /Inland/ Both	How applied to flood model (return period, reduction %, soil change, DEM edit, friction parameter)	Description
Acquisition	Both	Both	Soil change	Acquisition of a property in a floodway that is intended to reduce the risk of future flooding.*
Beach nourishment	Green	Coastal	DEM edit	The process of adding sediment to a beach to provide a buffer to coastal erosion as part of a coastal defense scheme.
Bioswale	Green	Inland	Soil change	Channels designed to convey stormwater runoff.
Buy-out	Green	Both	Soil change	Acquisition of a property in a floodway that is intended to reduce the risk of future flooding.
Coral reef	Green	Coastal	Friction parameter	Reef structures that protect the shoreline from wave action.
Culvert	Grey	Both	Reduction %	A structure that allows water to flow from one side to another, like in the case of a road.
Dam	Grey	Both	Return Period, Reduction %	A barrier constructed to hold back water.
Detention	Both	Inland	Soil change,	An area meant to store water to

basin			Return period	Protect against flooding for a limited period of time.
Ditch	Grey	Inland	Soil change	A narrow channel used for drainage.
Dune	Green	Coastal	DEM edit	A mound of sand or sediment that can act as a barrier to flooding.
Dike	Green	Both	Return period, Reduction %	A wall or embankment that works to prevent flooding.
Earthen berm	Green	Both	Return period, Reduction %	A ledge made of soil that can prevent flooding.
Elevated roads	Grey	Both	DEM edit	A road raised specifically to prevent flooding.
Flood wall	Grey	Inland	Return period, Reduction %	A wall that protects from flooding.
Floodplain restoration	Green	Inland	Soil change	The process of restoring a river's floodplain.
Infiltration basin	Grey	Inland	Soil change, Return period	A vegetated area where stormwater runoff is stored and then infiltrated into the soil
Levee	Grey	Both	Return period, Reduction %	An embankment built to prevent flooding from a river.
Living breakwater	Green	Coastal	Friction parameter	An offshore structure designed as a barrier to limit wave energy.
Living shoreline	Green	Coastal	Friction parameter, soil change, reduction %	A shoreline stabilization technique that uses vegetation and can slow down wave action.
Mangrove	Green	Coastal	Friction parameter, reduction %	A species of tree with an extensive root system that slows down wave action.
Marsh/wetland	Green	Both	Soil change,	Construction of a marsh or

creation			reduction	Wetland on a site that never was before. A place for water to be stored, therefore reducing flooding inland of it.
Marsh/wetland restoration	Green	Both	Soil change, reduction	Restoration of a marsh or wetland. A place for water to be stored, therefore reducing flooding inland of it.
Open space preserve	Green	Both	Soil change, reduction	An area of protected or conserved land.
Oyster reef	Green	Coastal	Friction parameter	An oyster habitat that can reduce wave momentum by increasing friction at the bed and/or surface.
Pervious pavement	Grey	Inland	Soil change	Porous concrete that allows rainwater to pass through it, avoiding runoff which exacerbates local flooding.
Pipe	Grey	Inland	Return period, Reduction %	A structure that moves water from one place to the next.
Pump, deployable	Grey	Both	Return period. Reduction %	A mobile structure that moves away large volumes of water.
Pump station	Grey	Both	Reduction %	A permanent structure that moves away large volumes of water.
Rain garden	Green	Inland	Soil change	An area that collects rainwater from a road, driveway, or street and allows time for water to soak into the ground or be carried away.
Retention pond	Green	Inland	Soil change, Reduction %, Return period	An area designed with additional storage capacity to hold surface water runoff during rainfall events.
Seawall	Grey	Coastal	Reduction %, Return period	A coastal defense structure that mitigates flooding by protecting for the action of the tides and waves.

Sediment accretion	Grey	Coastal	Soil change	Coastal sediment returning to the visible portion of a beach or shoreline.
Stormwater system upgrade	Grey	Both	Reduction %, return period	An update to an existing system that better handles flood water during rain events.
Spillway	Grey	Both	Return period	A structure used to provide controlled release of water from a dam or levee.
Stormwater vault	Grey	Both	Return period, soil change	An underground structure designed to manage excess stormwater runoff.
Tide gate	Grey	Coastal	Return period, Reduction %	An opening where the tide can move freely in one direction but then closes automatically or manually to prevent water from flowing in the other direction.
Valve	Grey	Coastal	Return period, reduction %	Also known as a backflow preventer, has an automatic mechanism that prevents water from flowing up from the water source through a stormwater pipe and onto the street once the pipe is at capacity.
Weir	Grey	Inland	Return period	A small dam built on a river to regulate the level of water or flow.

* While not all acquisitions result in the conversion of developed land to park land or a floodplain, for the purposes of this research only areas that have been converted from impervious to a pervious surface are included.

APPENDIX II. Review and Feedback of Preliminary Flood Models

Review and feedback of preliminary FSF flood data is key to assuring the accuracy of our flood models. The following describes some of the commonly used review and feedback techniques employed at FSF.

Overview

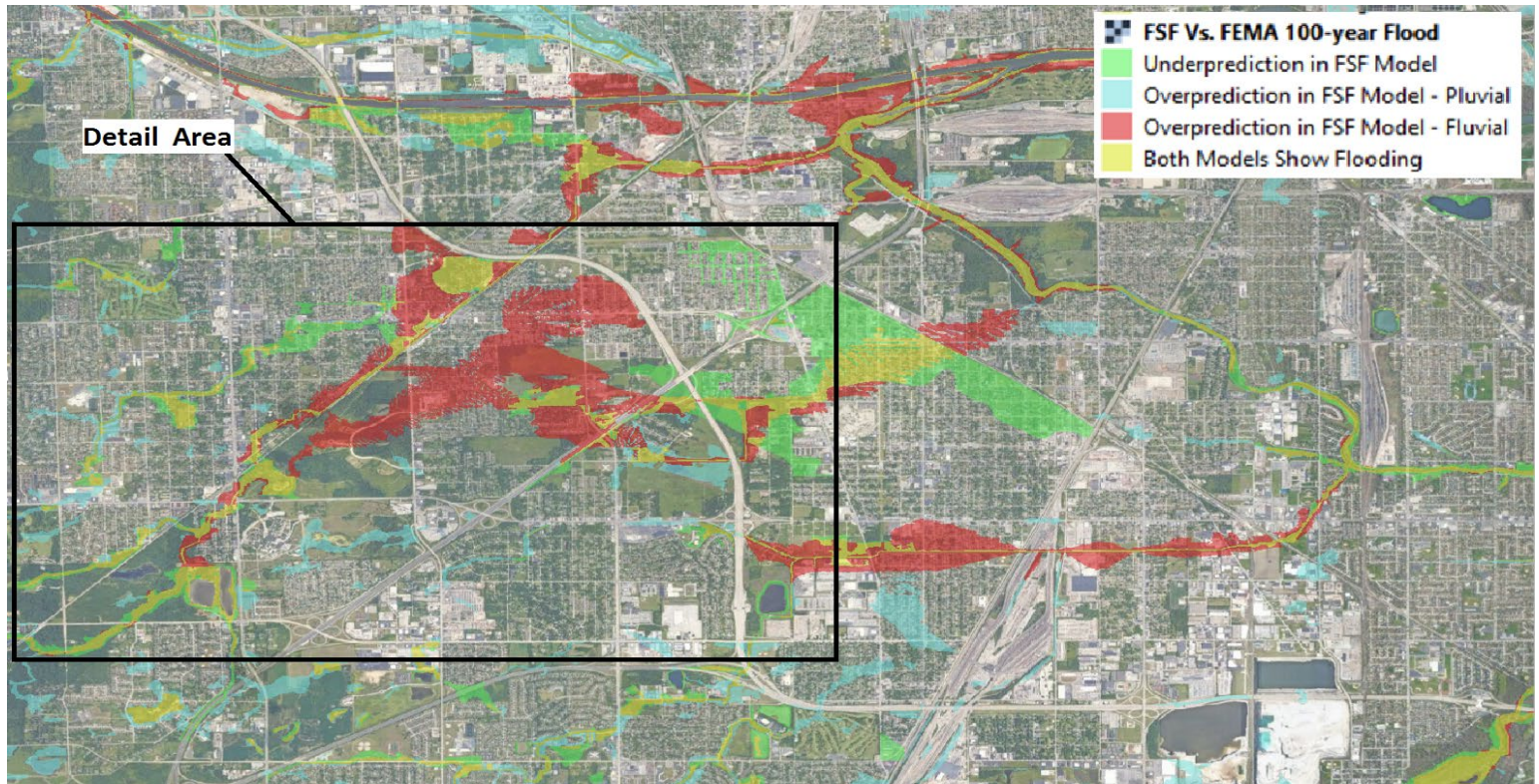
Much of the review and feedback of preliminary modeled flood data involves visual inspection of every tiled inundation layer produced by the flood modelling partners. Our basic flow was to compare the flooded outputs to realistic expectations in order to identify areas in which the models were producing unrealistic inundation, or were not identifying risk in areas where we expected risk to exist. Ultimately, we found it helpful to review this data in two formats:

1. A comparison of the 100-year flood model to FEMA's 1-100 SFHA. While we don't expect to perfectly align with FEMA, we do understand that the FEMA SFHAs are useful guides that help us to understand where flooding has occurred, where it is likely to occur, and where infrastructure is in place to mitigate potential flooding.
2. A comparison of the flood model outputs at benchmark return periods (e.g. the 5-, 10-, 20-, 50-, 75-, and 100-year flood events) in order to confirm realistic levels of flooding. This method was especially useful in urban/built up areas in low return period scenarios.

While there are a number of other approaches that were taken to ensure the accuracy of the models, these two were the most reliable in allowing us to quickly validate (review) and provide feedback to our modeling partners for new models where necessary.

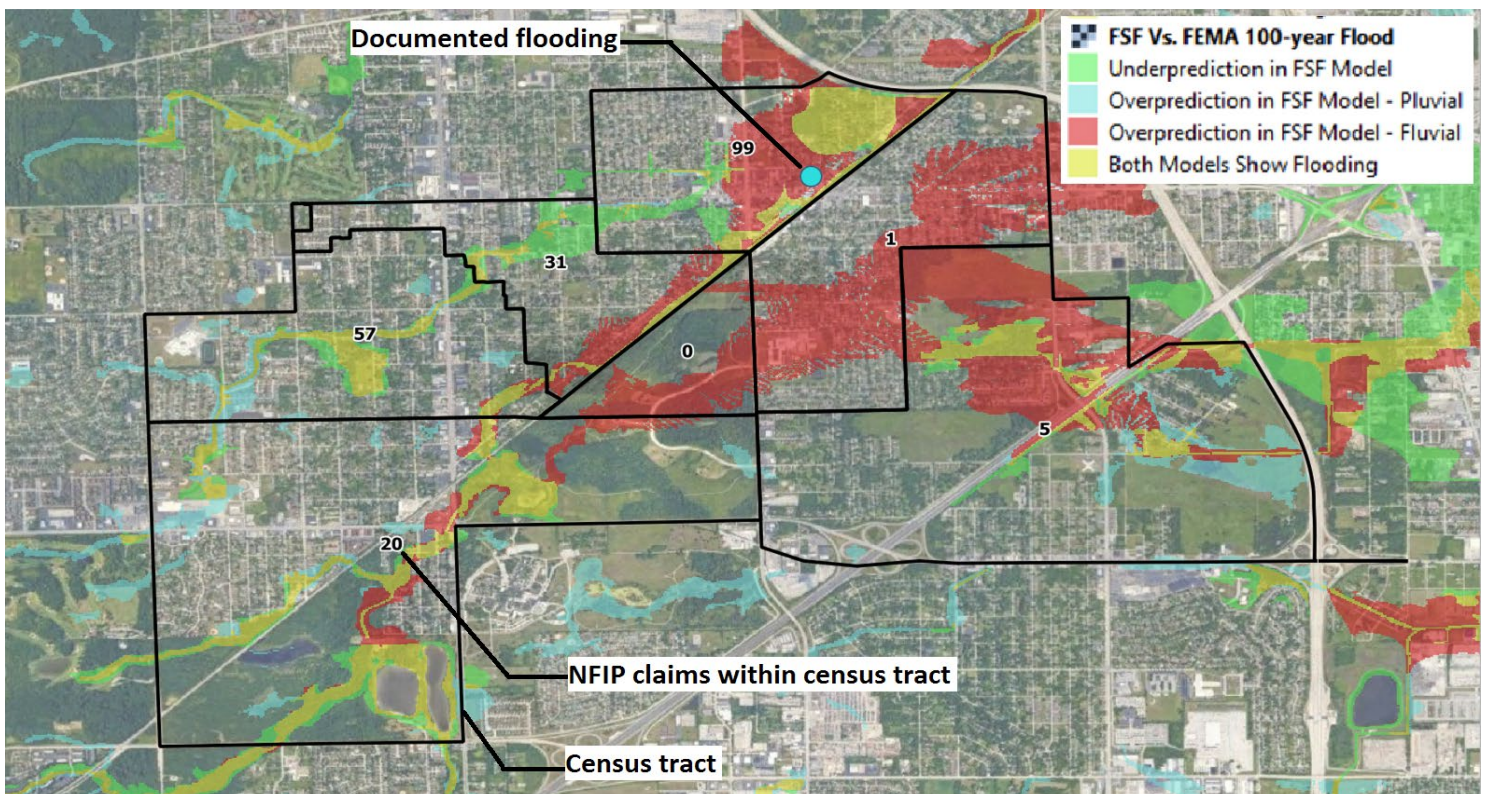
First Street vs. FEMA 100-year Flood Model Comparison

Comparing FSF and FEMA's modeled 100-year flood extents is useful because FEMA's flood layers are considered the gold standard in a publically available national flood model. Although FEMA's model is based on historic climate data (resulting in a general underprediction of flood extents), this data still offers a respectable approximation of modeled flooding. Therefore, if major differences exist between the extents of flooding across the two models, the legitimacy of these major differences is investigated further by FSF's data team.



The above screen capture shows a comparison between the extent of modeled flooding for the 100-year event between FSF and FEMA in dense suburbs southwest of Chicago. It's essentially an overlay of the two datasets to visualize where FSF and FEMA agree on where flooding should occur. Raster cells are broken into one of the following categories:

- **Yellow** -- Both models show flooding
 - These are areas where the FSF flood model and the FEMA flood model both predict flooding will occur.
- **Blue and red** -- Overprediction in FSF's model
 - These are areas where FSF shows flooding but FEMA's model does not.
 - Blue cells represent overprediction tied to pluvial events.
 - Red cells represent overprediction tied to fluvial events.
- **Green** -- Underprediction in FSF's model
 - These are areas where FEMA's model indicates flooding but FSF's does not.



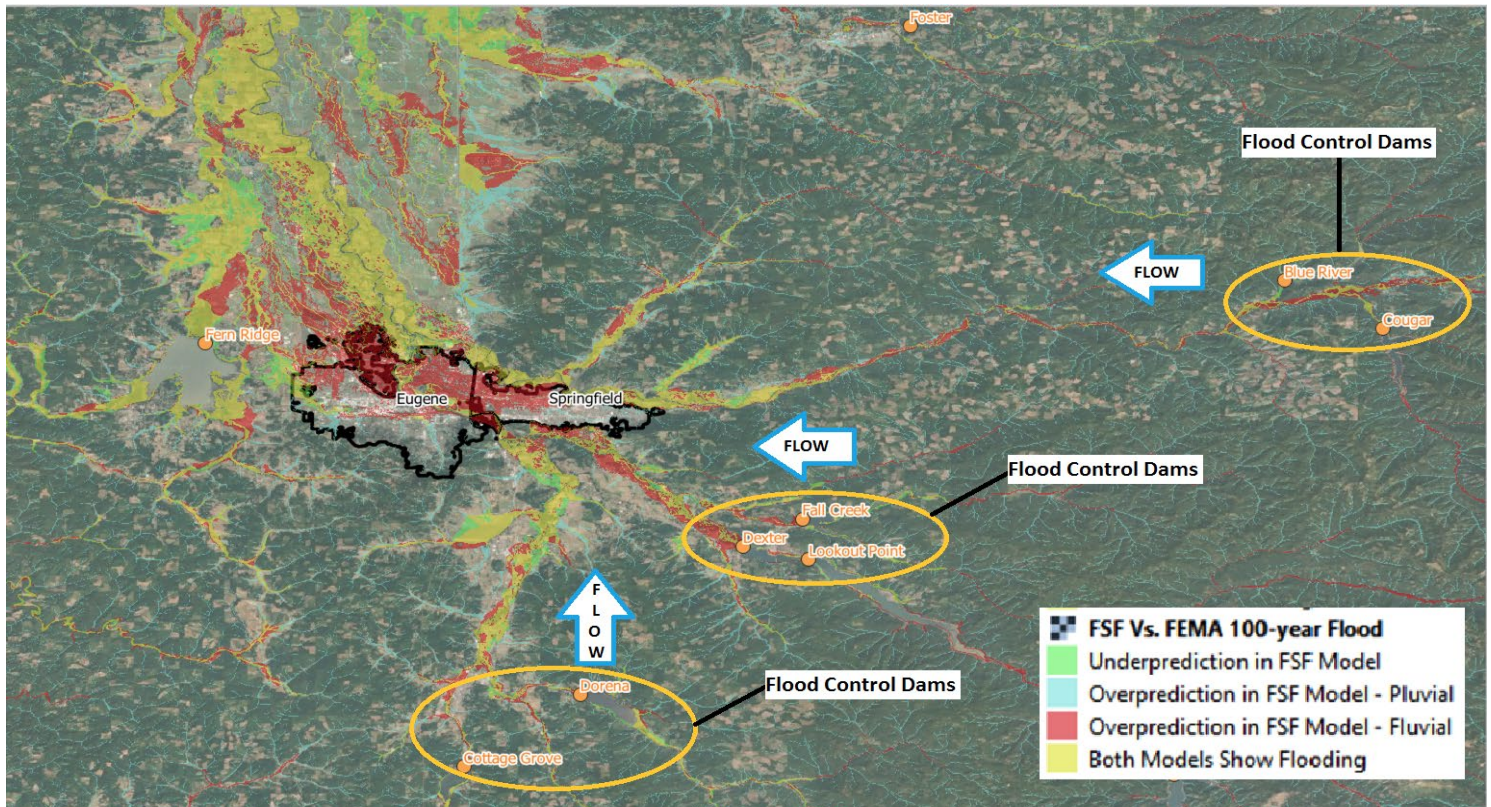
The above screen capture shows a more detailed portion of the flood comparison in Chicago's suburbs. This location generally shows extensive areas of overprediction in FSF's flood model compared to FEMA's (red cells). This is also an area the data team would research further to determine if our model really should diverge from FEMA's so radically.

To help validate the accuracy of our flood extents, FSF has developed a data layer of census tracts associated with counts of filed NFIP claims. In the area shown above, we can see large areas of flood overprediction that have no or very few claims (e.g. < 5 claims). Modeled flooding should therefore be reduced within these areas, and flood extents should more closely resemble the yellow extents where both models show flooding. Similarly, there are other portions of the overpredicted flooding that lie within census tracts with many NFIP claims (e.g. 20, 57, 31, and 99 claims). Based on the high numbers of claims, we can infer more extensive flooding in these areas, and that the larger extents of flooding better agree with the high numbers of claims.

Moreover, FSF also documents instances of historic flooding using events described in FIS reports and local news articles. This is accomplished through a combination of NLP machine learning techniques and targeted online searches during manual inspection of the preliminary flood data. In the screen capture above, we note that the existence of documented flooding within one of the more extensively modeled flood areas that overlaps a census tract with 99 NFIP claims. This further strengthens the validity of the FSF model in this area, and we can assume our flood extents are correct here.

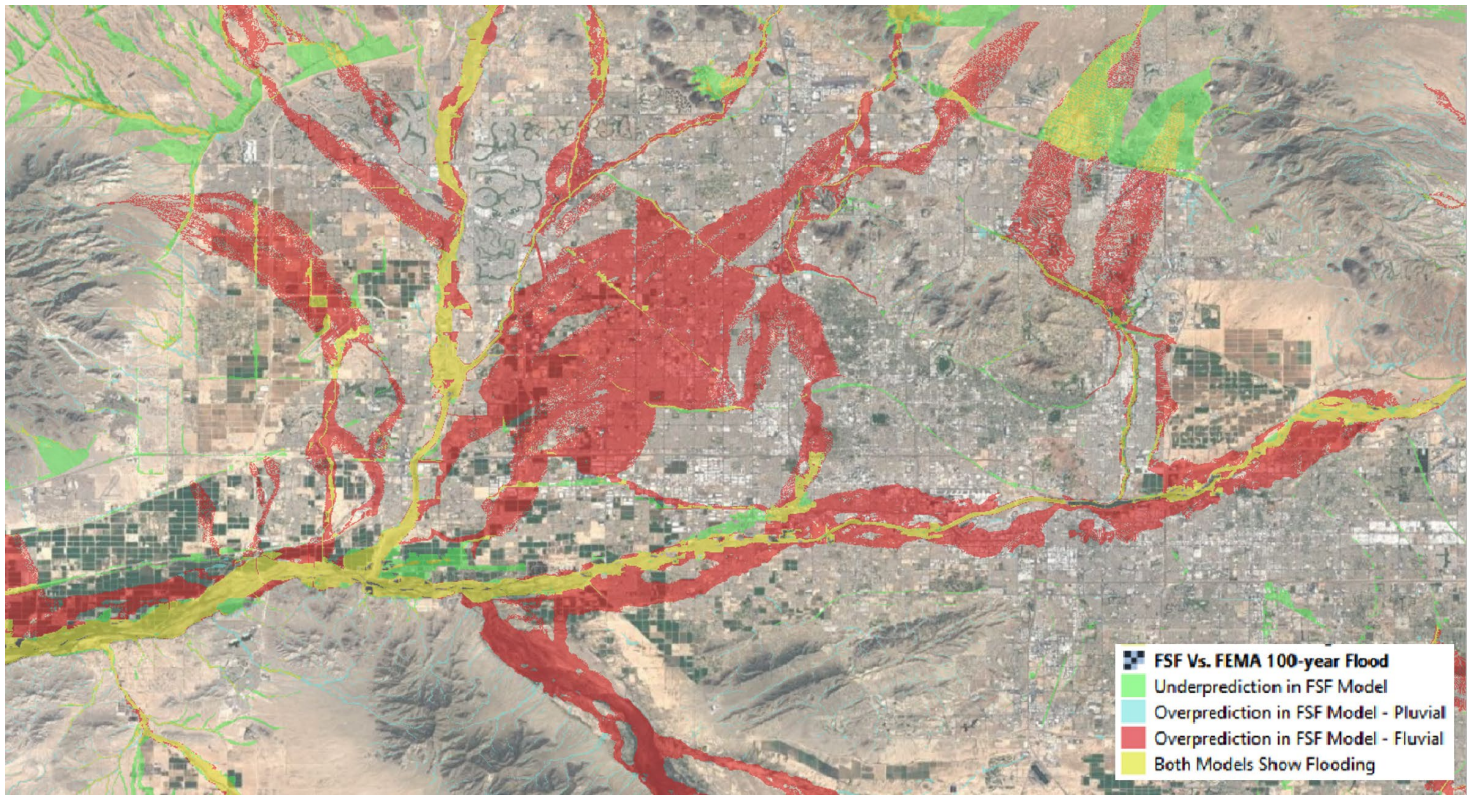
Flooding Due to Lack of Adaptation Data

FEMA has incorporated a fairly robust level of adaptation data into its flood model, thereby providing another compelling reason for comparing FSF and FEMA's modeled 100-year flood extents during the review and feedback process. This helps assure we are adequately incorporating existing adaptation projects into our data. For instance, if one observes an area of extensive flood overprediction compared to FEMA within our preliminary model, it's plausible that flood protection from adaptation infrastructure has been missed, and further research must be conducted.

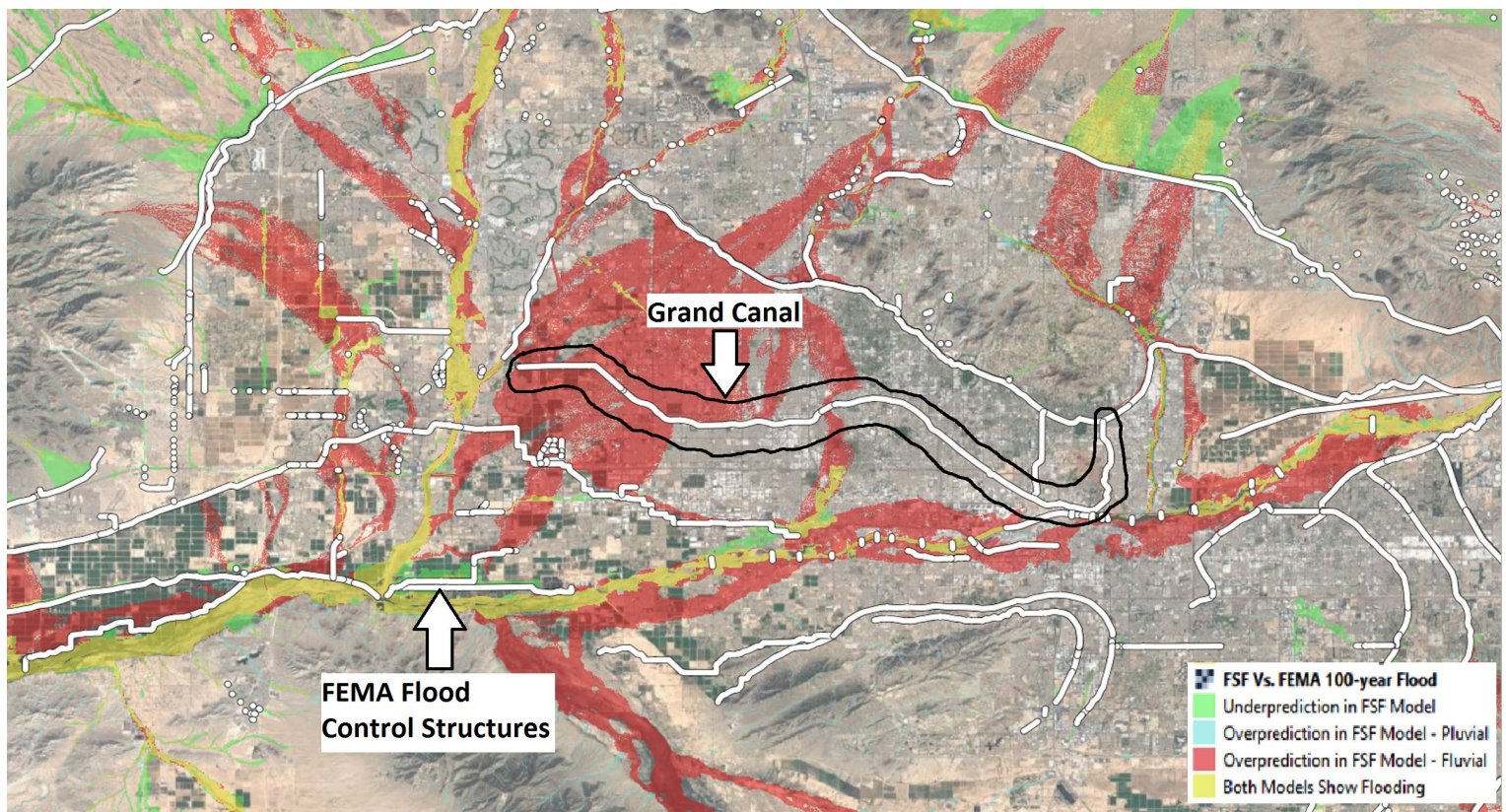


The above screen capture shows a comparison of FSF's preliminary modeled 100-year flood data with FEMA's around the cities of Eugene and Springfield, OR. These cities lie in The Willamette Valley - a relatively small, 150-mile long river valley, home to 70% of Oregon's population, and very prone to flooding from springtime melting snowpack. In order to mitigate flood risk, the Army Corps of Engineers built The Willamette Valley Project; a series of flood control dams in the surrounding mountains.

In the screen capture, extensive flood overprediction has been modeled for Eugene and Springfield. These cities, with a combined population of over 230,000, sit in the floodplain of the Willamette River and are downstream of numerous flood control dams built as part of The Willamette Valley Project (shown as orange points). Areas like this are flagged during the review and feedback process where the FSF preliminary flood model drastically overpredicts flooding compared to FEMA. This is an indication that our data hasn't accounted for the effect of dams on our model, but FEMA likely has. Our team will then know to adjust the model in these areas to better account for the effect of dams designed for flood control.



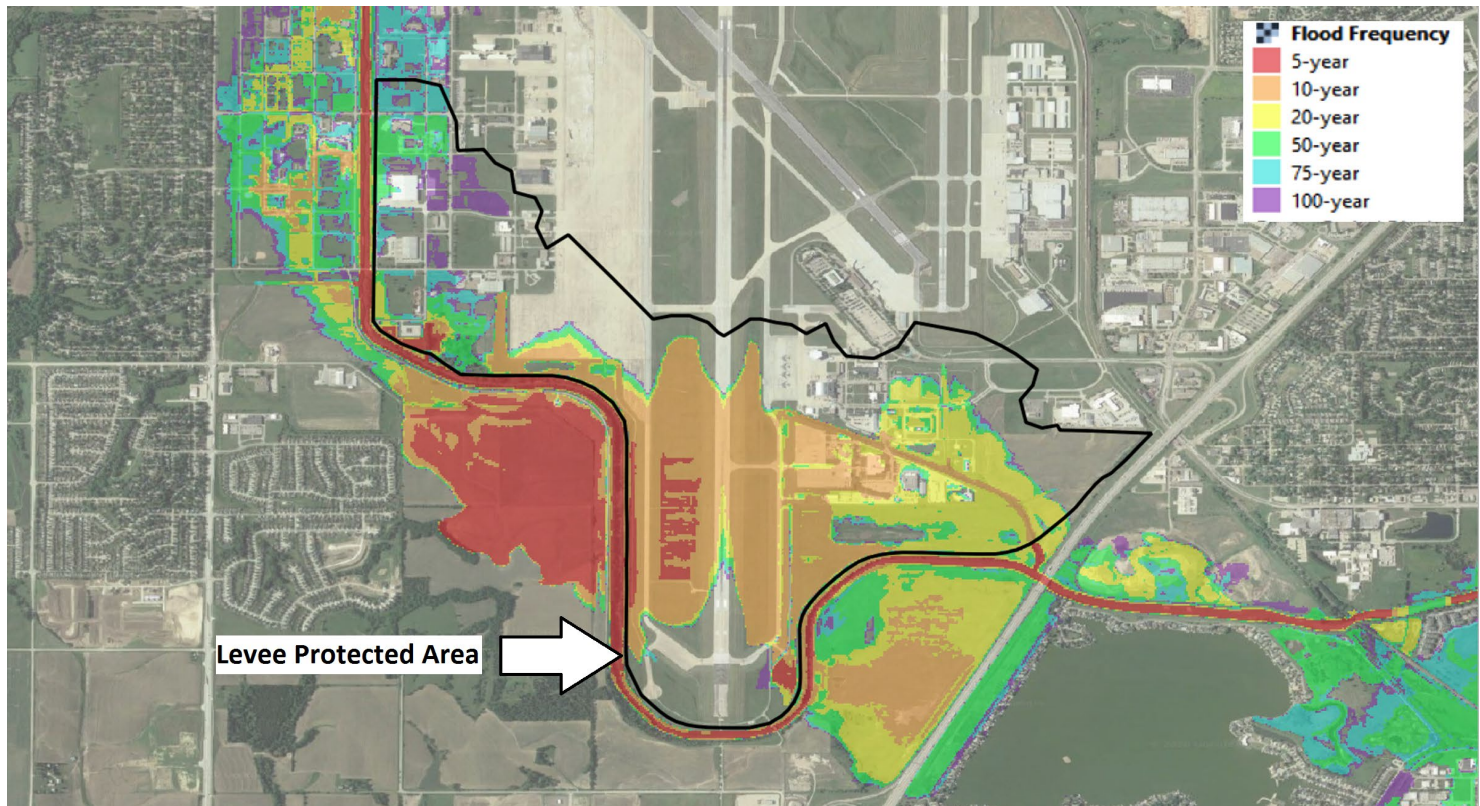
Comparison between FSF's preliminary flood model and FEMA is also useful in heavily urbanized areas. The above screen capture shows the Phoenix, AZ metro area; heavily developed and home to nearly 5 million people. It is unusual that our models disagree so widely in such a populated developed area. FEMA is likely accounting for some type of adaptation infrastructure to reduce flooding that we are missing.



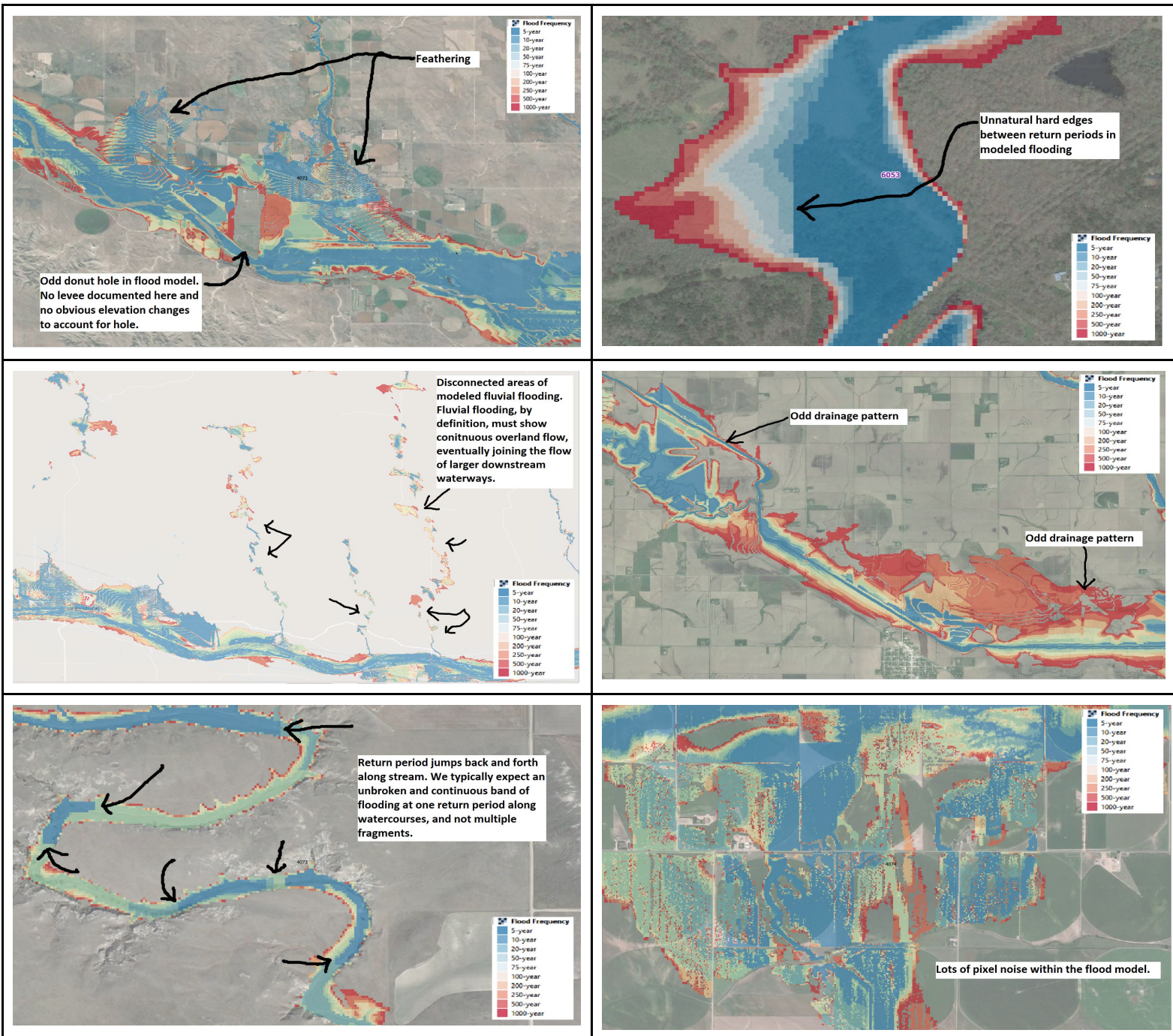
During review and feedback, FSF uses publicly available spatial data sources to investigate the presence of major flood control infrastructure that may have an influence on our model. The above screen capture shows one commonly-used layer: FEMA's dataset of general flood control structures associated with the national flood hazard layer (symbolized as white line features). When this layer is overlaid with our comparison of flood models, it becomes clear that the FSF model is likely not accounting for major pieces of adaptation infrastructure. For example, the above featured linear structure is Phoenix's Grand Canal. Further research quickly reveals that this feature is a man-made canal built to control the 100-year flood event. Because of access to this information, the extents of the modeled flooding were reduced within the Phoenix area, with final extents more closely resembling the yellow extents where both models show flooding.

Benchmark Return Period Comparison within First Street Flood Model

Taking a detailed look at FSF's flood model broken down by return period is another important technique in the review and feedback process. A visual breakdown across return period extents is particularly useful for assuring adaptation infrastructure is being properly incorporated into our model. It also allows for effective cosmetic inspection of our flood layers.



FSF modeled flood data displayed to show a breakdown of flood extents by return period is useful for verifying that adaptation flood protection areas have been incorporated correctly into our flood model. In the above screen capture, we see a protected area behind a levee that was found in the Army Corps' National Levee Database. Although this feature has been rated for the 50-year flood, we see the flood model predicts inundation within the service area at return periods as low as the 5-year. We can therefore conclude the flood model is not properly accounting for this adaptation feature, and the model would be flagged and adjusted so this area does not show flooding until the at least the 50-year event.



Displaying flood layers based on return period extents is also especially useful for spotting cosmetic errors in drainage patterns that are likely caused by issues with the underlying digital elevation model (DEM) used to create the flood layers. The above screen captures demonstrate common issues that are found during the review and feedback process. These issues are brought the attention of the FSFs flood modelers and corrected.